Towards the role of TatA and TatB in the activity and stability of thylakoidal Tat translocase

Dissertation

To obtain the academic degree
doctor rerum naturalium (Dr. rer. nat.)

submitted to

Faculty of natural sciences I – Biosciences

Martin-Luther-Universität
Halle-Wittenberg

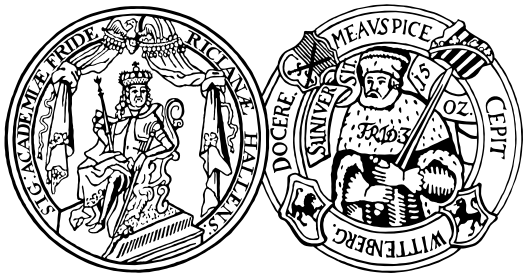

Submitted by Ming Zhou

Reviewers:
1. Prof. Dr. Ralf Bernd Klösgen
2. Prof. Dr. Gary Sawers
3. Prof. Dr. Jan Maarten van Dijl

Date of public defence: 09/12/2025

TABLE OF CONTENT

ABBREVIATIONS

% v/v	Percent volume per volume
% w/v	Percent weight per volume
AA	Acrylamide
ADP	Adenosine diphosphate
APH	Amphipathlic helix
APS	Ammonium persulfate
ATP	Adenosine triphosphate
BN	Blue Native
BN-PAGE	Blue Native Polyacrylamide Gel Electrophoresis
C-terminus	Xarboxyl-terminus; the end of a protein polypeptide
DEPC	Diethylpyrocarbonate
ECL	Enhanced Chemiluminescence detection
EDTA	Ethylenediaminetetraacetic acid
ER	Endoplasmic reticulum
GTP	Guanosine triphosphate
HEPES	4-(2-hydroxyethyl)-1-piperazineethanesulfonic acid
HPLC	High performance liquid chromatography
LB medium	Luria-Bertani (LB) broth, Luria-Bertani (LB) medium
LHCP	Light-harvesting chlorophyll-binding protein
NADP	Nicotinamide adenine dinucleotide phosphate
NMR	Nuclear magnetic resonance
N-terminus	Amino-terminus, NH 2 -terminus; the start of a protein polypeptide
PA	Polyacrylamide
Pi	Inorganic phosphate
PMF	Proton motive force
PMSF	Phenylmethylsulfonyl fluoride
PVDF	Polyvinylidene fluoride
RP-HPLC	Reversed-phase high performance liquid chromatography
RT	Room temperature
SDS	Sodium Dodecyl Sulfat
SDS-PAGE	Sodium Dodecyl Sulfate Polyacrylamide Gel Electrophoresis
Sec pathway	Secretory pathway
SP	Signal peptide
SPP	Stromal processing peptidase
SRP pathway	Signal Recognition Particle pathway
STD	Stroma-targeting domain
Tat pathway	Twin-arginine translocation
TEMED	Tetramethylethylenediamine
TFA	Trifluoroacetic acid
Tic complex	Translocon at the inner envelope membrane of chloroplasts
TMH	Transmembrane helix

Toc complex	Translocon at the outer envelope membrane of chloroplasts
TP	Transit peptide
TPP	Thylakoidal processing peptidase
TTD	Thylakoid-targeting domain
α-TatA	Antibodies against peaTatA
α-TatB	Antibodies against peaTatB
α-TatC	Antibodies against peaTatC
ΔpH	Transmembrane proton gradient

SUMMARY

Cellular protein sorting and transport are essential processes in all living organisms. During evolution, so-called organelles was developed inside eukaryotic cells as spatial compartments, for specific biochemical reactions. In order to maintain organelle function, the majority of required proteins are synthesized in the cytosol and subsequently transported into their target organelles. To facilitate the proper localization of proteins, cells have evolved various translocases that mediate both the transport of proteins across membranes and their insertion into membranes. Notably, some translocases can transport fully folded proteins. Among them, twin-arginine translocation (Tat) translocase, found in chloroplasts of plants and mitochondria of many eukaryotes, as well as in bacteria and archaea, is of particular interest.

In chloroplasts, Tat translocase is located in thylakoid membranes and comprises three subunits: TatA and TatB, both members of the TatAB protein family, and TatC. TatB and TatC together form the hetero-oligomeric TatBC complex, which is involved in substrate binding and recognition. TatA, on the hand, undergoes an assembly-disassembly cycle with TatBC complex in response to substrate presence. Although this general framework is widely accepted, the exact mechanism by which folded substrates are translocated across thylakoid membranes remains unclear. Due to the transient nature of the translocation process, elucidating the dynamic interplay among these three subunits, particularly under active transport conditions, remains a significant challenge.

To investigate the function of individual subunits, our group developed so-called *in thylakoidal* assays. In these assays, the intrinsic activity of a specific Tat subunit in thylakoid membranes is inhibited by specific antibodies, followed by the reconstitution of blocked Tat transport through the supplementation of external Tat proteins. In this study, we first evaluated three *in vitro* translation systems for synthesizing TatB used in reconstitution assays in anti-TatB-treated thylakoids. Surprisingly, only one system proved suitable for this propose. Moreover, high amounts of external TatB produced via *in vitro* translation seemed unable toachieve higher levels of reconstitution. Thus, to accurately assess the effect of TatB on Tat transport efficiency and to quantify protein concentrations in the assays, purified TatB obtained by heterologous overexpression was used in anti-TatA-treated, anti-TatB-treated and untreated thylakoids. The same experiments were also conducted with overexpressed TatA.

Unexpectedly, high concentrations of both TatA and TatB led to a decrease in intrinsic Tat transport. Notably, in our reconstitution assays, external TatB was able to functionally substitute for TatA whereas external TatA could not substitute for TatB. Next, the unexpected decrease in transport efficiency prompted further investigation into whether TatA and TatB could affect the stability of TatBC complex, the core unit of Tat translocase. BN-PAGE analysis revealed that three forms of TatBC complex could be extracted from thylakoid membranes and that external TatA destabilizes all three TatBC complexes. However, changes in TatBC signal intensity did not linearly corelate to transport efficiency, suggesting that the detection by BN-PAGE may not fully reflect the functional state of TatBC complexes. Thus, the underlying effect of TatA on TatBC stability remains to be clarified. Finally, given that TatA activity is driven by the proton motive force (PMF) across thylakoid membranes, the potential effect of PMF on the stability of TatBC complexes was also examined. Indeed, PMF was found to affect the stability of TatBC complexes. But whether this effect by PMF is directly related to TatA function requires further investigation.

1 Introduction

1.1 Protein transport into intracellular compartments

In both prokaryote and eukaryote, numerous biochemical reactions occur simultaneously inside the cell. During evolution, membrane-enclosed compartments, known as organelles, emerged in eukaryotic cells, serving as spatially distinct environments that organize various metabolic processes (Singer and Nicolson 1972). These organelles, such as the endoplasmic reticulum (ER), peroxisomes, mitochondria and chloroplasts, possess distinct protein compositions to carry out specific biochemical reactions. Except mitochondria and chloroplast proteins, those proteins required for other organelles are synthesized in the cytosol and subsequently transported into their target organelles (Robinson and Austen 1987; Verner and Schatz 1988). Mitochondria and chloroplasts, on the other hand, as endosymbiotic organelles, are capable of synthesizing proteins within their compartment. But the majority of their soluble and membrane proteins are also initially synthesized in cytosol (Ellis 1981; Schatz and Mason 1974). In chloroplasts, only about 5% of the more than 3000 proteins are synthesized within the organelle, while the remaining proteins are synthesized on cytosolic ribosomes (Leister 2003). In mitochondria, depending on the organism, approximately 500-1000 proteins are found in the compartment (Elstner, et al. 2009). Yet only a very small number of these are synthesized on mitochondrial ribosomes – e.g. 8 in yeast (Borst and Grivell 1978) and 13 in human (DiMauro and Schon 2003). Therefore, cytosolic-synthesized proteins play essential roles in maintaining the functionality of all organelles.

Proteins synthesized in the cytosol and subsequently transported into their target organelles are referred to precursors. These precursors typically consist of two parts: an N-terminal extension called transit peptide (TP) and the connected functional part called mature protein (Robinson and Austen 1987). TP is responsible for guiding proteins to the correct organelle and facilitating protein interaction with specific receptors on biological membranes (Robinson and Austen 1987; Schatz and Dobberstein 1996). After translocation, TP is removed by peptidases, leaving the mature protein in its target location - either in the organelle interior or embedded within the corresponding membrane.

1.2 Protein transport across thylakoid membranes

In the case of protein targeted to chloroplasts, cytosolically synthesized precursors have two possible final destinations: either the outer compartments of the chloroplast or the thylakoid. In both cases, all chloroplast-targeted proteins must first pass through two envelope membranes. Transit peptides (TPs) of precursor proteins, which contain a stroma-targeting domain (STD), are responsible for cytosolic targeting to chloroplasts. This domain also guides subsequent transport across the envelope membrane though the Toc complex (translocon at the outer envelope membrane of chloroplasts) and the Tic complex (translocon at the inner envelope membrane of chloroplasts) (Gutensohn, et al. 2006; Hinnah, et al. 2002; Smith, et al. 2004). After reaching the stroma, the TP of proteins destined to remain there is removed by stromal processing peptidase (SPP) (Fig.1.1, route①, TP: *red ellipse*) (Richter and Lamppa 1998; Robinson and Ellis 1984). Among these TPs, no conserved sequence motifs have been identified, although they share some general features, such as uncharged N-terminus and a lack of acidic residues in the central region (von HEIJNE, et al. 1989). If the final destination of the protein is on the thylakoid membrane or inside the lumen, TP processing becomes more complex (Fig.1.1, ②-⑤). Proteins targeted to thylakoids possess an additional signal peptide (SP) following the TP. The SP contains a thylakoid-targeting domain (TTD), which mediates the translocation of the protein across the thylakoid membrane (Fig.1.1, SP: *blue ellipse*) (Gutensohn, et al. 2006). After translocation, the SP is cleaved by thylakoidal processing peptidase (TPP). Like TPs, SPs also possess a common structure: a positively charged N-terminus, a hydrophobic core and small side chain residues at -3 and -1 positions of the end of C-terminal cleavage site (von HEIJNE, et al. 1989).

There are four pathways operating protein transport across the thylakoid membrane: Signal Recognition Particle (SRP)-dependent, Twin-arginine translocation (Tat)-dependent, Secretory (Sec)-dependent and spontaneous transport pathways (for a review, see Klösgen, et al. (2004)). Each of these pathways possesses a unique mechanism and specific set of protein substrates. According to their targeting properties, two classes of targeting sequences have been discovered. In this context, we refer to the N-terminal sequence that is responsible for thylakoid protein targeting as the 'targeting sequences', which may consist of both a SP and a TP, or only a TP.

The first class of targeting sequences consists solely of TP, while the TTD is embedded in the

uncleaved, mature body of the substrate proteins. Thylakoid proteins with this class of targeting sequences are transported via SRP-dependent pathway (Fig.1.1, route ②), with the representative of light-harvesting chlorophyll-binding protein (LHCP). The SRP-dependent protein transport process is driven by GTP hydrolysis (see review: Richter, et al. (2010)).

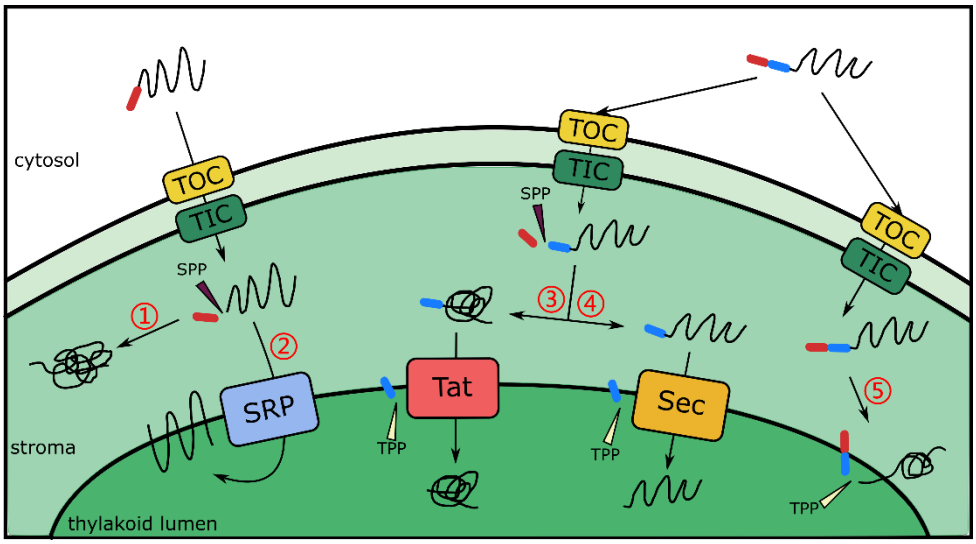

Fig.1.1 Protein transport into the chloroplast.
Nucleus-encoded chloroplast proteins are synthesized in the cytosol and imported into the chloroplast via the TOC complex (translocon at the outer chloroplast membrane) and TIC complex (translocon at the inner chloroplast membrane). Upon entry into the stroma, transit peptides (*red ellipse*) are cleaved by stromal processing peptidase (SPP). Proteins lacking a thylakoid targeting domain (TTD) remain in the stroma and folded there (①). Depending on the type of thylakoid targeting domains, proteins are subsequently directed to different thylakoid transport pathways. ② The SRP (Signal Recognition Particle) pathway mediates proteins inserted into the thylakoid membrane. The thylakoid targeting domain for SRP substrates is located inside the mature part which is not cleaved by thylakoidal processing peptidase (TPP). ③–④ Proteins containing signal peptides (*blue ellipse*) are transported across the thylakoid membrane into the lumen either by the Tat (Twin-arginine translocation) pathway or the Sec (Secretory) pathway, depending on the folding sate of mature domain. ⑤ Unfolded proteins spontaneously inserted into the thylakoid membrane which is directed by a SP. In the case of ③–⑤, the thylakoid targeting domain is located within the SP and the SP is removed by TPP after successful translocation.

The second class of targeting sequences is bipartite, consisting of a TP and a SP. Three pathways on the thylakoid membrane recognize SP, while SP can differentiate and direct proteins specifically into the targeted pathway (Fig.1.1, route ③④⑤).

The first pathway is the spontaneous transport pathway. It recognizes a bipartite targeting signal, in which both TP and SP are removed simultaneously after protein translocation (Fig.1.1, route ⑤). This pathway does not require stromal factors, nucleoside triphosphates or the proton gradient across the thylakoid membrane, which given the name of 'spontaneous'. This pathway appears to be responsible for a specific class of thylakoid membrane proteins that share a characteristic structural feature and

membrane topology: a relatively short hydrophilic N-terminal segment located in the lumen, followed by a single hydrophobic transmembrane domain positioned near the NH_2-proximity of mature polypeptide, and the mature domain located in the stroma. Representative substrates of this pathway include CFo-II (Michl, et al. 1994) as well as several photosystem II subunits such as PsbX, PsbW (Kim, et al. 1998) and PsbY (Thompson, et al. 1999).

Tat pathway and Sec pathway are the other two pathways recognizing a bipartite targeting signal. In these two pathways, TP is removed after the protein passes two layers of the chloroplast envelope membrane, and SP is removed after protein transport into the lumen (Fig.1.1, route ③④). Sec pathway is responsible for transporting unfolded protein across the thylakoid membrane (Randall and Hardy 1995) and it is driven by ATP hydrolysis (see review: Denks, et al. (2014)). Typical substrates of the Sec-dependent pathway include plastocyanin, the 33kDa protein of the oxygen evolving complex (Yuan and Cline 1994) and the subunit F of photosystem I (Karnauchov, et al. 1994).

Tat pathway, in contrast to other thylakoid transport routes, is special for its ability to transport folded proteins across the thylakoid membrane (Clark and Theg 1997; Creighton, et al. 1995; Hynds, et al. 1998). To date, only three known pathways are capable of translocating folded proteins into organelles: Tat pathway (Müller and Bernd Klösgen 2005), peroxisomal import pathway (Erdmann and Schliebs 2005) and Bsc1-mediated protein translocation (Wagener, et al. 2011). Another distinctive feature of Tat pathway is its strict dependence on proton motive force (PMF) across the thylakoid membrane as the sole energy source, rather than utilizing nucleoside triphosphates or stromal factors (Braun, et al. 2007; Klösgen, et al. 1992; Mould and Robinson 1991).

The name “Tat” is derived from a conserved twin-arginine (RR) motif which are consistently found in the SP of Tat substrates (Berks 1996; Chaddock, et al. 1995). Since both the Sec and Tat pathways utilize SPs for targeting, distinguishing features are required in the SP of their respective substrates to ensure pathway specificity. The RR motif, along with its vicinity, have been shown to play a crucial role in directing proteins to the Tat pathway and preventing mistargeting to the Sec pathway (Blaudeck, et al. 2003; Bogsch, et al. 1997; Brink, et al. 1998). Two representative substates of Tat pathway are the 16kDa and 23kDa proteins of the oxygen evolving complex (Klösgen, et al. 1992; Mould, et al. 1991). Importantly, the Tat pathway is not exclusive to thylakoid membranes. It also operates in cyanobacteria

(Frain, et al. 2016), at cytoplasmic membranes of bacteria and archaea, such as *Escherichia coli* (Jack, et al. 2001; Rose, et al. 2013; Stanley, et al. 2000), *Bacillus subtilis* (Goosens, et al. 2014; Jongbloed, et al. 2004), and *haloarchaea* (Dilks, et al. 2005), as well as at mitochondrial inner membranes of certain organisms, including plants (Petrů, et al. 2018; Schäfer, et al. 2020). Despite some variations in detail, the overall structure and mechanism of Tat pathway are conserved among all the systems.

1.3 The Tat translocation System

1.3.1 Subunits of Tat translocase

Generally, Tat translocase consists of three subunits, namely TatA, TatB, and TatC, as found in *E. coli* cytoplasmic membranes and thylakoid membranes (also called Tha4, Hcf106, and cpTatC in the thylakoid system, respectively) (Müller and Bernd Klösgen 2005). Loss of any of these subunits results in inhibition of Tat-dependent protein transport (Hauer, et al. 2013; Ize, et al. 2004; Lee, et al. 2002; Zinecker, et al. 2020). Additionally, a TatE protein is also present in *E. coli* and some enterobacteria, which shares high sequence similarity with TatA (Sargent, et al. 1998) but exhibits less functional importance (Jack, et al. 2001). In addition to the canonical TatABC system, a minimal Tat system requires only two proteins, TatA or TatB, and TatC, in certain organisms. In *Bacillus subtilis*, which represents the Tat machinery of most Gram-positive bacteria, a TatAC translocase mediates Tat-dependent protein transport (Jongbloed, et al. 2004). Similarly, in the jakobid *Andalucia godoyi*, a mitochondria-encoded TatAC system conducts minimal Tat transport activity (Petrů, et al. 2018). In addition, plant mitochondria possess a functional TatBC system that acts as the protein translocase (Schäfer, et al. 2020). It should be noted that TatA and TatB belong to the same protein family (Alcock, et al. 2016; Yen, et al. 2002). Therefore, the compositional diversity of Tat systems across organisms likely reflects a central role of TatC and a functionally adaptable role between TatA and TatB.

1.3.1.1 TatAB protein Family

Plant and bacterial TatA and TatB proteins were first identified in 1990s. They exhibit high sequence similarity, particularly in the amino (N-) -terminal region, but this similarity diminishes towards the carboxyl (C-) terminus (Mori, et al. 1999; Voelker and Barkan 1995; Walker, et al. 1999; Weiner, et al.

1998). Additionally, both TatA and TatB are relatively small proteins. The molecular weights of TatA and TatB from pea (*Pisum sativum*) are approximately 8.9 and 18.9 kDa, respectively. The N-terminus of the TatA/B proteins is located in the lumenal side of the thylakoid membrane (or the periplasmic side in *E. coli*), while the disordered C-terminal region located in the stroma (or the cytoplasmic side in *E. coli*) (Gouffi, et al. 2004; Koch, et al. 2012; Pettersson, et al. 2018; Zhang, et al. 2014). Via an α-helical transmembrane domain (TMH), TatA/B are integrated in the membrane (De Leeuw, et al. 2001; Lee, et al. 2006a; Mori, et al. 1999). While TatB is fully membrane-integrated protein in both bacteria and plants (De Keersmaeker, et al. 2007; Zinecker, et al. 2020), TatA has also been detected in soluble form in chloroplast stroma and bacterial cytosol (Dilks, et al. 2005; Frielingsdorf, et al. 2008; Pop, et al. 2003). TatA and TatB share highly structural similarity (Fig.1.2), but they show functional distinction (Lee, et al. 2002).

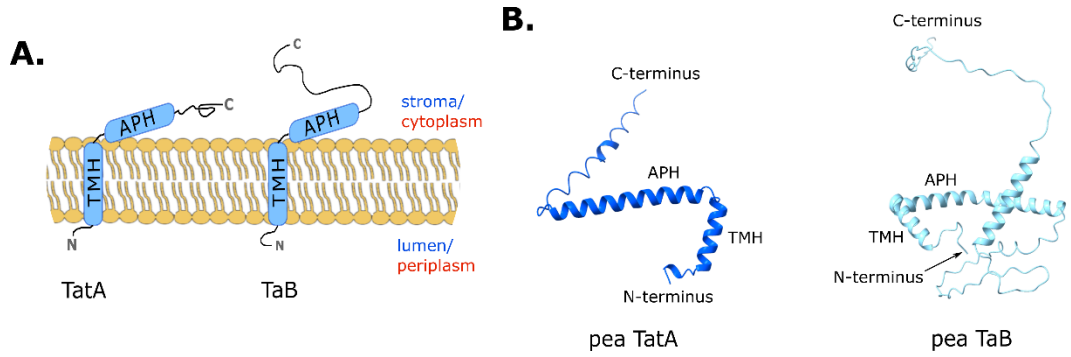

Fig.1.2 Structural features of TatA and TatB proteins.
(A) Schematic representation of TatA and TatB topology in the thylakoid membrane and *E. coli* cytoplasmic membrane. TatA and TatB proteins in these two organisms show highly structural similarity. Both proteins share a similar membrane orientation, with an N-terminal transmembrane helix (TMH) followed by an amphipathic helix (APH) lying almost parallel to the membrane surface. The N-terminus locates in the lumen/periplasm, while the C-terminus is exposed to the stroma/cytoplasm. (B) AlphaFold-predicted structures of pea (*Pisum sativum*) TatA (left) and TatB (right). Both proteins exhibit the conserved TMH–APH arrangement. However, TatB possesses a longer C-terminal domain, distinguishing it from TatA in structure and potentially in function.

1.3.1.2 TatC protein family

TatC consists of six TMHs with both the N- and C-terminus located at stromal/cytoplasmic side. These six TMHs are connected by the soluble loops S1/C1 and S2/C2 at stromal/cytoplasmic side and loops L1/P1, L2/P2 and L3/P3 at lumenal/periplasmic side (Fig.1.3A) (Punginelli, et al. 2007; Ramasamy, et al. 2013; Rollauer, et al. 2012). Sequence comparisons in the TatC family from different organisms reveal

a similar overall length and topology among TatC homologs, whereas they only show moderate conservation on residues that are located in TMH region (Allen, et al. 2002; Simone, et al. 2013; Yen, et al. 2002). Notably, a highly conserved residue is found on TMH4, glutamate (E170) in *E. coli* and glutamine (Q284) in pea TatC precursor, which is conserved as either E or Q among various organisms (Ramasamy, et al. 2013).

The crystal structures published by Rollauer, et al. (2012) and Ramasamy, et al. (2013) reveal the complex and unique structure of TatC protein from *Aquifex aeolicus*. This protein has a glove-like structure: the TMHs are not tightly packed but are lined up next to each other, with TMH3 serving as a backbone connecting them; while the cytoplasmic proximity of the protein is oriented more vertically relative to the lipid surface, the periplasmic proximity bends inwards, forming a bulge shape; this bulge region is almost parallel to the membrane surface. This parallel interface also refers to as 'TatC cap' (Fig.1.3B, cyan-shade). Consistently, the AlphaFold prediction suggest a similar structural arrangement for pea TatC (Fig.1.3B). Additionally, due to this parallel interface, TatC oligomers are predicted to assemble into a cap-like structure that remain open at the stromal/cytoplasmic side and closed at the lumenal/periplasmic side. Intriguingly, TMH5 and TMH6 are significantly shorter than the other TMHs, resulting in the position of loop L3/P3 within the membrane interior and away from the lumenal/periplasmic cap region (Fig.1.3B).

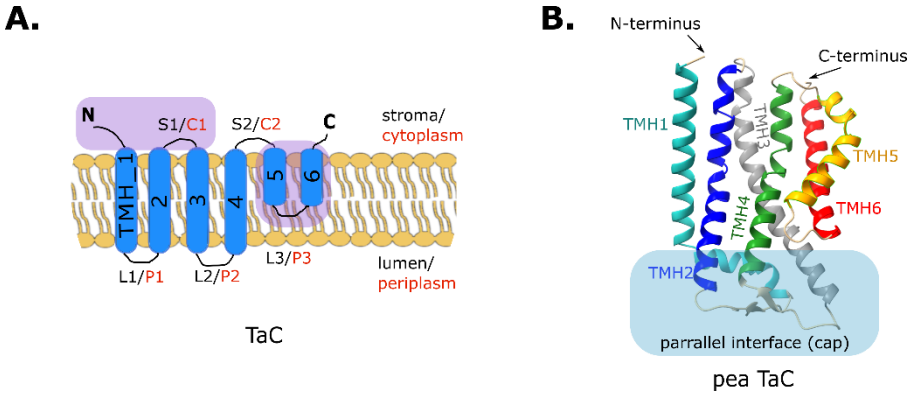

Fig.1.3 Structural features of TatC protein.
(A) Schematic topology of TatC in the thylakoid membrane and *E. coli* cytoplasmic membrane. TatC in these two systems also shows highly structural similarity, which consists of six transmembrane helices (TMH1–6) and the stromal/cytoplasmic orientation of both the N- and C-terminus. *Purple-shaded* regions indicate the hypothetical binding sites of signal peptides (SPs). (B) AlphaFold-predicted structure of pea (*Pisum sativum*) TatC, viewed from the membrane side. TMHs are individually colored (TMH1–6), and the N- and C-terminus are labeled with *black arrows*. The *cyan-shaded* region highlights the "parallel interface", so-called TatC cap.

1.3.2 Tat substrates

Tat substrates consist of two parts, an N-terminal targeting sequence that directs the protein to Tat translocase and a folded (mature) protein that serve as the functional unit. The targeting sequence typically comprises both a transit peptide (TP) and a signal peptide (SP). The SP usually contains a thylakoid-targeting domain (TTD), which is responsible for directing protein targeting and mediating transport across the thylakoid membrane. An exception is the thylakoid Rieske protein, where the TTD is located within the mature protein sequence (Molik, et al. 2001; Schäfer, et al. 2020). Moreover, SPs share a common structure consisting of a positively charged n-region, a hydrophobic h-region and a polar c-region. At end of c-region, the cleavage site for thylakoidal processing peptidase (TPP) is present (Lüke, et al. 2009; Teixeira and Glaser 2013)(Fig.1.4). After translocation across the thylakoid membrane, SP is cleaved by TPP, releasing the mature part of the protein into the lumen (Frielingsdorf and Kloösgen 2007; Lüke, et al. 2009). The cleaved SP remains in the membrane and is subsequently degraded there (see Enguo Fan dissertation, MLU, 2008).

The RR motif in the SP of Tat substrates has been shown to be essential for specific targeting to Tat translocase in the earlier time (Chaddock, et al. 1995; Halbig, et al. 1999; Stanley, et al. 2000). Whereas, the presence of an RR motif alone does not necessarily direct proteins to Tat pathway, indicating that this motif alone is insufficient to determine the destination of proteins. For instance, in *Bacillus subtilis*, a large number of proteins containing an RR motif, yet only a small subset of them has been confirmed to be transported via Tat translocase (van Dijl, et al. 2002).Moreover, recently studies have shown that increasing the hydrophobicity of Tat SP can compensate for the loss of the RR motif and restore Tat transport activity (Huang and Palmer 2017; Ulfig and Freudl 2018). Thus, while the RR motif is important for Tat-specific targeting, it seems not strictly required. The precise mechanism of substrate selection by Tat pathway remains to be elucidated.

Unlike SPs which share common structural features, mature domains of Tat substrates are highly diverse. Their molecular weights range from 9kDa to 90kDa (Berghöfer and Klösgen 1999; Brüser, et al. 2003; Mould, et al. 1991; Rodrigue, et al. 1999) and they lack conserved sequence motifs or structural features. The only established requirement of mature parts for efficient Tat transport is that they must be fully folded (DeLisa, et al. 2003; Frain, et al. 2019; Müller and Bernd Klösgen 2005). Albeit, in some

rare cases, partially folded (Hynds, et al. 1998; Stolle, et al. 2016) or even unfolded proteins (Richter, et al. 2007) have also been shown to be transported via Tat pathway. Therefore, the precise role of the mature protein domain on Tat-dependent translocation remains poorly understood.

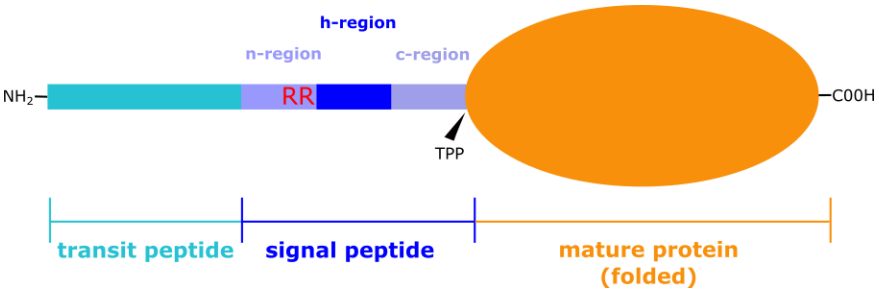

Fig.1.4 Scheme of a Tat substrate. A Tat substrate contains an N-terminal targeting sequence that directs the protein to Tat translocase and a folded mature part that serves as the functional unit. The targeting sequence typically comprises both a transit peptide (TP, *cyan*) and a signal peptide (SP, *blue*). The SP is responsible for directing proteins to the Tat pathway. The SP (*blue*) consists of three domains: a positively charged n-region, a hydrophobic h-region and a polar c-region. A conserved twin-arginine motif (RR, shown in *red*) is located within the n-region and just before the h-region. Following translocation, the SP is cleaved by TPP at the cleavage site in c-region end, releasing the mature folded protein (*orange*) in the thylakoid lumen.

1.3.3 Tat-dependent protein transport

In both *E. coli* cytoplasmic membranes and thylakoid membranes, Tat pathway is operated by TatA, TatB, and TatC. The subunits TatB and TatC form the hetero-oligomeric TatBC complex, which is involved in substrate binding and recognition. TatA, on the other hand, functions more dynamically: its activity is closely linked to the presence of substrate. Mechanically, Tat-dependent protein transport can be divided into four consecutive steps (see review: Müller and Bernd Klösgen (2005)): (1) TatBC receptor complex recognizes the SP of Tat substrates; (2) substrate-binding triggers the recruitment of TatA into TatBC complex, initiating membrane translocation of the substrate protein; (3) TatA dissociates from the TatBC complex after protein translocation; (4) mature protein is released into the lumen/periplasm by proteolytic cleavage of the SP (Fig.1.5). However, despite agreement on this overall framework of Tat-dependent protein transport, the details of molecular cooperativity for Tat pathway remain under debate.

For example, the initial binding location of substrates is not clear. Several studies suggest that Tat substrates may initially interact with the membrane lipid bilayer prior to the recognition by TatBC complex (Bageshwar, et al. 2009; Brüser and Sanders 2003; Frielingsdorf and Kloösgen 2007; Shanmugham, et al. 2006). However, it has been also suggested that substrates interact directly with TatBC receptor (Gé and Cline 2007; Maurer, et al. 2010; Mori, et al. 2001). Additionally, one report

showed that soluble stromal factors bound with Tat substrates prior to translocation, may assisting in substrate sorting and facilitating docking to the Tat machinery (Ouyang, et al. 2020).

Besides, the biggest debate on Tat pathway is around the working models of TatA. Currently, three major models have been proposed: (1) TatA pore model - TatA forms translocation pores of variable diameters to facilitate membrane transport of Tat substrates of various sizes (Alcock and Berks 2022; Hao, et al. 2023); (2) membrane weakening model - TatA induces local membrane weakening, allowing substrates pass directly through the lipid bilayer (Hou, et al. 2018; Mehner-Breitfeld, et al. 2022); (3) enzymatic model - TatA works in a catalytic or regulatory role to functionally activate TatBC complex (Hauer, et al. 2013).

The idea of TatA pore model arose from the observation that in *E. coli*, the expression level of TatA is approximately 20-fold higher than that of other Tat components (Jack, et al. 2001) and TatA can be purified as homo-oligomeric complexes independently of the other Tat subunits (Peltier, et al. 2002). Importantly, TatA has been shown to form a 'ladder' of discrete bands on BN-PAGE (Behrendt, et al. 2007; Oates, et al. 2005), indicating the existence of TatA complexes of varying sizes in *E. coli* cytoplasmic membranes. Additionally, NMR data has demonstrated that TatA forms a pore-like structure whose size depends on the number of TatA molecules applied in the experiment (Rodriguez, et al. 2013). Furthermore, Gohlke, et al. (2005) observed ring-shaped TatA structures of variable diameters via electron microscopy. However, this TatA pore model does not address the question of why no proton leakage occurs during transport.

On the other hand, experimental data from thylakoids, which are isolated from wild type species such as *Pisum sativum* or *Arabidopsis thaliana*, does not support this pore model. In plants, TatA also forms homo-oligomers by BN-PAGE detection, but these appear in only one or two sizes (Jakob, et al. 2009). Additionally, the TatA:TatB ratio is approximately 1:1 and TatC is present at a similar, or even less, abundance compared to them (Jakob, et al. 2009; Mori, et al. 2001). Given the relatively low abundance of TatA in thylakoid membranes and its necessity for Tat transport, it seems unlikely that TatA forms pores of varying sizes in this system. Thus, an alternative model, the enzymatic model, has been proposed that TatA acts as a regulatory role in Tat translocase (Hauer, et al. 2013). Hauer, et al. (2013) observed a sigmoidal curve when Tat transport activity was plotted against TatA concentration. Such

curves are a characteristic of cooperative interactions observed in allosteric enzymes, leading to the hypothesis that TatA may act as a coenzyme for TatBC complex, catalyzing a specific step during Tat-dependent protein transport (Hauer, et al. 2013).

Moreover, Brüser and Sanders (2003) proposed a membrane-weakening model of TatA in which the short TMH of TatA destabilizes the membrane near the Tat substrate. This allows a pulling of substrate through the membrane and meanwhile maintains the membrane proton. Later, their group demonstrated that the N-terminal part of TatA, including TMH, destabilized the cytoplasmic membrane of *E. coli*, and that this destabilizing effect was triggered by substrate binding and counter-balanced by APH of TatA in the resting state (Hou, et al. 2018). A linear arrangement of TatA was subsequently proposed to locally weaken the membrane and enable protein transport (Mehner-Breitfeld, et al. 2022). Moreover, the length of TatA TMH has been shown to be crucial for successful translocation, underscoring the role of TatA in membrane-destabilization (Stockwald, et al. 2023).

Besides, rather than working independently as one of three models mentioned above, TatA may perform multiple functions simultaneously in the Tat-dependent protein transport. Recently, it has been proposed that TatA does not form a proteinaceous pore, as seen in Sec pathway, but instead participates in the formation of a toroidal pore consisting of both lipid and TatA/B/C proteins (Asher and Theg 2021). In this model, substrate-binding triggers the opening of TatBC receptor, while recruited TatA connects TatBC protomers to assemble a pore structure. Simultaneously, TatA weakens the lipid bilayer within the pore, thereby facilitating the substrate translocation across the membrane (Hao, et al. 2023).

Why is the Tat machinery under such intense debate? A particular challenge in studying Tat pathway lies in the transient and dynamic nature of the translocase. Although TatA is known to play an essential role in Tat transport (Zinecker, et al. 2020), its transient interactions with TatBC complex prevents the capture of TatA-associated TatBC complex in a native state (Cline and Mori 2001; Geise, et al. 2019). The role of TatA has therefore been suggested by indirect evidence, including crossing linking, mutagenesis and fluorescent tracking (Alcock, et al. 2013; Barrett and Robinson 2005; Blummel, et al. 2015). Thus, the molecular mechanism of TatA action remains one of the least understood aspects of the Tat pathway. As a result, even though TatBC complex is a relatively stable structure which can be

readily examined by BN-PAGE and immunoblotting (Cline and Mori 2001) (Matthias Reimers Dissertation, MLU, 2021), the structure and assembly of the active translocase remain incompletely understood.

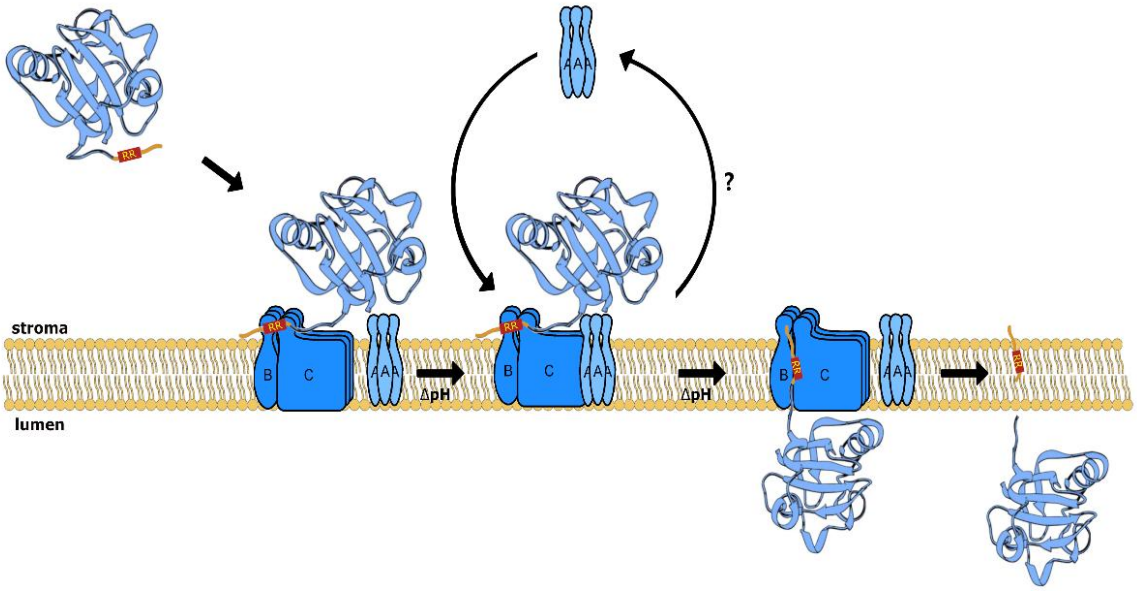

Fig.1.5. Proposed model of Tat-dependent protein transport across the thylakoid membrane.
The folded precursor protein carrying an N-terminal twin-arginine (RR) signal peptide is recognized by the membrane-embedded TatBC complex. Substrate binding triggers the recruitment of TatA, which interacts with TatBC complex to activate translocase. The folded protein is then translocated across the membrane into the lumen with ΔpH as the major energy source. Following translocation, the signal peptide is cleaved by thylakoidal processing peptidase (TPP), and TatA is proposed to dissociate from TatBC complex and recycle for subsequent transport cycles. Whether dissociated TatA back to the stroma remains under investigation (indicated by "?").

1.4 Function of Tat components

1.4.1 Architecture of TatBC complexes

TatB and TatC form hetero-oligomers as substrate receptors (Bolhuis, et al. 2001; Cline and Mori 2001; Fincher, et al. 2003). These TatBC complexes are stable and exist independently of substrate binding, while their stability and apparent size are sensitive to the type and concentration of detergents used in solubilization. Depending on the detergent applied, the molecular weight of TatBC complexes usually ranges between 400 and 650kDa (Cline and Mori 2001; McDevitt, et al. 2006; Richter and Brüser

2005). But whether all these forms function as substrate receptor is still unclear. Unlike TatB, which also freely presents in the membrane as homo-oligomers (Cline and Mori 2001; Oates, et al. 2005), TatC is always incorporated within TatBC complexes (Behrendt, et al. 2007; Cline and Mori 2001). Behrendt, et al. (2007) further demonstrated that in the absence of TatC, TatB assembled into multiple homo-oligomers; whereas in the presence of TatC, TatB predominantly formed TatBC complexes with TatC protomers, and formed only one homo-oligomer around 140kDa. This finding underscores the intrinsic tendency of TatB and TatC to form hetero-oligomers and the potential regulatory role of TatC in modulating TatB organization. The ratio of TatB to TatC on the membrane is presumably 1:1 in both *E. coli* and thylakoids (Jack, et al. 2001; Jakob, et al. 2009; McDevitt, et al. 2006). However, the precise number of TatBC protomers within a receptor complex remains unclear, with suggested ranging from two to eight (Alcock, et al. 2016; Blummel, et al. 2015; Tarry, et al. 2009). Recently, our group observed a three-step conversion of TatBC complexes, associated with a progressive dissociation of TatB. Hence, we propose that the predominant form of TatBC complexes consists of three TatB protomers independently associated with a homo-oligomeric three-TatC core (Matthias Reimers Dissertation, MLU, 2021).

The exact binding sites of TatB on TatC remains unknown. Indirect approaches, such as site-specific crosslinking, have shown that the most critical contacts between TatB and TatC mediates by the TMH and a conserved glutamate residue at position 8 of TatB (Alcock, et al. 2016; Behrendt and Brüser 2014; Ma, et al. 2018). Whereas, the C-terminal disordered region of TatB appears to be dispensable for the TatB-TatC interaction (Ma, et al. 2018; Maldonado, et al. 2011). The TMH of TatB shows contact with TMH5 and TMH6 of TatC, while the N-terminus of TatB contacts with loop P3 of TatC (Alcock, et al. 2016; Blummel, et al. 2015; Habersetzer, et al. 2017; Rollauer, et al. 2012). TatB also contacts TMH1 and TMH2 of TatC, indicating that TatB may be intercalated between two TatC protomers (Alcock, et al. 2016; Fröbel, et al. 2019). Intriguingly, although this glutamate residue at position 8 of TatB has been shown to be essential for stable binding between TatB and TatC (Alcock, et al. 2016), a site mutation at this position does not completely abolish TatB function (Zinecker, et al. 2020). These findings suggest that tight or stable binding between TatB and TatC may not be strictly required for the function of TatBC complexes.

1.4.2 Substrate binding on TatBC complexes

TatBC complexes are detected in several forms by BN-PAGE with the molecular weight ranges between 400 and 650kDa (Cline and Mori 2001; McDevitt, et al. 2006), while whether all these forms are capable of binding substrates is still unclear. Thus, 'TatBC complex' or 'TatBC receptor' are used in the context to generally refer to functional TatBC complexes.

It is widely accepted that substrate proteins ultimately interact with TatBC complex, where their signal peptides (SPs) are recognized and bound (Berghöfer and Klösgen 1999; Gé and Cline 2007; Mori, et al. 2001), although the precise initial binding location of the SP remains under debate (see Section 1.3.3). The initially contact between Tat substrates and TatBC receptor is weak and reversible (Gé and Cline 2007; Whitaker, et al. 2012). Subsequently, TatBC complex mediates a more stable and stronger substrate–receptor connection. This process has been suggested to involve the conserved RR motif in the SP (Blummel, et al. 2015; Gé and Cline 2007; McDevitt, et al. 2006). However, since substrate binding can still occur in its absence albeit no active protein transport occurs (Kreutzenbeck, et al. 2007; McDevitt, et al. 2006), the RR motif likely contributes more to the initiation of translocation than to substrate binding. Moreover, mutations in TatC and in the N-terminus of TatB can suppress the transport defect caused by RR mutations (Kreutzenbeck, et al. 2007; Lausberg, et al. 2012; Strauch and Georgiou 2007), indicating that other regions in TatBC complex surrounded the RR motif can partially compensate for its loss. Altogether, these findings suggest that the RR motif plays an important, but not indispensable, role in SP recognition and the initiation of Tat-dependent transport. The exact mechanism of SP binding and recognition needs further investigation.

The proposed binding domains of TatBC complex for the SP involve two distinct regions (Lausberg, et al. 2012; Rollauer, et al. 2012; Zoufaly, et al. 2012). The first region includes the extreme N-terminus and the 1st cytosolic loop of TatC, which are located on one side of TatC and near cytosolic surface (Fig.1.3A, left shadow). The second region comprises the N-terminal part of TatB and TMH5 of TatC, which are located on the opposite side of TatC and in the central of the membrane (Fig.1.3A, right shadow). Given the spatial separation of these regions, it has been proposed that a SP may bind on two adjacent TatC protomers (Aldridge, et al. 2014; Ma and Cline 2010). However, other studies suggest that the SP only binds on one TatC protomer (Ramasamy, et al. 2013; Tarry, et al. 2009). So far, the exact

binding site of SP within the TatBC complex requires further investigation.

After proper binding, the SP is inserted into the TatBC receptor in a hairpin-like structure (Gé and Cline 2007; Hamsanathan, et al. 2017; Ulfig and Freudl 2018). TatC presumably mediates this subsequent insertion of SP and the extreme N-terminal region of the mature protein into the receptor complex (Blümmel, et al. 2017; Fröbel, et al. 2012).This deep binding of SP is driven by proton gradients (∆pH) across biological membranes, while the initial binding of SP is independent of ∆pH (Gé and Cline 2007; Musser and Theg 2000; Whitaker, et al. 2012). Furthermore, SP remains bound to the receptor until translocation is completed, after which it is released by proteolytic cleavage (Fincher, et al. 1998).

During SP binding, TatBC receptor also possesses a way to discriminate the correct SP, as inactive SP can still bind to TatBC complex but fail to trigger a proper Tat translocation (Kreutzenbeck, et al. 2007; McDevitt, et al. 2006). TatB may play a crucial role in this discrimination process. Unlike TatC, whose interaction with SP is primarily focused around the RR motif, TatB engages more extensively with SP: TatB contacts nearly the entire length of SP (Alami, et al. 2003; Gérard and Cline 2006; Maurer, et al. 2010; Ulfig, et al. 2017). TatB also shows its importance in substrate recognition (Fröbel, et al. 2019). Therefore, this extensive interaction between TatB and SP may play an essential role in substrates, or SP, recognition.

In addition to this SP contact, the unstructured C-terminal region of TatB also shows strong interaction with the surface of folded Tat substrates before the translocation occurs (Fröbel, et al. 2012; Kreutzenbeck, et al. 2007; Maurer, et al. 2010). NMR study has revealed high flexibility in this unstructured C-terminal region (Zhang, et al. 2014), suggesting that, following the correct match between TatBC receptor and SP, the C-terminal region of TatB may bind to the substrate and subsequently assist its translocation.

The numbers of substrates that are able to bind with the TatBC complex still unclear. Since the TatBC complex is suggested to contain two to eight TatBC protomers (Alcock, et al. 2016; Blummel, et al. 2015; Tarry, et al. 2009), it is conceivable that a single complex can bind multiple substrates simultaneously. However, this is the subject of intense debate (Aldridge, et al. 2014; Celedon and Cline 2012; Wojnowska, et al. 2018).

1.4.3 Interaction of TatA with TatBC and substrate

Given the high similarity between TatA and TatB (Section 1.3.1.1), one might assume that TatA exhibits similar interaction patterns as TatB with other Tat components. Nevertheless, TatA and TatB display distinct interaction and function in Tat translocation. Absence of TatA leads to a completely loss in Tat transport (Greene, et al. 2007; Hauer, et al. 2013), while TatB is unable to functionally replace TatA in *E. coli* (Lee, et al. 2002). These results indicate the functional specificity of each protein. Moreover, as described above (Section 1.4.1 and 1.4.2), the interaction between TatB and TatC, as well as between TatBC and substrates, are relatively robust. In contrast, the interaction of TatA with other subunits or with substrates is much less well-defined. So far, no native structure or direct isolation of TatA-BC or TatA-substrate complexes has been reported. Thus, this lack of structural information makes the functional role and mechanistic involvement of TatA within Tat machinery particularly intriguing.

TatA was initially presumed to interact with TatC via TatB (Sargent, et al. 2001). However, subsequent studies have demonstrated that TatA can directly interact with TatC independently of TatB presence in the membrane (Alcock, et al. 2016; Fröbel, et al. 2011). TatC serves as a core scaffold for recruiting and organizing TatA within the translocase (Aldridge, et al. 2014; Bolhuis, et al. 2001; Cléon, et al. 2015). The primarily indication of TatA-TatC interaction is between the TMH of TatA and TMH5 of TatC (Aldridge, et al. 2014; Rollauer, et al. 2012).

Two conserved residues in *E. coli* TatA (Hicks, et al. 2003) have been identified as functionally critical for TatA-TatC interaction: a hydrophilic residue at position 8 (Q8) in the TMH (E10 in pea TatA), and a phenylalanine residue at position 39 in the APH (F41 in pea TatA). Mutations at these sites result in complete loss of Tat-dependent transport (Barrett and Robinson 2005; Dabney-Smith, et al. 2003; Hicks, et al. 2003). Interestingly, these TatA mutants are still able to associate with TatC, but appear to destabilize TatBC complexes, evidenced by their continued, albeit reduced, co-purification with TatB and TatC (Alcock, et al. 2016; Barrett and Robinson 2005). These findings may reflect a distinct mode of TatA interaction, compared to TatB interaction, to influence the functionality of Tat translocase.

The Q8 residue is located in N-terminal proximity of TatA TMH. This region has been shown substrate- and ΔpH-dependent interaction with TMH5 of TatC (Aldridge, et al. 2014; Fröbel, et al.

2011). Therefore, the loss of Tat transport activity observed by Q8 mutation may reflect a disruption in the substrate-induced interaction between TatA and TatC. On the other hand, the F39 residue, located within APH of TatA, is suggested to be crucial for proper oligomer assembly. Mutation at this position leads to the formation of aberrant TatA oligomers (Barrett and Robinson 2005) whereas Q8 is not essential for TatA oligomerization (Alcock, et al. 2016). These findings suggest that proper TatA oligomer assembly is critical for the functional integrity o Tat translocase. Notably, although Q8 is not required for TatA oligomerization, the TMH of TatA still contributes to this process (Fröbel, et al. 2011; Pettersson, et al. 2021). Together, these results indicate that different domains of TatA may play specialized roles in mediating Tat-dependent protein transport.

In addition, TatA has been shown to interact with TatB in the presence of TatC (Barrett and Robinson 2005; Bolhuis, et al. 2001; Mori and Cline 2002). In one study, TatA was copurified with TatB in a complex form under overexpression conditions, indicating a direct interaction between the two proteins (Sargent, et al. 2001). Moreover, The TMH of TatB is proposed to regulate the access of TatA into the complex (Blummel, et al. 2015; Habersetzer, et al. 2017; Huang and Palmer 2017), suggesting that TatB may modulate TatA recruitment and possibly interact with TatA during this process. Additionally, TatA is suggested to adopt an orientation similar to that of TatB along with TMH5 of TatC (Dabney-Smith, et al. 2003; Habersetzer, et al. 2017; Zoufaly, et al. 2012), placing TatA and TatB in close spatial proximity. Collectively, it is conceivable that TatA and TatB may interact with each other.

Furthermore, TatA also interacts with substrates, and this interaction depends on the proton motive force (PMF) across biological membranes and the presence of a functional SP of substrates (Alcock, et al. 2013; Blummel, et al. 2015). TatA undergoes an assembly-disassembly cycle in response to substrate presence, dynamically associating with and dissociating from the TatBC complex (Mori and Cline 2002; Rose, et al. 2013). Additionally, TatA has been suggested to interact directly with substrates independently of TatBC complex (Taubert, et al. 2015). The interaction may lead to the binding of the C-proximal APH of TatA to TatBC (Aldridge, et al. 2012; Hou, et al. 2018). Moreover, Evidence indicates that TatA may engage in two distinct modes of interaction with substrates. Taubert, et al. (2015) showed that mutations in surface-exposed residues of the substrate reduced the interaction between TatA and mature protein, without affecting its interaction with the SP. These findings suggest that TatA interacts with both mature domain and the SP, and that these interactions are functionally independent.

The region encompassing TMH5, loop L3, and TMH6 of TatC (Fig. 1.3A, right shadow) appears to function as a coalescence region for the interaction between TatA, TatB, TatC and SP of substrates (Alcock, et al. 2016; Blummel, et al. 2015; Rollauer, et al. 2012). TatA has also been suggested to interact with TMH4 of TatC (Aldridge, et al. 2014). Given that TMH4, TMH5 and TMH6 are spatially adjacent in the folded structure of TatC (Fig.1.3B), it is plausible that TatA dynamically associates within this region. Notably, TatA appears to interact with this region even in the absence of substrate stimulation, which is presumably caused by a certain dynamic conformational change of TatBC complexes (Aldridge, et al. 2014). Despite its essential role, TatA remains a poorly understood in Tat translocase, and its precise functional mechanisms require further investigation.

1.5 Objectives

The unique feature of Tat translocase lies in its ability to transport fully folded proteins of various shapes and sizes across cellular membranes without disrupting the membrane potential. Elucidating the underlying mechanism is therefore of considerable interest but remains a major challenge. A key obstacle is the transient nature of the translocation process, which makes it difficult to study the active state of the translocase. In particular, TatA precipitation only occurs in the presence of functional Tat substrates, therefore, in the active state. To date, the dynamic interplay among Tat subunits under native conditions remains poorly understood. In this study, we aim to investigate the roles of TatA and TatB - two members of the same protein family but with distinct functions- in the activity and stability of Tat translocase. For this purpose, four objectives were pursued in this work.

First, *in vitro* translation systems were evaluated for synthesizing TatB proteins used in the reconstitution of Tat transport in anti-TatB-treated thylakoids (Chapter 4.1). Secondly, to determine the effects of TatA and TatB on Tat-dependent protein transport, external TatA and TatB proteins were supplemented into anti-TatA-treated, anti-TatB-treated and untreated thylakoids. In particular, the combined effect of TatA and TatB was also assessed (Chapter 4.2). Since TatBC complex serves as the core unit in Tat pathway, thirdly, the influence of TatA and TatB on the stability of TatBC complex was examined (Chapter 4.3, Chapter 4.4). Finally, due to the essential role of PMF in Tat transport, the effect of PMF on the stability of TatBC complex was also examined (Chapter 4.5).

2 Materials

2.1 Chemicals

All chemicals, enzymes, and kits used in the present work were provided by well-known companies, including Carl Roth GmbH & Co. KG (Germany), QIAGEN GmbH (Germany), Sigma-Aldrich GmbH (Germany), Thermo Fisher Scientific (USA), NEB (USA), etc.

2.2 Size ladders

Type	Name	Manufacturer
DNA	GeneRuler™ 50 bp DNA Ladder	Thermo Fisher Scientific (USA)
DNA	1 kb plus DNA Ladder	Sigma-Aldrich (USA)
Protein (SDS-PAGE)	PageRuler™ Prestained Protein Ladder	Thermo Fisher Scientific (USA)
Protein (BN-PAGE)	High Molecular Weight Native Protein Marker	GE Healthcare (USA)

2.3 Enzymes

Name	Manufacturer
Restriction enzyme: NOT I, Xbal I, Hind III and etc.	Thermo Fisher Scientific (USA)
Thermolysin	Sigma-Aldrich (Germany)
T3-RNA-Polymerase	Thermo Fisher Scientific (USA)
T7-RNA-Polymerase	Thermo Fisher Scientific (USA)

2.4 Kits

2.4.1 Plasmid purification kits

Name	Manufacturer
QIAGEN® Plasmid Midi Kit	QIAGEN (Hilden)
Wizard® Plus Minipreps DNA purification System	Promega (Madison, WI, USA)

2.4.2 *in vitro* translation kits

Name	Manufacturer
Flexi® Rabbit Reticulocyte Lysate System (L4540)	Promega (Madison, WI, USA)
S30 T7 High-Yield Protein Expression System (L1110)	Promega (Madison, WI, USA)
Wheat Germ Extract (L4380)	Promega (Madison, WI, USA)

2.5 Primers

Those primers used for sequencing were obtained from MWG Biotech (Ebersberg).

Name	Sequence
M13 for	GGT TTT CCC AGT CAC GAC G
M13 rev	GGT TTT CCC AGT CAC GAC G
T7 prom	TAA TAC GAC TCA CTA TAG GG
T7 terminator	TAG TTA TTG CTC AGC GG

2.6 Plasmids

2.6.1 Vectors

Name	Origin
pBAT	Obtained from Dr. Bationa Bennewitz (AG Klösgen), described in Annweiler et al. (1991)
pBluescript KS+ (pBSC)	Obtained from Dr. Bationa Bennewitz (AG Klösgen), described in Clausmeyer et al. (1993)
pET30a	Obtained from Dr. Mario Jacob (AG Klösgen), produced by Novagen GmbH

2.6.2 Clones

Name	spieces	mutation	Vector	Promoter	Definition
mTatA	*Pisum sativum*	E72D	pBAT	T3	Mature part of TatA, the functional unit in Tat translocase
		83M	pBAT	T3	
		84stop	pBAT	T3	
		E72D	pET30a	T7	
preTatA	*Pisum sativum*	E127D	pBAT	T3	Precursor TatA, including transit peptide
		138M	pBAT	T3	
		139stop	pBAT	T3	
mTatB	*Pisum sativum*	V180M	pBAT	T3	Mature part of TatB, the functional unit in Tat translocase
		V180M	pET30a	T7	
preTatB	*Pisum sativum*	V245M	pBAT	T3	Precursor TatB, including transit peptide
TatAB	*P.sativum/ P.sativum*	V138M	pBAT	T3	Chimeric protein, N-terminus of mTatA until TMH + C-terminus of mTatB starting from Hinge-region
		V138M	pET30a	T7	
TatBA	*P.sativum/ P.sativum*	64M	pBAT	T3	Chimeric protein, N-terminus of mTatB until TMH + C-terminus of mTatA starting from Hinge-region
		65stop	pBAT	T3	
		65stop	pET30a	T7	
OEC16	*Spinacia oleracea*		pBSC	T7	Precusor form of 16kDa subunit of Oxygen Evolving Complexes
16/23	*S.oleracea/ S.oleracea*		pBSC	T7	Chimeric protein, OEC16-transit peptide + OEC23-mature part

2.7 Bacteria

Strain	Genotype	Source
TOP10	F- *mcrA* Δ(*mrr-hsdRMS-mcrBC*) ϕ80*lacZ*Δ*M15* Δ*lacX74 nupG recA1 araD139* Δ(ara-leu)7697 *galE15 galK16 rpsL*(*Str*$_R$) *endA1* λ-	Invitrogen (Carlsbad, USA)
DH5α	F– *endA1 glnV44 thi-1 recA1 relA1 gyrA96 deoR nupG purB20* ϕ80d*lacZ*ΔM15 Δ(*lacZYA-argF*)U169, hsdR17($r_{K-}m_{K+}$), λ–	Invitrogen (Carlsbad, USA)
BL21 (DE3)	F– *ompT gal dcm lon hsdS*$_B$*(*r_{B-} m_{B-}*)* λ(DE3 [*lacI lacUV5-T7 gene 1 ind1 sam7 nin5*])	Novagen (Darmstadt)

2.8 Antibiotics and inhibitors

Name	Manufacturer
Kanamycin	Carl Roth
Ampicillin	Carl Roth
Gramicidin	Sigma-Aldrich
RiboLock™ RNase-Inhibitor	Thermo Fisher Scientific

2.9 Nucleotides and amino acids

Name	Manufacturer
RNA *Cap Structure Analog*	New England Biolabs
^{35}S-Methionin	PerkinElmer (Waltham, MA, USA)
Amino Acid Mixture Minus Methionine	Promega

2.10 Proteins used

Name	Organism	Molecular weight (Mw)	
		precusor	mature
TatA	*Pisum sativum*	14.8kDa	8.9 kDa
atTatA	*Arabidopsis thaliana*	15.7 kDa	9.3 kDa
atTatA-E10C	*Arabidopsis thaliana*	15.7 kDa	9.3 kDa
ecoTatA	*E.coli*	——	9.6 kDa
TatB	*Pisum sativum*	28.4 kDa	19.1 kDa
16/16	*S.oleracea*	24.9kDa	16.5kDa
16/23	*S.oleracea*	28.5KDa	20.2kDa

2.11 Protein purification

2.11.1 Affinity chromatography

Name	Charactertisitcs	Manufactuer
Ni Sepharose Fast Flow	Ni_2^+-NTA-Sepharose	GE Healthcare (German)
Econo-PacR Cromatography Columns (20 ml)	Gravity column loaded with 5 ml of Ni_2^+-NTA-Sepharose	Bio-Rad (USA)
EC 125/4 Nucleosil 500-5 C3 PPN	HPLC column	Macherey-Nagel (German)

2.11.2 Dialysis tubes

Name	Charactertisitcs	Manufactuer
ZelluTrans 1.0V	MWCO 1000	Roth (Karlsruhe)
MEMBRA-CELR dialysis tubing	MWCO 3500	Serva (Heidelberg)

2.11.3 RP-HPLC

Name	Charactertisitcs	Manufactuer
Chromaster HPLC-System	5430 Diode Array 5310 Column Oven 5260 Auto Sampler (Foxy 18 mm) 5110 Pump	VWR (German)
HPLC control program	EZChrom *Elite*	Agilent Technologies (German)
PR-HPLC column	EC 125/4 Nucleosil 500-5 C3 PPN	Macherey-Nagel (German)

2.12 Antibodies

Antibodies	Characteristics	Dilution for use	Source
anti-TatB	specific for stromal domain of *P.sativum* TatB; developed from rabbit, by antigen-specifically purification	1:1000	Dr. Mario Jacob (AG Klösgen)
anti-TatC	specific for N-terminal of *P.sativum* TatC; developed from rabbit, by antigen-specifically purification	1:1000	Dr. Mario Jacob (AG Klösgen)
anti-TatA	specific for stromal domain of *P.sativum* TatA; developed from rabbit, by antigen-specifically purification	1:500	Dr. Mario Jacob (AG Klösgen)
anti-rabbit-HPR (antiserum)	specific for Fc part of rabbit antibodies conjugated with horseradish peroxidase (HRP)	1:1000	Sigma-Aldrich (St. Louis, USA)

2.13 Plant materials

Pisum sativum (var. *Feltham First*) was grown under long-day conditions at 20–22 ℃ on coco-fiber-containing soil. For chloroplast and thylakoid preparation, leaves were harvested from 7- 8 days old pea seedlings.

3 Methods

3.1 Protein preparation

3.1.1 *In vitro* synthesis of proteins

3.1.1.1 Plasmid preparation

Electrocompetent *E. coli* cells (strain DH5α or TOP10) were transformed with 50–200 ng of plasmid DNA (maximum volume: 2µl). The DNA was gently mixed with 40µl of competent cells and transferred into a pre-cold electroporation cuvette (Carl Roth, Karlsruhe). Electroporation was performed using the *E. coli* Pulser™ electroporator (Bio-Rad, USA) at 1.8 kV. Immediately after the pulse, 1ml LB medium was added to the cuvette and mixed it gently with the *E. coli* culture by pipetting. The entire volume was transferred to the Epi tube which used before to store the electrocompetent *E. coli* cells. The cell culture was subsequently incubated on a rotator for 45min at 37℃ to allow recovery and expression of the targeted gene. The speed of rotation should not be too quick, gently mixing. Following recovery, 10-100µl of the transformed culture was plated on LB-agar plates containing the appropriate antibiotic and incubated overnight at 37℃. Next day, a single colony was picked up from the agar-plate and inoculated into 50ml LB medium at 37℃, overnight. Plasmid DNA was subsequently purified from overnight cultures using QIAGEN plasmid Midi Kit (QIAGEN, Germany) according to the manufacturer's protocol. The purified DNA was dissolved in 1xTE buffer and stored at −20 ℃.

LB medium	1% (w/v)	Peptone from Casein
	0.5% (w/v)	Yeast Extract
	1% (w/v)	NaCl
	1.5% (w/v)	Agar
Antibiotics	100µg/mL	Ampicillin
	50µg/mL	Kanamycin
10xTE buffer	100mM	Tris
	1mM	EDTA
		pH 8.0 adjust by HCl

3.1.1.2 Plasmid precipitation

If the concentration of purified DNA was insufficient for subsequent linearization, the plasmid was precipitated by ethanol to concentrate the DNA. For this purpose, the plasmid solution was mixed with 1/20 Vol. of 4M NaCl and 2.5 Vol. of 100% ethanol (store in -20℃). The mixture incubated either overnight at -20℃ or for 30 min in -80℃ for precipitation. Subsequently, the DNA was pelleted by centrifugation for 30min at 13300rpm, 4℃. The pellet was then washed once with 70% Ethanol and centrifuged again for 5min at 13300rpm, 4℃. Then the supernatant was discarded and the pellet was air-dried at room temperature (RT) for at least 10min. Finally, the DNA pellet was resuspended in 1xTE buffer to a suitable concentration for further use.

3.1.1.3 Linearization of plasmid

Circular plasmids prepared as described above were linearized using appropriate restriction enzymes before *in vitro* transcription process, as linear DNA templates generally are more efficient for transcription. After complete digestion with the selected enzyme, the reaction was stopped by adding 1/20 Vol. of 0.5M EDTA. Then the linear DNA was purified by extraction with phenol-chloroform-isoamyl alcohol (25:24:1, v/v/v)(Sambrook, et al. 1989), followed by ethanol precipitation. For precipitation, 2.5 Vol. of 100% ethanol (store in -20℃) were added to the aqueous phase, and the mixture was incubated either overnight at −20 ℃ or for 30 min at −80 ℃. The precipitated DNA was then collected by centrifugation as described in Section 3.1.1.2. At end, the DNA pellet was resuspended in 1xTE buffer to a concentration approx. 1µg/µl.

Linerization	
Plasmid-DNA (20µg)	X µl
Buffer (10x)	20µl
Enzyme (10µ/µl)	2µl
DEPC water	Fill up to 200µl

3.1.1.4 *In vitro* transcription and translation

The linearized and purified DNA was used as a template for *in vitro* transcription and subsequent in *in*

vitro translation, as described below. To enable radioactive labeling of the newly synthesized polypeptides, the translation reaction was conducted with the addition of ^{35}S-methionine.

For *in vitro* transcription, the linearized DNA was mixed with transcription components as shown below. The reaction mixture was first incubated for 1h at 37℃. After that, 1µl of 25x GTP was added, and incubation continued for an additional 30min at 37℃. Transcribed RNA was subsequently precipitated by adding 1/10 Vol. of 3M NaCl (pH 5.2) and 2.5 Vol. of 100% ethanol (store in -20℃). The mixture was stored at −20 ℃ for RNA precipitation.

***In vitro* transcription**	
5 x Buffer	5µl
5x NTPs, red. GTP	5µl
RNA-Cap	1.2µl
0,1 M DTT	2.5µl
Plasmid-DNA (linearisiert)	Vol. entspr. 2µg DNA
RNase-Inhibitor	0.5µl
Polymerase	1µl
DEPC water	fill up to 25µl

For *in vitro* translation, the corresponding volume (as shown below for each translation kit) of precipitated RNA obtained by *in vitro* transcription was first pelleted by centrifugation at 13000 rpm, 4℃ for at least 30min. After centrifugation, the supernatant was carefully removed, and the pellet was air-dried. The dried RNA pellet was then resuspended in the *in vitro* translation mixture, as shown blow:

***In vitro* translation**	
Flexi® *Rabbit Reticulocyte Lysate System* (Promega)	
Transcription	60ul
DEPC water	36µl
AA Mix, minus Met	4µl
0,1 M DTT	4µl
2,5 M KCl	2µl
Reticulocytes	50µl
^{35}S-Met	4µl
Total volume	100µl
The reaction was conducted at 30°C for 90min	
***Wheat Germ* Extract *System* (Promega)**	
Transcription	10ul
DEPC water	4.65µl
AA Mix, minus Met	1µl
Wheat germ extract	6.25µl
^{35}S-Met	0.6µl
Total volume	12.5µl
The reaction was conducted at 25°C for 2h	
S30 T7 High-Yield Protein Expression *System* (Promega)	
Circular DNA (>0.5µg/µl)	Vol. 1µg DNA
S30 Premix Plus	20µl
S30 T7-Extrakt	18µl
DEPC water	Add to 50µl
^{35}S-Met	2µl
Total volume	50µl
The reaction was conducted at 30°C for 1h	

3.1.2 Heterologous expression and purification of Tat proteins

3.1.2.1 Heterologous expression in *E. coli*

Electrocompetent *E. coli* cells (strain BL21) were transformed with 50–200 ng of plasmid DNA (with pET30a vector) (details of electroporation procedure, see Section 3.1.1.1). A single colony was picked up from the agar-plate and inoculated into 5ml of M9 medium containing 50µg/ml kanamycin. Incubation was conducted for at least 16h at 37°C with shaking at 200rpm. Next day, the overnight culture was used to inoculate a 500ml main culture (1:100) in fresh M9 medium containing 50µg/ml

kanamycin. This 500ml-culture was incubated at 37℃ with shaking at 200rpm until optical density at 600nm (OD_{600}) reached approximately 1.0. Protein expression was then induced by the addition of 1M IPTG (final concentration: 1mM), followed by incubation overnight at 28℃ with same shaking speed at 200rpm. For harvest, the overnight culture was pelleted for 20min at 4000rpm, 4℃ using a TX-750 swing-bucket rotor (Heraeus Multifuge X3R, Thermo Fisher Scientific, USA). The supernatant was discarded and the pellet was resuspended in 25ml of 1xPBS buffer. The suspension was either stored at -20℃ or directly disrupted by three cycles of French press (1000 psi) with the addition of 200mM PMSF (dissolve in 100% ethanol, final concentration: 1mM).

5xM9-salt	239mM	Na_2HPO_4
	110mM	KH_2PO_4
	42.8mM	NaCl
	93.5mM	NH_4Cl
M9 medium	1x	M9-salt
	20.6mM	$MgSO_4$
	0.41% (w/v)	Glucose
	1mM	$CaCl_2$
	1% (v/v)	LB Medium
10xPBS	750 mM	NaCl
	30 mM	KCl
	45 mM	Na_2HPO_4
	15 mM	KH_2PO_4

3.1.2.2 Purification of His-tag-fusion proteins

Before starting protein purification, 25ml of the cell suspension obtained by French press was mixed with 75ml of Gua-HCl binding buffer. This mixture was then incubated with gently stirring at 4℃ for at least 1h to ensure fully protein binding. After incubation, the suspension was subjected to ultracentrifugation at 28000rpm for 1h at 4℃ using a SW32-Ti swing rotor (L8-50M/E Ultracentrifuge, Beckmann, Krefeld). In parallel, gravity flow columns (one column per 25ml of initial cell suspension) were prepared and pre-incubated with Gua-HCl binding buffer. Each column contained 5ml of Ni-affinity resin matrix (GE Healthcare, München). Following ultracentrifugation, the clear supernatant was applied to the Ni-affinity columns at 4℃ at a flow rate of minimal 40µl/min. Once the entire lysate

has passed through the columns, at least 25ml of Gua-HCl binding buffer was used for washing columns. The flow-through (*washing fraction*) was collected. Bound proteins were eluted by sequentially using Gua-HCl elution buffer: 3ml (*fraction E1*), 9ml (*fraction E2*), and 6ml (*fraction E3*). From each fraction, a 50µl aliquot was taken and mixed with 950µl of 80% acetone, and then was incubation for at least 2h at -20℃ for protein precipitation. The precipitated proteins were pelleted by centrifugation for 30min at 13000rpm, 4℃ (Heraeus Biofuge Fresco 17, Thermo Fisher). Then pellets were resuspended in 50µl of 1xLaemmli sample buffer and subsequently analyzed by SDS-PAGE (see Section 3.2.1).

Gua-HCl binding buffer	20 mM	Hepes
	500 mM	NaCl
	20 mM	Imidazole
	6M	GuaHCl
		pH 7.5, adjust by HCl
Gua-HCl elution buffer	20 mM	Hepes
	500 mM	NaCl
	500 mM	Imidazole
	6M	GuaHCl
		pH 7.5, adjust by HCl

3.1.2.3 Cleavage of the N-terminal His-tag

Elusion fractions containing His-tagged fusion proteins were first freeze-dried in -80℃ for at least 2 days. The resulting freeze-dried pellets were resuspended with cyanogen bromide (present in acetonitrile, stored at -20℃, dissolve in RT for 30 min prior to use) and 85% formic acid at a volume ratio of 1:5 for cleavage. The cleavage reaction was conducted at 25℃ with shaking at 500rpm for 5h. The reaction was terminated by adding 15ml of distilled water. To neutralize the acid in the reaction mixtures, 1.5ml of 10M NaOH was added to each sample. Then the mixtures were frozen at -80℃ for at least 3h and subsequently lyophilized until completely dry. The resulting pellets, containing the cleaved protein and sodium formate salts, were dissolved in distilled water containing 1% SDS, and then dialyzed at 4℃ against at least 1L of distilled water with 1%SDS to remove residual salts and small molecular weight by-products (MEMBRA-CELR dialysis tubing, MWCO 3500). The dialyzed samples were then checked by SDS-PAGE (see Section 3.2.1) to assess cleavage efficiency. If the cleavage was not complete, the sample was then separated by 12.5% SDS-PAGE gel (see Section 3.1.2.4).

3.1.2.4 Separation of complete and incomplete cleavage proteins

To separate proteins with or without the N-terminal His-tag (see Section 3.1.2.3), the dialyzed sample was mixed with Laemmli buffer to a final concentration of 1x and loaded on a preparative gel. A preparative midi SDS-gel containing 12.5% acrylamide with a thickness of 1.5 mm was used for protein separation (see Section 3.2.1). The stacking gel was prepared without sample wells to allow loading of a large sample volume. A total of 5mL of sample in 1xLaemmli buffer was loaded directly onto the gel. Electrophoresis was performed at 70V overnight at RT. The preparation of SDS-PAGE gels and Laemmli buffer followed the protocol described in Section 3.2.1.

Following protein separation by preparative SDS-PAGE, the gel was stained using the zinc-imidazole method as described by Castellanos - Serra, et al. (1999) (see Section 3.3.3). The gel band corresponding to the correctly cleaved target protein was excised and finely minced into small pieces using a scalpel. The gel pieces were transferred into a 50ml Falcon tube, and 1xSDS running buffer with an additional 1%SDS was added for protein elusion. The elution process was performed at RT overnight. This elution step was repeated three times. Each elution fraction was collected on the following day, and samples taken from individual fraction were loaded to a mini-SDS-gel for checking (see Section 3.2.1).

3.1.2.5 Reversed-Phase High-Performance Liquid Chromatography (RP-HPLC)

Proteins obtained by SDS elution (see Section 3.1.2.4) were further purified using RP-HPLC (see Materials 2.11.3) with an acetonitrile-water gradient at a constant flow rate of 1ml/min. Prior to sample loading, the HPLC tubing and pump were rinsed with distilled water to remove any residual contaminants. The PR-HPLC columns were equilibrated to the appropriate starting conditions by loading corresponding buffer used for protein dissolving. Two solvent systems were used for gradient elution: Solvents A - consisted of 10% acetonitrile in distilled water and 0.05% trifluoroacetic acid (TFA); Solvents B - consisted of 100% acetonitrile and 0.05% TFA. The specific gradient program used for protein purification is described as follows:

Time	Solvent A	Solvent B
0min	90%	10%
5min	80%	20%
10min	60%	40%
15min	50%	50%
20min	40%	60%
25min	10%	90%
30min	90%	10%

3.1.2.6 Dialysis of purified Tat proteins

Proteins obtained from RP-HPLC purification in acetonitrile/water were transferred into a dialysis tube (ZelluTrans 1.0 V, MWCO 1kDa) and dialyzed against 1L of HM buffer with gentle stirring at 4℃ for at least 16h prior to use in *in thylakoidal* reconstitution experiments (see Section 3.4.4.2). To ensure sufficient protein concentration for quantification by Bradford method (Bradford 1976) after dialysis, only RP-HPLC elution fractions with high protein content (A_{220}≥500 mAU, as detected during RP-HPLC) were selected for dialysis. To avoid excessive increase in final volume and to minimize sample dilution, the dialysis tube was cut to an appropriate length corresponding to the sample volume.

3.1.2.7 Masurement of Protein concentration

The concentration of proteins containing aromatic amino acids like tryptophan, tyrosine, and phenylalanine, was determined by UV absorption spectroscopy at 280nm (Aitken and Learmonth 1996). These amino acids have specific absorbance peaks in the UV spectrum, with tryptophan absorbing most strongly around 280 nm. The peptide bonds in proteins also absorb UV light, particularly in the far UV region (around 200 nm). This property allows for the use of UV absorption spectroscopy to quantify protein concentration. For example, the concentration of TatB can be measured by this method.

For other proteins that do not contain aromatic amino acids, such as TatA, the concentration of them was determined using the Bradford protein assay (Bradford, 1976). To remove aggregates from protein solutions, the dialyzed RP-HPLC elution fractions were centrifuged at 13000 rpm for 5 min at RT, and the resulting supernatants were then carefully transferred to new reaction tubes. The proteins

quantification was performed in triplicate using Bradford reagent (ROTI®Quant; Roth, Karlsruhe) and absorbance was measured at 595nm (A_{595nm}). Protein concentrations were calculated against a standard curve generated with bovine serum albumin (BSA).

$$protein\ (ug) = \frac{A_{595nm}}{0.0393}$$

3.2 Polyacrylamide gels

3.2.1 Sodium Dodecyl sulfate–Polyacrylamide Gel Electrophoresis（SDS-PAGE）

SDS-PAGE was used for the electrophoretic separation of proteins (Laemmli 1970). Protein samples were mixed with Laemmli buffer to a final concentration 1x and denatured by heating at 95℃ for 3min before loading to the gel. SDS binds uniformly to the denatured proteins, resulting in a constant charge-to-mass ratio. Electrophoresis was conducted using 1xSDS running buffer at both the cathode and anode with an electric field at 80-100V. Proteins were separated by the molecular sieving effect of the polyacrylamide gel matrix according to their molecular weight. The compositions of the required buffers and the SDS-PA-gels are listed as below.

Laemmli buffer (4x)	1% (w/v)	SDS
	8.7 % (v/v)	Glycern
	300mM	TRIS/HCl (pH 6.8)
	0.02%(w/v)	Bromopheol Blue
	0.08 % (v/v)	Mercaptoethanol
SDS running buffer (10x)	250 mM	TRIS/HCl (pH 8.3)
	1920 mM	Glycin
	1 % (w/v)	SDS

Midi-SDS-PA-gradient gel (10%-17.5% Acrylamide) -- 1mm

Composition	Seperating gel 10%(w/v) AA	Seperating gel 17.5%(w/v) AA	Stacking gel 5%(w/v) AA
H_2O	6.53ml	---	6.95ml
2M Tris/HCl (pH 8.8)	3ml	3ml	---
1M Tris/HCl (pH 6.8)	---	---	1.25ml
80% Saccharose	0.93ml	3.47ml	---
30% Acrylamide	5.3ml	9.3ml	1.67ml
10% SDS	160µl	160µl	100µl
10% APS	110µl	110µl	130µl
TEMED	20µl	20µl	22µl
Total volume	16ml	16ml	10ml

Midi-SDS-PA-gel (12.5% Acrylamide) -- 1.5mm

Composition	Seperating gel 12.5%(w/v) AA	Stacking gel 5%(w/v) AA
H_2O	18.5ml	13.9ml
2M Tris/HCl (pH 8.8)	9ml	---
1M Tris/HCl (pH 6.8)	---	2.5ml
30% Acrylamide	20ml	3.34ml
10% SDS	480µl	200µl
10% APS	200µl	260µl
TEMED	40µl	40µl
Total volume	48.2ml	20ml

4x Mini-SDS-PA-gel (15% Acrylamide)

Composition	Seperating gel 15%(w/v) AA	Stacking gel 5%(w/v) AA
H_2O	8ml	10.8ml
2M Tris/HCl (pH 8.8)	6ml	---
1M Tris/HCl (pH 6.8)	---	1.5ml
30% Acrylamid	15ml	2.4ml
10% SDS	300µl	150µl
10% APS	115µl	60µl
TEMED	30µl	20µl
Total volume	29.4ml	14.9ml

3.2.2 Blue Native Polyacrylamide Gel Electrophoresis (BN-PAGE)

BN-PAGE was used for electrophoretic separation of solubilized protein complexes (Schagger, et al. 1994). Using Coomassie Brilliant Blue dye (SERVA, Heidelberg) is able to impart an overall negative charge of protein complexes, allowing the separation to be based mainly on the size (mass + shape) of the whole complexes. Due to the integrity of protein complexes, the molecular size (mass + shape) of them is not equal to the sum of molecular weight of individual proteins. Electrophoresis was performed overnight at a voltage of 100V using anode buffer and the Coomassie-containing cathode buffer I (as shown below). Next day, cathode buffer I was replaced with cathode buffer II (without Coomassie), and electrophoresis was continued at a voltage of 400V for approximately 3h.

Cathode buffer I	15mM	Bis-Tris
	50mM	Tricin
	0.01%(w/v)	Coomassie Brilliant Blue G-250
Cathode buffer II	15mM	Bis-Tris
	50mM	Tricin
Anode buffe	50mM	Bis-Tris

Midi-BN-PA-gradient gel (10%-17.5% Acrylamide)

Composition	**Seperating gel 5%(w/v) AA**	**Seperating gel 13.5%(w/v) AA**	**Stacking gel 4.5%(w/v) AA**
H_2O	6.6ml	1.4ml	4.9ml
0.5M BisTris pH7.0	1.6ml	1.6ml	1.0ml
30% Acrylamide	2.7ml	7.2ml	1.5ml
2M ε-aminocaproic acid	4.0ml	4.0ml	2.5ml
87% Glycerin	1.0ml	1.7ml	----
10% APS	70µl	70µl	90µl
TEMED	7µl	7µl	9µl
Total volume	16ml	16ml	10ml

3.3 Visualization of proteins in polyacrylamide gels

3.3.1 Autoradiography

To visualize ^{35}S-labeled proteins or complexes, samples were loaded in an SDS-PA gel or a BN-PA gel, respectively. After electrophoresis, gels were incubated in fixation solution for 30min, and then dried in vacuum at 80°C for 2.45h (Midi-gel) or 45min (Mini-gel). The dried gels were exposed to Phospho-imager screens. The radiolabeled proteins were analyzed using a Fujifilm scanner FLA-3000 (Fujifilm, Düsseldorf), BASReader (version 3.14) and AIDA Image Analyzer (versions 3.25, Raytest, Straubenhardt). Quantification of signal intensities was performed using the AIDA Image Analyzer (version 5.0).

3.3.2 Coomassie-Colloidal staining

According to Neuhoff, et al. (1985), a high sensitive protein staining with clear background on polyacrylamide gels was developed. The gel staining with Coomassie-Colloidal was incubated in fixation solution for 30 min with slow shaking, and then incubated in staining solution for overnight. Water was used for destaining.

Fixation buffer	40%(v/v)	Methanol
	10%(v/v)	Acetic Acid
Solution A	2%(w/v)	orthophosphoric acid
	10%(w/v)	Ammonium sulfate
Solution B	5%(w/v)	Coomassie Brilliant Blue G-250
Staining Buffer	20%(v/v)	Methanol
	78.4%(v/v)	Solution A
	1.6%(v/v)	Solution B

3.3.3 Zinc-Imidazole staining

In order to conduct SDS-elution of proteins from SDS-PA gels, a reversible Zinc-Imidazole staining was performed (Castellanos-Serra, et al. 1999). The gel was incubated for 30min in imidazole solution followed by washing with water for 30s. Then gel was transferred in zinc-sulfate solution until the desired staining was achieved. The reaction was stopped with water washing.

Imidazole solution	200mM	Imidazole
	0.1%(w/v)	SDS
Zinc-sulfate solution	200mM	$ZnSO_4 \bullet 7H_20$

3.3.4 Western Blot

3.3.4.1 Protein transfer - blotting

After electrophoresis, both BN-PA gels and SDS-PA gels were equilibrated in a denaturing solution prior to blotting procedure. In the case of SDS-PA gels, the gels were incubated with an SDS running buffer; whereas for BN-PA gels, it is critical that they are not incubated with an SDS running buffer, as it will result in a failure of peaTatC detection. Instead, BN-PA gels were incubated with the cathode buffer as shown below.

The electrophoretic transfer of proteins to Roti-PVDF 2.0 membrane whith pore size 0.2µm (Carl Roth, Karlsruhe) was carried out by semi-dry blotting. For this purpose, the membrane and six pieces of filter paper (Gel Blotting Paper Whatman 3MM, Carl Roth, Karlsruhe) were cut approximately to the same size of the gel. In the case of BN-PA gels blotting, the blot was set up as follows: after electrophoresis, the gel was incubated for 15 min in 200ml of cathode buffer. The PVDF membrane was wetted with methanol and then briefly washed with water. It was then equilibrated for 5min with anode buffer II. To set up the blot (cathode plate below, anode above), three pieces of filter paper soaked in cathode buffer are placed as the first layer. Then the gel was placed on top, and then followed by the membrane on top. The final layers were a layer of filter paper soaked in anode buffer II, followed by two layers of filter paper soaked in anode buffer I. Air bubbles must be removed. After each step, the stack was unrolled using a Falcon tube to expel air bubbles. When constructing a blot with BN-PA gels, it is important to note that they are very soft and fragile, especially in the upper region of the gel. In the case of SDS-PA gels blotting, the set-up was simpler: all six pieces of filter paper were soaked in SDS-running buffer and the order was same as mentioned above – three layers of filter paper, the gel placed on top, then the membrane, at end three layers of filter paper. The transfer time and current for blotting are shown as below:

	SDS-PA gels	BN-PA gels	
Anode buffer I	SDS-running buffer	300 mM	Tris
Anode buffer II	---	25mM	Tris
Cathode buffer	SDS-running buffer	25mM	Tris
		40 mM	ε-Aminocaproic acid
Current	1.5mA pre cm^2	1.2mA pre cm^2	
Time	2h	1h	

3.3.4.2 Immunodetection of proteins

Specific detection of proteins was performed using two-step antibody treatment and enhanced chemiluminescence (ECL) detection. After protein transfer, the PVDF membrane was briefly washed in water. Then the membrane was incubated with washing solution I for 2h. For BN-PA gels, 0.09% (v/v) H_2O_2 was also added to the solution in this step to eliminate nonspecific signals of the thylakoid cytochrome b_6f complex. Followed by the first incubation, another 2h incubation was conducted with fresh washing solution I added with the desired primary antibody at the appropriate dilution (see Materials, Section 2.12). After that, four time washing steps of 5min for each were performed using washing solution I. After washing, the membrane was incubated with the secondary antibody at the appropriate dilution in washing solution I for 1h. Subsequently, four time washing steps of 10 min each were performed with washing solution II. Since the secondary antibody was a non-affinity purified antiserum, the relatively long time of the final wash steps was important for reducing the nonspecific background.

10xPBS	750 mM	NaCl
	30 mM	KCl
	45 mM	Na_2HPO_4
	15 mM	KH_2PO_4
washing solution I	1x	PBS
	0.5%(v/v)	Tween 20
	5%(w/v)	Milk powder
washing solution II	1x	PBS
	0.5%(v/v)	Tween 20

For ECL detection, the membrane was incubated with ECL solution for 1 minute and then transferred to an open plastic bag. Detection was performed by a digital camera setup (FUSION FX, Vilber, Collégien, France) using the associated software. The exposure time was chosen to allow the signals of interest were clear enough but not saturated. For detection with α-TatC antibody, it ranged from 2-5 minutes; with α-TatB antibody, 1-2 minutes were usually sufficient; with α-TatA antibody, it normally needs 10-15min.

ECL solution	50mM	Tris/HCl, pH 8.3
	1.25mM	Luminol
	198µM	Coumaric acid
	2.7mM	H_2O_2

3.4 Methods for working with plant materials

3.4.1 Isolation of chloroplasts from pea plants

In the isolation of intact chloroplasts, all steps were performed in a cold room at 4℃ or on ice. Centrifuge rotors and adaptors were pre-cooled at 4℃. Pipettes with cut-off tips were used in the whole process.

First, 7-day-old pea seedlings (80-100 g) were harvested and blended in 500ml of SIM buffer in a Waring blender (5 x 2s). The smooth-like mixture was then filtered through two layers of Millipore Miracloth (Merck, Darmstadt) into 2x250ml centrifuge bottles. The filtrate was centrifuged for 5min at 2000g, 4℃. All centrifugation steps were performed using an Avanti J-25 centrifuge (Backmann Coulter, Krefeld) (rotors: JA 14 rotor, JS-13.1 swing out rotor). The pellet was then carefully resuspended with a brush in 5ml of 1xSRM buffer. Then the suspension was layered onto a percoll gradient in a Corex tube (percoll gradient from bottom to top: 4 mL 80%, 10 mL 35%), followed by 7 minutes of centrifugation at 2000g, 4°C. After centrifugation, the intact chloroplast was presented in the layer in between of 35% and 80% percoll. Thus, the top layer was removed and discarded by a glass pipette. Using a pipette with cut-off tips to take out the intact chloroplast and put it into a new ice-cold Corex tube filled with 1xSRM buffer. Then the chloroplast-containing solution was centrifugated for 2min at 1000g, 4℃. The pellet was then washed twice with 1xSRM buffer at same speed. After washing steps, the sedimented chloroplasts

were finally resuspended in 1ml of 1xSRM buffer and were transferred into an Epi tube (1.5ml) which was wrapped with aluminum foil to protect the chloroplasts from light.

SIM buffer	350mM	Saccharose
	25mM	HEPES
	2mM	EDTA
		pH 7.6 by KOH
5xSRM buffer	1650mM	Sorbitol
	250mM	HEPES/KOH
		pH 8.0 by KOH
35% percoll	35%(v/v)	Percoll
	1x	SRM
80% percoll	80%(v/v)	Percoll
	1x	SRM

3.4.2 Determination of chlorophyll concentration

To determine the chlorophyll concentration, three repeats were prepared with 990µl of 80% acetone and 10µl of chloroplast suspension, mixing completely by vortex. Then samples were incubated for 5min at RT, followed by centrifugation for 5min at 13000rpm at 4℃ (Heraeus Biofuge Fresco 17, Thermo Fisher). The supernatant was transferred to polystyrene cuvettes (Carl Roth, Karlsruhe), and the absorbance was measured at 663nm and 645nm. Averages of the measured data were calculated for each wavelength and were used to calculate the chlorophyll concentration using the equation shown below:

$$c\left(\frac{\mu g\ \text{Chlorophyll}}{\mu L}\right) = \frac{(20.2 * A645 + 8.02 * A663)}{10}$$

3.4.3 Preparation of thylakoids

To isolate thylakoids, freshly prepared chloroplasts corresponding to a chlorophyll of 750µg were taken for centrifugation at 10000rpm, 4℃ for 1min. The pellet was then dissolved in 1ml HM buffer for

osmotic lysis for 10min on ice. The lysed chloroplasts were washed twice with 1ml HM buffer. The centrifuge steps for washing were performed at 10000rpm, 4°C for 5min. Finally, the pellet of thylakoid was dissolved in 1ml HM buffer, reaching a chlorophyll concentration of 0.75µg/µl.

HM buffer	10mM	HEPES
	5mM	$MgCl_2$
		pH 8.0 by KOH

3.4.4 *In thylakoido* transport experiments

3.4.4.1 Import experiments

40µl of thylakoid suspension (concentration: 0.75µg chlorophyll/µl) was mixed with 5µl of Tat substrate synthesized by *in vitro* translation. The transport mixtures were incubated for 20min in a temperature-controlled water bath (25°C) at a light intensity of 20µE. To stop the transport reaction, the samples were mixed with ice-cold 50µl of HM buffer and centrifuged for 4min at 10000rpm, 4°C (Heraeus Biofuge Fresco 17, Thermo Fisher). The pellet was washed with 170µl of HM buffer, and centrifuged again. The pellet then resuspended in 200µl of HM buffer which was divided into 2x100µl in new Epi-tubes. One fraction with 100µl was treated with 10µl of 2mg/ml thermolysin solution (final concentration: 182µg/ml) and the other fraction with 100µl was untreated. Samples were incubated on ice for 30 min. The protease treatment was stopped by adding 5µl of 0.5M EDTA solution (final concentration: 20mM). The protease-treated and the remaining untreated fraction were pelleted for 4 min at 10000rpm, 4°C. Then pellets were dissolved in Lammli buffer and loaded on an SDS-PA gel for protein separation (Section 3.4.5).

Thermolysin solution	0.2%(w/v)	thermolysin
	25mM	$CaCl_2$

3.4.4.2 Reconstitution experiments

For antibody treatments, 40µl of thylakoid suspension is required for each treatment. According to experiment design, the total volume of required thylakoids was mixed with the respective antibody to

block intrinsic TatA or TatB function - anti-TatA antibody (*Arabidopsis thaliana*): 0.25 x volume; anti-TatB antibody (*Pea sativum*): 1 x volume. The blocking reaction was conducted on ice for 45 min. The thylakoids were then pelleted for 4min at 10000rpm, 4°C. Pellets were washed twice with HM buffer and finally resuspended in HM buffer to the starting concentration of 0.75µg chlorophyll/µl. Then the resuspension was divided into 40µl of each into new Epi tubes.

To reconstituted antibody-blocked Tat transport, external Tat subunits was added into this 40µl of antibody-treated thylakoids. For a positive control, one assay was same as import set-up (Section 3.4.4.1) that without antibody treatment, but conducted same incubation period and washing times as antibody-treated samples. No external Tat subunits were added to this positive control. For a negative control, one antibody-treated sample was not added with external Tat subunits. Then 5µl of Tat substrate added to all assays. Samples were then incubated for 20min in a temperature-controlled water bath (25°C) at a light intensity of 20µE. The following steps were same as described before (Section 3.4.4.1). Tat subunits, or variants, were synthesized either by heterologous overexpression and purification (see Section 3.1.2) or by *in vitro* translation (see Section 3.1.1). In the case of purified proteins, they needed to be dialyzed against HM buffer before use (see Section 3.1.2.6).

3.4.5 Separation of proteins from thylakoid membranes

To separate individual proteins from thylakoid membranes, an SDS-PAGE was conducted (see Section 3.2.1). Each pellet obtained after transport experiments (Section 3.4.4) was resuspended in 25µl of 4xLaemmli sample buffer. Finally, all samples were denatured for 3min at 95°C. The 25µl Laemmli-samples (corresponding to a chlorophyll concentration of 15µg) was all loaded onto an SDS-PA gradient gel.

3.4.6 Solubilization of protein complexes from thylakoid membranes

To solubilize protein complexes from thylakoid membranes, a BN-PAGE was conducted (see Section 3.2.2). The experiment set-up is similar with Section 3.4.4, but without protease treatments. Thus, the pellet obtained after transport experiments contained 30µg chlorophyll. Each pellet was resuspended in 15µl of BN-lysis buffer and 7.5µl of 5% digitonin (final concentration: 1.66%). The thylakoids were

then solubilized for 1h at 4 ℃ on a rotator. After that, samples were ultracentrifuged for 20min at 55000rpm, 4 ℃ (OPTIMA MAX-XP Ultracentrifuge, rotor: MLA-80, Beckman Coulter, Krefeld). Carefully taking out the supernatants, no green sediments. The supernatants were then mixed with 1.5µl of BN sample buffer and incubated on ice for 10min. The supernatant was applied to a 5–13.5% BN-PA gradient gel (see Section 3.2.2).

BN-lysis buffer	50mM	Bis-Tris, pH 7.0
	1M	ε-aminocaproic acid
	5mM	EDTA
	0.5mM	MgCl2
	1mM	PMSF
	1mM	DTT
BN sample buffer	5% (w/v)	Coomassie G-250 dissolve in 0.5M ε-aminocaproic acid

4 Results

4.1 Functional reconstitution of Tat transport in pea thylakoids

In thylakoids, so-called *in thylakoido* assays were developed to analyze the function of Tat subunits in Tat transport (Hauer, et al. 2013; Zinecker, et al. 2020). In the reconstitution assays (Fig.4.1, route ②), the intrinsic activity of Tat subunits is inhibited by specific antibodies, resulting in the loss of Tat-dependent protein transport. Therefore, ^{35}S-methioine-radiolabeled Tat substrates are not able to be transported into the thylakoid lumen and remain in the stroma, where they are degraded by externally added protease. Subsequently, the blocked transport can be reconstituted by supplementing the assays with soluble Tat subunit proteins obtained from *in vitro* translation or heterologous overexpression. A successful reconstitution is indicated by the accumulation of radiolabeled mature substrate proteins in the thylakoid lumen, where they are protected from external proteolysis. On the other hand, in import assays (Fig.4.1, route ①), as control, the intrinsic Tat transport is not blocked by antibodies. Here, radiolabeled Tat substrates are directly added to isolated thylakoids to demonstrate the import competence of the thylakoids. Again, the success of substrate transport is confirmed by protease treatment, since mature substrate proteins, which are located inside the lumen, are protected from proteolysis.

In the case of antibody-blocked Tat transport reconstitution, TatA and its derivatives synthesized by *in vitro* translation wer able to successfully reconstitute Tat transport in anti-TatA-treated thylakoids (Hauer, et al. 2017; Hauer, et al. 2013). Albeit TatB synthesized by *in vitro* translation appearsed to not function well in Tat transport reconstitution (Zinecker, et al. 2020). While Zinecker, et al. (2020) examined only one *in vitro* translation system for synthesizing TatB protein, three other *in vitro* translation systems are routinely used in our laboratory. Compared with heterologous overexpression, *in vitro* translation is more time-efficient and can produce less-soluble proteins. Therefore, we aimed to investigate whether TatB synthesized by these alternative three *in vitro* translation systems could be effectively used in our reconstitution assays.

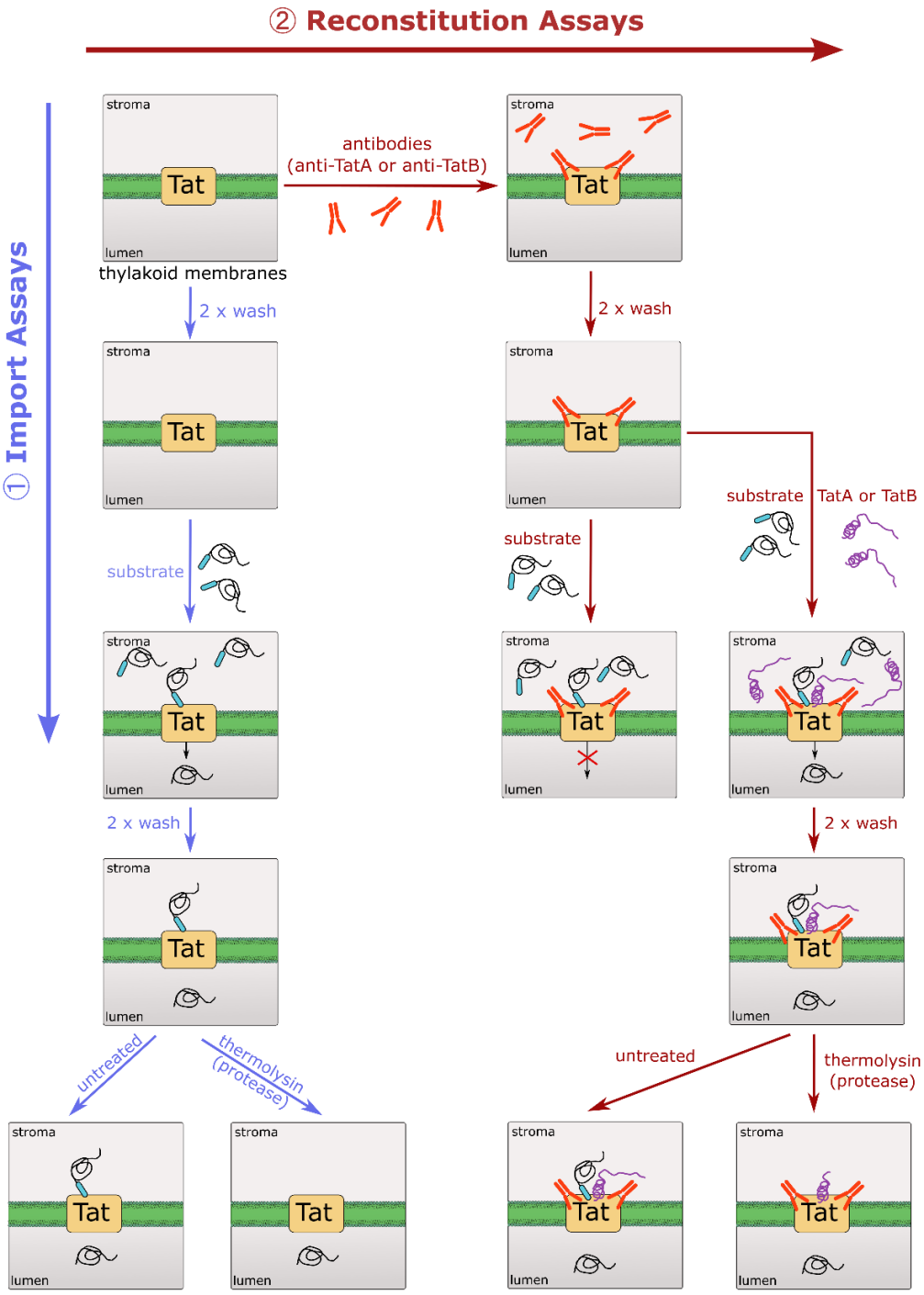

Fig.4.1 Scheme of *in thylakoido* transport assays.
① **Import Assays (left, blue arrows):** Isolated thylakoids are washed twice to match the washing steps used in reconstitution assays, and then incubated with radiolabeled precursor substrates under standard transport conditions (25℃, 20min, light). After transport, thylakoid membranes are washed twice again and equally divided into two fractions: one remains untreated while the other is subjected to thermolysin treatment. Protease treatment enables discrimination between successfully translocated substrates in the lumen (protease-protected) and those remaining in the stroma or bound to the membrane surface. ② **Reconstitution Assays (right, red arrows):** Isolated thylakoids are pre-incubated with specific antibodies (anti-TatA or anti-TatB) to inhibit intrinsic Tat subunit function. After two washing steps, either HM buffer or exogenously supplied TatA or TatB proteins is added. Radiolabeled substrates are included in all assays to evaluate the transport competence of the thylakoids. Subsequently, samples are incubated under standard transport conditions followed by twice washing. After that, thermolysin treatment is applied to distinguish translocated from non-translocated substrates. This dual assay approach allows functional analysis of individual Tat subunits.

4.1.1 Reconstitution by TatB obtained from *in vitro* translation

4.1.1.1 Testing TatB proteins obtained from *in vitro* translation systems

In our laboratory, three different *in vitro* translation systems are routinely used: the *Rabbit reticulocyte Lysate System* (Promega), the *S30 T7 High-Yield Protein Expression System* (Promega) and the *Wheat Germ Extract* (Promega), shorten as 'Reti', 'S30', 'WG' respectively. Therefore, TatB was synthesized using these three *in vitro* translation systems and subsequently tested for its ability to reconstitute Tat transport in anti-TatB-treated thylakoids (Fig.4.2).

The autoradiogram shown in Fig.4.2 presents the results of reconstitution experiments in anti-TatB-treated thylakoids, using the Tat substrate pOEC16 (*p*), the precursor form of 16kDa subunit of the oxygen-evolving complex. In SDS-PAGE, pOEC16 migrates at approximately 26kDa, while the mature form (mOEC16) migrates at approximately 16kDa. When untreated thylakoids were incubated with pOEC16 under light conditions, efficient translocation occurred, as evidenced by unaffected mOEC16 bands in both protease treated and untreated lanes (*con, +* and - lanes). Upon protease treatment, the non-translocated pOEC16 was degraded by protease, while the translocated product mOEC16 was resistant to protease degradation (*con*, *+* lane). The accumulation of mOEC16 in the lumen (*con* lanes) indicates the functional competence of isolated thylakoids for Tat-dependent protein transport. In contrast, pre-treatment of thylakoids with TatB-specific antibodies inhibited Tat transport, as evidenced by no accumulation of mOEC16 (*HM* lane). To reconstitute this inhibited Tat transport, TatB proteins obtained from Reti, S30, WG systems were added to anti-TatB-treated thylakoids (lane ①-④). In lane ①, 20µl of TatB synthesized by wheat germ extract (WG) successfully restored transport activity, as indicated by the accumulation of mOEC16 under protease treatment condition (*+* lane). In contrast, the same amount of TatB synthesized by rabbit reticulocyte lysate (Reti) lacked this capability (lane②). In addition, TatB synthesized by S30 system also reached successful reconstitution (lane ③). This differential reconstitution capacity within these three systems was unexpected, especially since both Reti and WG systems are eukaryotic cell-free systems. One possible explanation is that rabbit reticulocyte lysate introduces post-translational modifications (Tymms 1998) that may interfere with TatB function, while wheat germ extract and *E. coli* S30 lysate introduce fewer post-translational

modifications and contain low levels of endogenous mRNA (David, et al. 2019; Van Herwynen and Beckler 1995). Intriguingly, only a lower amount of TatB obtained from S30 translation restored Tat transport (lane ③), whereas a higher amount of TatB did not (lane ④). Given that *in vitro* translation reactions inevitably contain perturbing proteins from the translation system itself (Frielingsdorf, et al. 2008), it is conceivable that certain components in the S30 translation mixture may interfere with the reconstitution process. Therefore, we next tested whether the empty translation product from S30 system could affect Tat-transport reconstitution or not (Fig.4.3A).

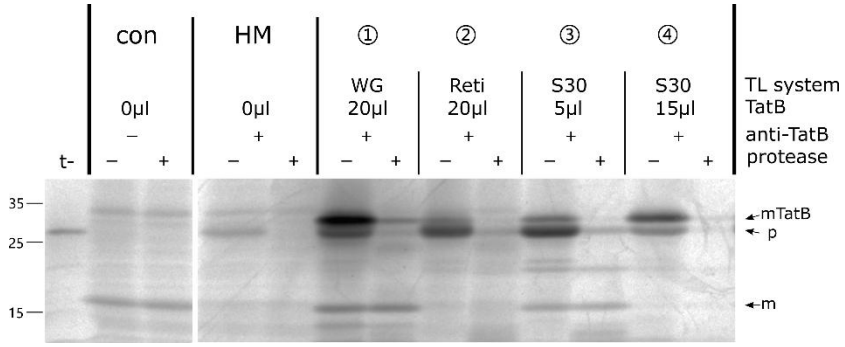

Fig.4.2 Reconstitution of Tat transport in anti-TatB-treated thylakoids with TatB obtained from *in vitro* translation.
Thylakoids isolated from pea leaves were either mock-treated (*con*) or anti-TatB-treated (*anti-TatB*). The anti-TatB-treated thylakoids were subsequently supplemented with either HM buffer (*HM*) or with TatB synthesized by *in vitro* translation with ^{35}S-methionine (*WG, Reti, S30*). 5µl of radiolabeled substrates were added to each assay. In this experiment, the precursor OEC16 was used as substrate. The substrate proteins were generated by *in vitro* translation using *Rabbit reticulocyte Lysate System* in the presence of ^{35}S-methionine. After adding substrates, samples were incubated under standard transport conditions (25℃, 20min, light). Subsequently, thylakoids were washed once with HM buffer and then equally divided into two fractions. One fraction was incubated with thermolysin (182µg/ml, *lanes+*) and the other was with HM buffer (*lanes-*) for 30min. For each lane, samples corresponding to 15µg of chlorophyll were loaded on a 10–17.5% SDS-polyacrylamide (SDS-PA) gradient gel. In *lane t-*, 1µl of the radiolabeled substrate translation was loaded. The bands representing the precursor (*p*), mature proteins (*m*) and TatB (*mTatB*) are indicated by *black arrows*. Radioactive signals were detected by phosphorimaging.

The effect of empty S30 translation product on Tat transport reconstitution

To investigate the potential effect of S30 translation system on Tat transport reconstitution, 2µl of TatB synthesized by S30 system was added to anti-TatB-treated thylakoids as a baseline for reconstitution (Fig.4.3A, lanes ①-③). Upon this, 13µl of either empty S30 translation product (lane ②) or HM buffer (lane ③) was supplemented, bringing the total reaction volume to 15µl. For comparison, 2µl and 15µl of TatB were also directly added to anti-TatB-treated thylakoids (lanes ① and ④, respectively). Those treatments allow assessment of the effects of both TatB dosage and translation system mixtures on reconstitution efficiency.

Consistent with previous observations, a lower amount of TatB (2µl) synthesized by S30 system achieved a low but detectable level of the Tat transport reconstitution in anti-TatB-treated thylakoids, whereas a higher amount (15µl) did not (Fig.4.3A, lanes ① and ④). A faint band at the same migration position as mOEC16 was also observed in the antibody-treated control (*HM* lane), indicating that antibody-mediated inhibition of Tat transport was not complete. Notably, the mOEC16 bands observed in samples with successful reconstitution (lanes ① and ③) were shaper and more defined compared to the faint bands in the *HM* lane, whereas the mOEC16 bands in samples with failed reconstitution (lanes ② and ④) were barely detectable. Taken together, the signals at the position of mOEC16 in reconstitution assays indeed represent successful reconstitution of TatB-blocked Tat transport.

Notably, even with the same amount of TatB in the assays (Fig.4.3A, lanes ①-③), the addition of 13µl of empty S30 translation product markedly reduced the reconstitution efficiency compared to the condition without any additional supplement (compare lanes ② and ①). In contrast, adding 13µl of HM buffer had no obvious inhibitory effect (compare lanes ③ and ①). These findings indicate that the reduced transport efficiency observed upon addition of the empty S30 translation product is not simply due to dilution, but it is the result of an inherent inhibitory effect of the translation system. Moreover, when the thylakoid concentration was kept constant across these conditions (Fig.4.3A, lanes ②-④), we could clearly observe that the inhibitory effect by S30 translation mixture counteracted the positive effect of increased TatB dosage, leading to a failure of reconstitution even with higher TatB supplementation (lane ④). Additionally, we observed reduced precursor (*p*) signal intensity in samples containing 15µl of S30 translation product (lanes ② and ④), compared to those with 2µl product (lanes ① and ③). This difference suggests that some components in the S30 system may interfere with substrate binding to thylakoid membranes. These components may include endogenous *E. coli* Tat substrates present in the S30 lysate, which could compete with the radiolabeled substrates for binding to thylakoid Tat translocase. Previous studies have shown that *E. coli* Tat substrates could be efficiently transported by thylakoidal Tat pathway (Hauer, et al. 2017; Mori and Cline 1998; Wexler, et al. 1998), suggesting a potential competition between *E. coli* and thylakoid Tat substrates on the binding of thylakoidal Tat translocase. Since many bacterial Tat substrates are soluble in the cytoplasm (Lee, et al. 2006b), they likely remain in the lysate after cell disruption. Furthermore, 15µl of TatB supplementation (lane④, *p* signal) showed better substrate binding than 2µl of TatB (lane②, *p* signal), suggesting that

TatB may assist substrate binding to thylakoid membranes. However, the overall reconstitution efficiency with TatB synthesized by S30 system was fairly low, and the inhibitory effect of the S30 translation system itself was evident. Therefore, the *S30 T7 High-Yield Protein Expression System* is not suitable for *in vitro* protein synthesis which are used in *in thylakoido* reconstitution assays for TatB-blocked Tat transport reconstitution.

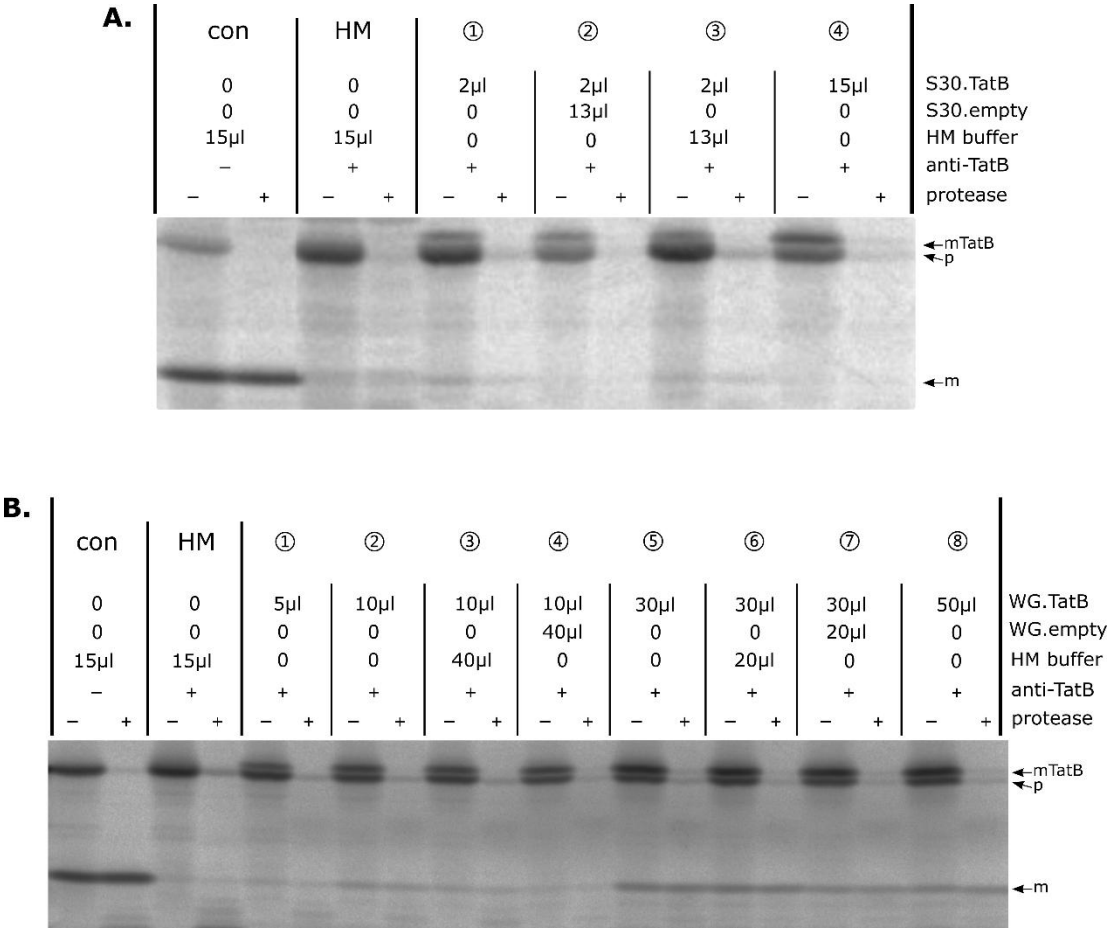

Fig.4.3 The effect of empty translation products on the Tat transport reconstitution in anti-TatB-treated thylakoids.
In thylakoido reconstitution assays of OEC16 transport by TatB and empty products obtained from *S30 T7 High-Yield Protein Expression System (S30)* (A) and *wheat germ extract system (WG)* (B) were analyzed. Substrate OEC16 was synthesized by *Rabbit reticulocyte Lysate System*, and TatB proteins and empty products were obtained from *S30* and *WG* systems. All the translation processes were performed in the presence of ^{35}S-methionine, while translation mixtures of empty products did not contain *in vitro* transcription of the respective TatB. The composition of each treatment, i.e. the volume of TatB and empty products are given above the lanes. For further details see the legend to Fig.4.2.

The effect of empty wheat germ translation product on Tat transport reconstitution

As shown in Fig.4.2, TatB synthesized by *wheat germ extract system* (*WG*) also successfully reconstituted TatB-blocked Tat transport (lane ①). Therefore, we next examined whether WG system

exhibited a similar inhibitory effect as S30 system on the Tat transport reconstitution (Fig.4.3B). Unlike S30 system, where a higher amount of TatB failed to reconstitute the transport (Fig.4.3A, lane④), higher amounts of TatB synthesized by WG system resulted in improved transport efficiency (Fig.4.3B, compare lane ① with lane ② and ⑤). Those results indicate that WG system exerts less suppressing effect on TatB-blocked Tat transport reconstitution. As observed previously, antibody-mediated TatB inhibition was not entirely complete, evidenced by faint signals at the migration position of mOEC16 in the antibody-treated control (*HM* lane). Therefore, the mature protein bands observed in the 5µl-TatB supplementation are difficult to confidently interpret as successful reconstitution (lane ①). However, when higher amounts of TatB were added, (10µl, 30ul and 50ul; lanes ③, ⑤, ⑧) distinct and stronger signals of mature proteins were observed compared with *HM* control, confirming the effective reconstitution by TatB obtained from WG system.

To evaluate whether WG system itself has any negative effect on the reconstitution of TatB-blocked Tat transport, 10µl and 30µl of TatB synthesized by WG system were used as baselines for the reconstitution (Fig.4.3B, lanes ②-④, ⑤-⑦, respectively). Upon these conditions, either empty WG translation product or HM buffer were added to bring the total reaction volume to 50µl (lanes ③ and ④, ⑥ and ⑦), keeping the final thylakoid concentration consistent across these assays. For comparison, 50µl of TatB was also directly added to anti-TatB-treated thylakoids (lane ⑧). Compared to the baseline samples, the addition of HM buffer resulted in similar signal intensities of mOEC16 (compared lanes ② and ③, ⑤ and ⑥), indicating that dilution by the respective buffer volume had minimal impact on the efficiency of reconstituted Tat transport. Whereas, the addition of an equivalent volume of empty WG translation product led to a moderate reduction in Tat transport efficiency (compared lanes ② and ④, ⑤and ⑦). Those results suggest that the observed mild reduction in Tat transport caused by WG translation product was not due to buffer dilution but rather attributable to intrinsic components present in the WG translation mixture. These inhibitory factors are unlikely to be endogenous Tat substrates, as hypothesized for the S30 system. The WG extract is derived from wheat embryos, which lack fully developed chloroplasts. Therefore, they are not expected to contain Tat substrates localized in thylakoids. Although it would be of interest to identify potential inhibitory factors, such as Tat substrates or competing proteins within *E. coli* S30 lysate and wheat germ extract, this lies beyond the scope of the present study and is not the focus of this thesis.

A comparison of Fig.4.3A and Fig.4.3B clearly demonstrates that the inhibitory effect of WG system is substantially weaker than that of S30 system. In the presence of S30 translation products (Fig.4.3A), overall reconstitution levels remained low (lanes① and ③) and no detectable transport was observed only with 15µl TatB supplementation (lane ④). In contrast, with WG translation products (Fig.4.3B), the signal intensity of mOEC16 increased progressively from 5µl to 30µl TatB supplementation (lanes①②⑤). Higher amounts of TatB led to better reconstitution evidenced by clearer and more robust mOEC16 signals (lanes ⑤ and ⑧). These results indicate that the *Wheat-Germ-Extract* is suitable for *in vitro* protein synthesis which is used for *in thylakoido* reconstitution assays in anti-TatB-treated thylakoids.

Intriguingly, supplementation with 50µl of TatB synthesized by WG system resulted in a similar reconstitution level compared to 30µl TatB (Fig.4.3B, compared lanes ⑦ and ⑧), rather than the expected further increase in transport efficiency. One possibility is that 30µl of TatB may have reached a saturating concentration, beyond which additional TatB no longer enhances reconstitution level. Alternatively, higher TatB concentrations may suppress the reconstitution level, suggesting a biphasic response with an initial increase followed by a decrease in transport efficiency between 30µl and 50µl TatB. To investigate these possibilities, we next performed a quantitative analysis of Tat transport efficiency across a range of TatB concentrations (Section 4.1.2).

4.1.1.2 Kinetics of reconstituted Tat transport by TatB obtained from WG translation

Before proceeding to the next section, we aimed to determine an appropriate transport reaction time for reconstitution assays using TatB obtained from WG system. For this purpose, we performed a time-course analysis of OEC16 transport in anti-TatB-treated thylakoids supplemented with 20µl TatB obtained from WG system. For comparison, mock-treated thylakoids were analyzed in parallel (Fig.4.4). In control assays, a rapid and nearly linear accumulation of mOEC16 was observed during the initial phase (0-10min), reaching approximately 60% of the maximal signal by 10min (Fig.4.4B, blue line). Beyond this time point (>10min), the further increase in mOEC16 became slow, likely due to the less availability of precursor proteins. In contrast, reconstitution assays exhibited a slow but steady linear accumulation of the mOEC16 over the entire 70-minute period (Fig.4.4B, red line). Although 10min appeared to be a suitable time point for assessing TatB activity, as both import and reconstitution

reactions remained within their respective linear phases, the signal strength at 10min in reconstitution assays was relatively weak (Fig.4.4A). Therefore, to ensure sufficient signal intensity as well as allow the analysis of TatB activity, we selected a compromise incubation time of 20min for reconstitution assays using TatB proteins obtained from WG system.

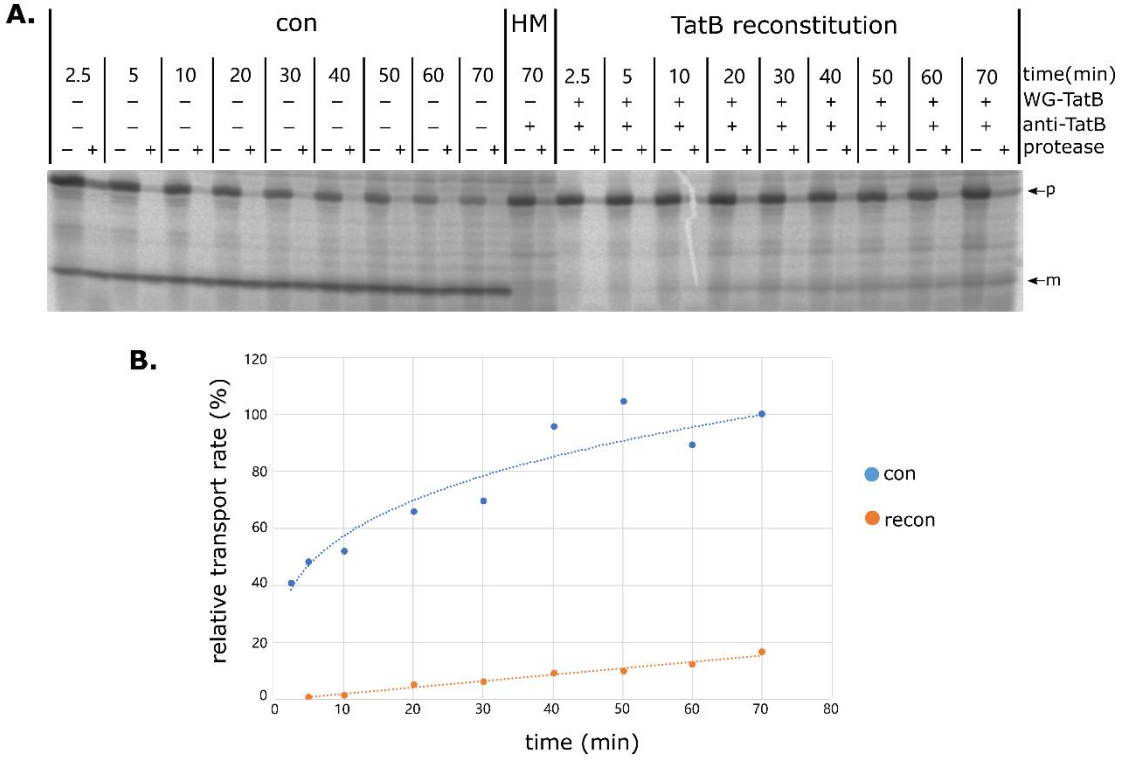

Fig.4.4 Time-course of OEC16 transport after supplementing anti-TatB-treated thylakoids with TatB obtained by wheat germ extract *in vitro* translation.
(A) Radiolabeled pOEC16 was incubated with mock-treated thylakoids *(con)* or anti-TatB-treated thylakoids supplemented with 20ul of TatB obtained from WG system *(TatB reconstitution).* As a negative control, pOEC16 was also incubated with anti-TatB-treated thylakoids supplemented with HM buffer for the maximum time period *(HM)*. The incubation was performed at 25℃ in the light for the time periods indicated on top of the lanes. All further processing steps were performed as described in the legend to Fig.4.2. (B) Quantification of the amount of translocated OEC16 *(m)* corresponding to that shown in (A). The results obtained with mock-treated thylakoids are given with *blue circles*, those of reconstitution assays are with *orange circles*. For each time-point, the relative amount of mature OEC16 *(m)* was calculated in terms of percentage of the value obtained in the 70min control reaction in *+ protease* lanes.

4.1.2 Reconstitution by TatB obtained from heterologous overexpression

As shown in Section 4.1.1 (Fig.4.3B), supplementation with 50µl of TatB synthesized by WG system failed to further enhance the reconstitution level of Tat transport in anti-TatB-treated thylakoids. However, *in vitro* translation systems inherently contain numerous proteins to conduct protein

synthesis, raising uncertainty about whether TatB, or other components in WG system, affected the efficiency of Tat reconstitution. Compared with proteins obtained by *in vitro* translation, heterologously overexpressed proteins are purified by HPLC, which are free from contamination by other proteins, and can be accurately quantified (Method 3.1.2). To eliminate potential effects from translation system components and to directly quantify TatB concentrations, we therefore used purified TatB by heterologous overexpression in reconstitution assays with anti-TatB-treated thylakoids (Fig.4.5).

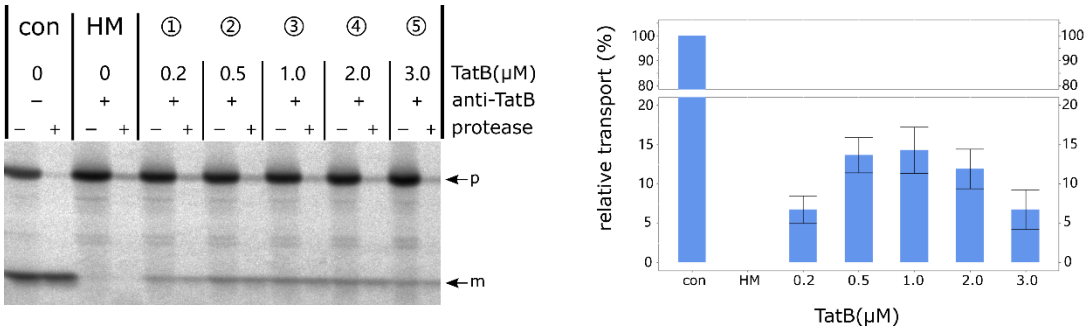

Fig.4.5 The effect of TatB on Tat transport in anti-TatB-treated thylakoids.
Thylakoids were pre-treated with TatB antibodies for 45min to block intrinsic TatB activity. Those anti-TatB-treated thylakoids were incubated with radiolabeled pOEC16 *(p)* and soluble TatB proteins for 20min at 25℃ in the light. Substrate OEC16 was synthesized by *Rabbit reticulocyte Lysate System* in the presence of ^{35}S-methionine. TatB was produced by heterologous expression and subsequently purified by HPLC. Left pane: a representative of an autoradiogram of this experiment. Right pane: quantification of the amount of translocated protein *(m)* from transport reactions which is identical to that shown in left pane. For each TatB concentration, the relative amount of translocated protein *(m)* was calculated in terms of percentage of the corresponding control reaction *(con)* in *+ protease* lanes. Both mean values and standard deviations were calculated from at least three independently repeated experiments. For further experimental details see the legend to Fig.4.2.

As expected, overexpressed TatB successfully reconstituted TatB-blocked Tat transport (Fig.4.5), consistent with previous results (Zinecker, et al. 2020). Within a certain concentration range (⩽1uM), increasing amounts of TatB led to higher reconstitution levels (Fig.4.5). Although the maximal transport efficiency remained relatively low, reaching only approximately 15%-18% by 1μM TatB compared to mock-treated thylakoids (Fig.4.5 right pane), the signals of mature proteins could be clearly observed on an SDS-PA gel (Fig.4.5, left pane). These results indicates that purified TatB obtained by heterologous overexpression is suitable for reconstituting Tat transport in anti-TatB-treated thylakoids.

Surprisingly, when anti-TatB-treated thylakoids were supplemented with more than 1μM TatB, a decrease in reconstituted transport activity was observed from 1μM to 3μM TatB (Fig.4.5, right pane).

The corresponding autoradiogram (Fig.4.5 left pane) also showed a weaker signal of mature proteins at 3µM TatB supplementation compared to 1µM supplementation (compare lanes ③ and ⑤). Since TatB is an essential subunit in Tat machinery, a negative effect of TatB on Tat transport efficiency was not initially anticipated. We expected that beyond a certain concentration, increasing TatB levels would lead to a plateau in reconstitution efficiency, rather than a decrease. This unexpected result raised the question of whether the reduced transport was a direct effect of TatB on Tat machinery or was a result from other factors, e.g. the aggregation of external TatB protein. Since the reconstitution assays depend on antibody blocking and the activity of external protein, any disturbance on external TatB would affect the reconstitution level. To clear this point, various concentrations of TatB were supplemented into non-antibody-treated thylakoids, where Tat transport only relies on the intrinsic Tat pathway. We aimed to check whether this negative effect could also be observed in intrinsic Tat transport (Section 4.2.1).

4.2 The effect of external TatA and TatB on thylakoidal Tat transport efficiency

Since the TatB-mediated reconstitution of Tat transport in anti-TatB-treated thylakoids exhibited an unexpected response to increasing supplementation of TatB (Section 4.1.2), we next aimed to determine whether TatB exerts a similar effect on intrinsic Tat transport activity and on TatA-blocked transport activity in thylakoid membranes. Additionally, we investigated whether TatA, another key component of the Tat machinery, influences Tat-dependent protein transport in a manner comparable to or distinct from that of TatB.

4.2.1 The effect of external TatB on Tat transport

Non-antibody-treated thylakoids

When TatB was supplemented into thylakoids without antibody treatment, a pronounced decrease on Tat transport activity was observed at 1.5µM TatB compared to non-TatB added thylakoids (Fig.4.6, right pane). Further increases in TatB concentration led to a progressive decline in transport efficiency. At 3µM TatB supplementation, only approximately 30% of transport activity remained compared to mock-treated thylakoids (Fig.4.6, right pane). This reduction in transport activity was paralleled with a

decrease in the intensity of radioactive signals of mature proteins on the autoradiogram. The signal intensity was progressively diminished with increasing TatB concentrations (Fig.4.6, left pane). These observations suggest that the decrease in reconstituted Tat transport induced by high TatB concentrations (Fig.4.5) is not due to nonspecific protein aggregation, but rather an indication of a direct interference of excessive TatB with Tat machinery.

Conversely, at relatively low concentrations of TatB (≤1 µM), no significant effect on intrinsic Tat activity was observed (Fig.4.6, right pane), with neither enhancement nor inhibition effect. Together with findings from TatB-blocked Tat reconstitution assays (Fig.4.5), they indicate 1µM as a threshold concentration, above which TatB begins to perturb both intrinsic and reconstituted Tat transport. This threshold may reflect a common underlying mechanism through which excessive TatB interferes with Tat translocation (see Discussion 5.1.3).

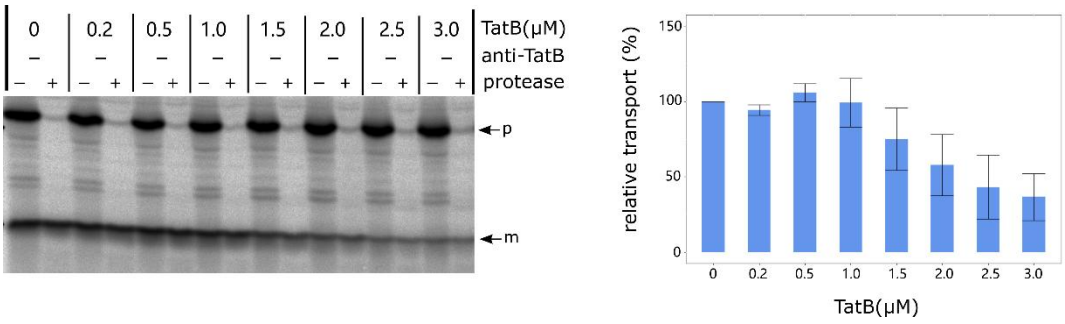

Fig.4.6 The effect of external TatB on Tat transport in non-antibody-treated thylakoids.
Mock-treated thylakoids were incubated with ^{35}S-radiolabeled pOEC16 *(p)* and purified TatB proteins for 20min at 25℃ in the light. Left pane: a representative of an autoradiogram of this experiment. Right pane: quantification of the amount of translocated protein *(m)* from transport reactions which is identical to that shown in left pane. For each TatB concentration, the relative amount of translocated protein *(m)* was calculated in terms of percentage of the corresponding control reaction *(con)* in *+ protease* lanes. Both mean values and standard deviations were calculated from at least three independently repeated experiments. For further experimental details see the legend to Fig.4.2.

Anti-TatA-treated thylakoids

Having both purified TatB proteins and affinity-purified antibodies against intrinsic TatA available, we next asked whether TatB was able to reconstitute transport activity on TatA-blocked Tat transport. To address this, we supplemented various concentrations of purified TatB into anti-TatA-treated thylakoids (Fig.4.7).

First, antibody treatment against TatA completely abolished intrinsic Tat transport, as evidenced by no accumulation of mOEC16 in the lumen (lane ①). Then upon antibody blocking, supplementation with TatB led to a restoration of Tat transport activity (lanes ②-⑥). While 0.2µM TatB resulted in only slight reconstitution of TatA-blocked Tat transport, higher concentrations of TatB (0.5µM, 1µM, 2µM and 2.5µM) progressively enhanced reconstitution level, as confirmed by both autoradiography and signal quantification (Fig.4.7). Notably, 2µM TatB restored transport efficiency up to ca.50% of the level in mock-treated thylakoids (Fig.4.7, right pane), which surpasses the maximum reconstitution level observed in anti-TatB-treated thylakoids (Fig.4.5). Intriguingly, in anti-TatA-treated thylakoids, the reconstitution level by TatB supplementation was positively correlated with TatB concentrations across the tested range (Fig.4.7), whereas in other assays (Fig.4.5, Fig.4.6), excessive TatB supplementation led to a decrease in transport efficiency. This discrepancy may reflect different roles of TatA and TatB within Tat translocase (see Discussion 5.1).

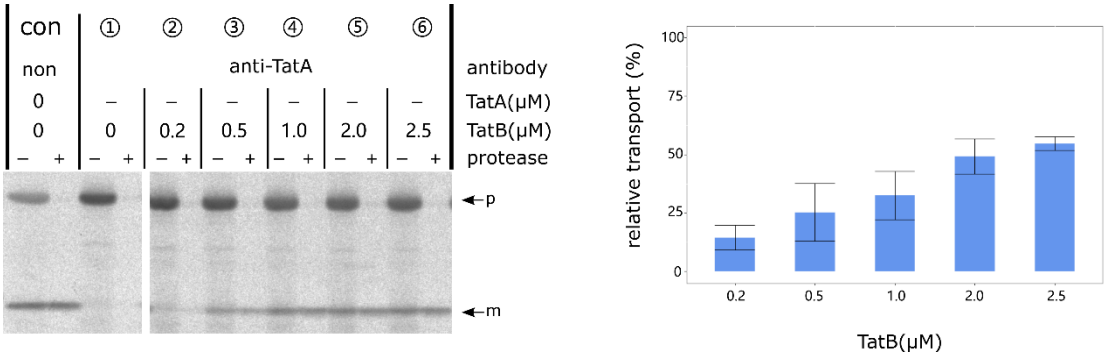

Fig.4.7 Analysis of TatB functional substitution for TatA in thylakoidal Tat translocase.
Thylakoids were pre-treated with specific TatA antibodies for 45min to block intrinsic TatA activity. Those anti-TatA-treated thylakoids were then incubated with ^{35}S-radiolabeled pOEC16 *(p)* and purified TatB proteins for 20min at 25℃ in the light. TatB was obtained by heterologous overexpression. Left pane: a representative of an autoradiogram of this experiment. Right pane: quantification of the amount of translocated protein*(m)* from transport reactions which is identical to that shown in left pane. For each TatB concentration, the relative amount of translocated protein *(m)* was calculated in terms of percentage of the corresponding control reaction *(con)* in *+ protease* lanes. Both mean values and standard deviations were calculated from at least three independently repeated experiments. For further experimental details see the legend to Fig.4.2.

4.2.2 The effect of external TatA on Tat transport

Anti-TatA-treated thylakoids

Since TatA and TatB belong to same protein family and share structural and sequence similarities in some extent (see Introduction 1.3.1.1), we next investigated whether TatA affects thylakoidal Tat

transport in a manner similar to TatB. First, we examined the effect of external TatA on the reconstitution of Tat transport in anti-TatA-treated thylakoids. Remarkably, even at a relatively low concentration (0.2µM), TatA reconstituted Tat transport to a level exceeding it in mock-treated thylakoids (Fig.4.8, right pane). Supplementation with 0.5µM TatA further increased reconstituted transport to approximately 125% of the mock control. However, increasing TatA concentrations beyond 0.5µM did not lead to further enhancement. Importantly, no significant decrease in Tat transport efficiency was observed with high concentrations of TatA supplementation in anti-TatA-treated thylakoids (Fig.4.8, right pane). Consistent with this, the corresponding autoradiogram (Fig.4.8, left pane) showed uniformly strong signals of mOEC16 across all TatA-supplemented assays, reflecting the high reconstitution efficiency by TatA.

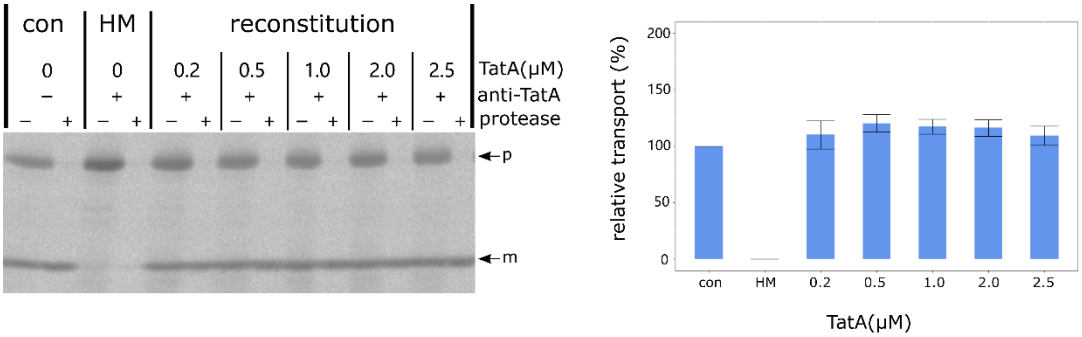

Fig.4.8 The effect of external TatA on Tat transport in anti-TatA-treated thylakoids.
Thylakoids were pre-treated with TatA antibodies for 45min to block intrinsic TatA activity. Those anti-TatA-treated thylakoids were incubated with radiolabeled pOEC16 *(p)* and purified TatA proteins for 20min at 25℃ in the light. TatA was obtained by heterologous overexpression. Left pane: a representative of an autoradiogram of this experiment. Right pane: quantification of the amount of translocated protein*(m)* from transport reactions which is identical to that shown in left pane. For each TatA concentration, the relative amount of translocated protein *(m)* was calculated in terms of percentage of the corresponding control reaction *(con)* in *+ protease* lanes. Both mean values and standard deviations were calculated from at least three independently repeated experiments. For further experimental details see the legend to Fig.4.2.

Non-antibody-treated thylakoids

Next, we examined the effect of external TatA on Tat transport in non-antibody-treated thylakoids (Fig.4.9). Due to the high efficiency of OEC16 transport, differences between treatments were difficult to distinguish on an autoradiogram (left pane, upper). To have a better visual comparison, the contrast of the gel image was increased (left pane, below). Signal intensities were also quantified and subjected to statistical analysis (right pane).

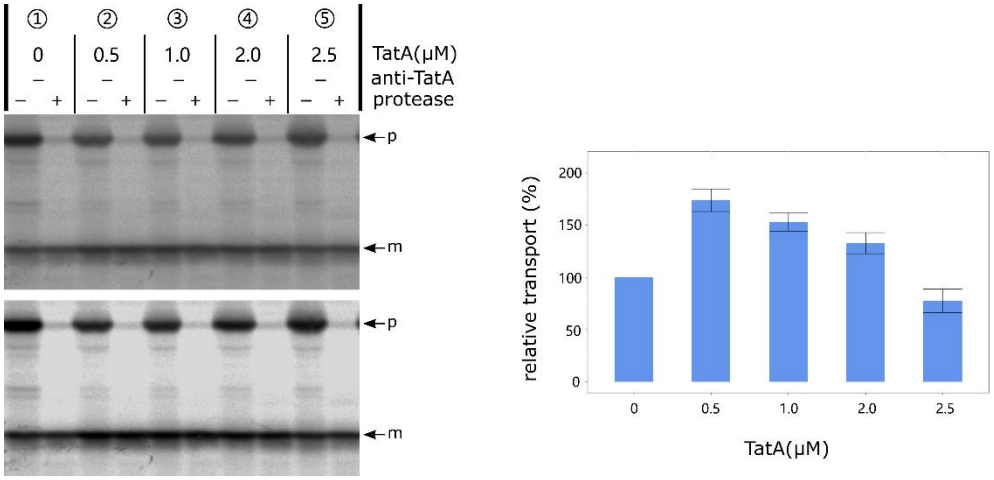

Fig.4.9 The effect of external TatA on Tat transport in non-antibody-treated thylakoids.
Mock-treated thylakoids were incubated with ^{35}S-radiolabeled pOEC16 *(p)* and purified TatA proteins for 20min at 25℃ in the light. Left pane: The two autoradiograms are the same pictures. The below one with increased contrast, in order to have a better visual comparison. Right pane: quantification of the amount of translocated protein *(m)* from transport reactions which is identical to those shown in left pane. For each TatA concentration, the relative amount of translocated protein *(m)* was calculated in terms of percentage of the corresponding control reaction *(con)* in *+ protease* lanes. Both mean values and standard deviations were calculated from at least three independently repeated experiments. For further experimental details see the legend to Fig.4.2.

With 0.5μM, 1μM and 2μM supplementation, TatA clearly facilitated Tat transport, evidenced by higher transport efficiency under these conditions compared to samples without TatA added. However, a progressive decrease on Tat transport activity was also observed from 0.5μM TatA to 2μM TatA (Fig.4.9, right pane). When a higher TatA concentration was supplemented (2.5μM), the transport efficiency was further decreased to a similar level as it in control sample (right pane). These observed decrease in Tat transport from 0.5μM TatA to 2.5μM TatA indicates a concentration-dependent reduction in Tat transport efficiency beyond the optimal TatA concentration. To determine whether this decreasing trend persisted at even higher concentrations, 3.6μM TatA was tested (Fig.S1). At this TatA concentration, the Tat transport was further reduced to a level below it in control, as evidenced by the clearly weaker signals of mOEC16 in lanes of 3.6μM TatA compared to 0μM TatA lanes (Fig.S1). However, since this experiment (Fig.S1) was only performed twice with smaller concentration differences compared to the experiments shown in Fig.4.9, it was not included in the statistical analysis in Fig.4.9. Nevertheless, it supports the conclusion that higher concentrations of TatA become less effective to facilitate, and even inhibit, intrinsic Tat transport.

Anti-TatB-treated thylakoids

Given that TatB is capable of reconstituting transport activity in anti-TatA-treated thylakoids (Fig.4.7), it was of particular interest to investigate whether the reverse was also true - whether TatA could functionally reconstitute TatB-blocked Tat transport. To address this, TatA was supplemented at two concentrations (0.5μM and 2μM) into anti-TatB-treated thylakoids (Fig.4.10). At 2μM TatA, TatA-mediated reconstitution of Tat transport in anti-TatA-treated thylakoids had already reached saturation phase (Fig.4.8) and intrinsic Tat transport even in the decreased phase (Fig.4.9). Thus, 2μM was selected in this experiment representing a TatA concentration which is more than sufficient for supporting Tat transport. Surprisingly, TatA was unable to reconstituted Tat transport activity in anti-TatB-treated thylakoids (Fig.4.10). Even at 2μM TatA, no mature OEC16 signal was detectable, indicating that the transport remained completely blocked by TatB antibodies. These results demonstrate that, unlike TatB, TatA cannot functionally substitute for its counterpart in thylakoidal Tat translocase.

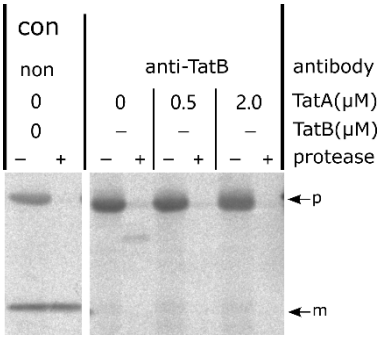

Fig.4.10 Analysis of TatA functional substitution for TatB in thylakoidal Tat translocase.
Thylakoids were pre-treated with TatB antibodies to block intrinsic TatB activity. Those anti-TatB-treated thylakoids were then incubated with radiolabeled pOEC16 *(p)* and soluble TatA proteins for 20min at 25℃ in the light. Here is a representative of an autoradiogram of this experiment. For further experimental details see the legend to Fig.4.2.

4.2.3 The effect of external TatA on TatB-mediated reconstitution

As shown previously, the maximal reconstituted Tat transport activity by TatB supplementation in anti-TatB-treated thylakoids remained relatively low, less than 30% of the transport activity in mock-treated thylakoids (Section 4.1.2, Fig.4.5). This raised the question that whether additional TatA supplementation could enhance TatB-mediated reconstitution, since TatA could facilitate both intrinsic and TatA-blocked reconstituted transport within a certain concentration range (Section 4.2.2). Moreover, the decline in transport efficiency at higher TatB concentrations (Fig.4.5 and Fig.4.6) may

due to the competition between TatB and TatA for their binding sites (Habersetzer, et al. 2017). Therefore, analyzing TatA behavior in TatB- mediated reconstitution assays could provide insights into potential binding-site competition between these two subunits (see Discussion 5.1.2). To address these questions, we assessed the effect of TatA on TatB-mediated reconstitution in anti-TatB-treated thylakoids (Fig.4.11).

Two concentrations of TatB (0.5μM and 2μM) were selected to establish reconstitution in anti-TatB-treated thylakoids (Fig.4.11). These concentrations represent two distinct regimes with similar Tat transport efficiency: 0.5μM falls within the facilitating range (≤1μM), while 2μM falls within the decreasing range (>1μM) (Fig.4.5). Based on these two conditions, varying amounts of TatA were supplemented to assess its impact on TatB-mediated reconstitution (Fig.4.11). To quantify the effect of TatA, a "TatA effect rate" was calculated for each treatment. This was defined as the ratio of the mature protein signal intensity in '+ protease' lane with TatA supplementation to that in the absence of TatA (0μM), under the same TatB condition. For example, the 'TatA effect rate' of 2μM TatA on 2μM TatB-mediated reconstitution was calculated by dividing the signal intensity of the mature protein band in lane ⑪ '+ protease' by that in lane ⑦ '+ protease'; similarly, for 0.5μM TatB, the 'TatA effect rate' of 2μM TatA was calculated by comparing lanes ⑤ and ①. Hence, 'TatA effect rate' of 1 indicates no net effect of TatA on TatB-mediated reconstitution (Fig.4.11, the solid line on bottom pane), while values above or below 1 reflect a positive or negative effect, respectively.

Compared to TatB-mediated reconstitution without TatA supplementation, the addition of 0.2μM, 0.5μM and 1μM TatA enhanced reconstitution efficiency at both TatB concentrations tested (Fig.4.11, bottom pane). Consistently, the facilitative effect of TatA exhibited a concentration-dependent decline: 0.2μM TatA yielded the greatest enhancement in both cases, while 0.5μM and 1μM TatA resulted in progressively decline on transport efficiency. When TatA concentration was further increased to 2μM, no significant effect was observed on 2μM TatB-mediated reconstitution (Fig.4.11, bottom pane, *blue dot* at 2μM TatA), and a slight inhibitory effect was observed on 0.5μM TatB-mediated reconstitution (Fig.4.11, bottom pane, *red dot* at 2μM TatA), indicated by both the average "TatA effect rate" and its standard error falling below 1. When at 3μM TatA, a clear inhibitory effect was observed in both cases, evidenced by transport efficiency dropping below the control level (Fig.4.11, bottom pane; upper pane, lanes ①⑥ and ⑦⑫). Interestingly, for each TatA concentration tested, the effect of TatA appeared

more favorable (higher facilitation or less inhibition) under 2μM-TatB condition compared to 0.5μM TatB (Fig.4.11, bottom pane, compare blue line and red line). However, due to the large standard errors, these differences were not statistically significant.

Overall, TatA exhibited similar effects on TatB-mediated reconstitution with both TatB concentrations tested – showing initial facilitation at low TatA concentrations, followed by a progressive decline starting from 0.2μM TatA, and eventual showing inhibition at 3μM TatA. Consequently, no significant difference in the TatA effect was observed between the two TatB-mediated reconstitution conditions.

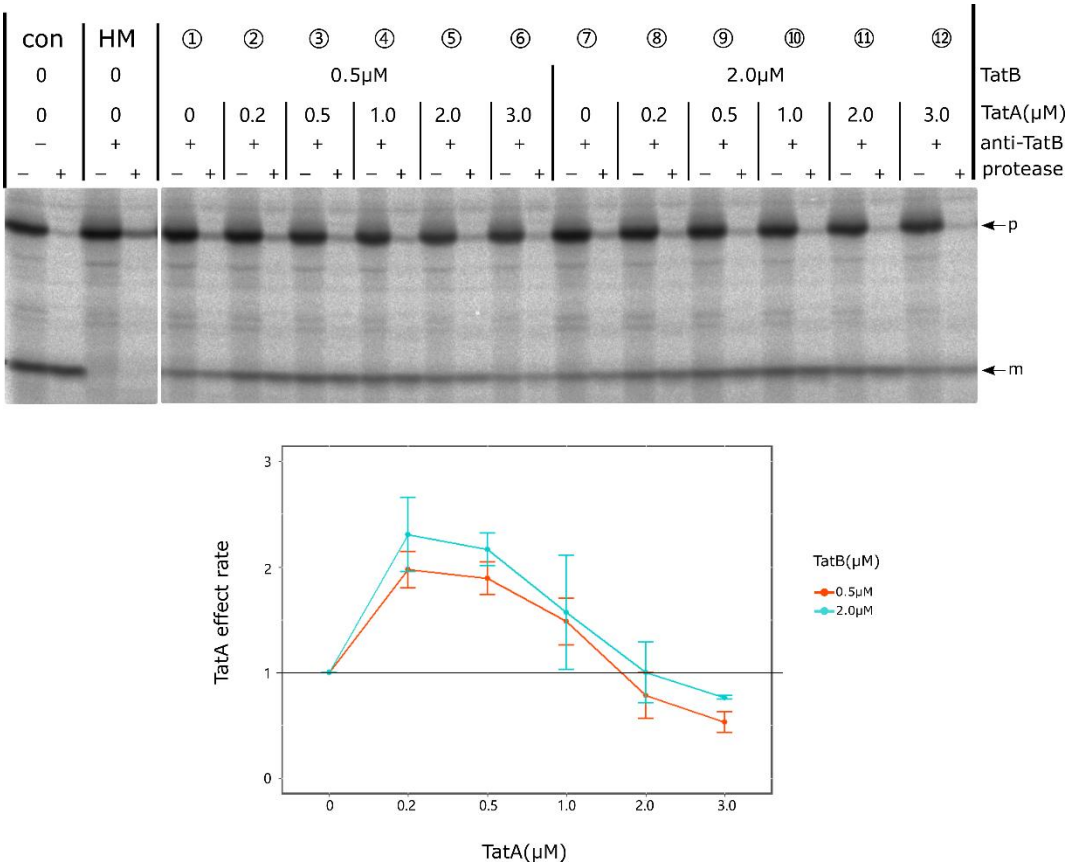

Fig.4.11 The effect of external TatA on Tat transport reconstituted by external TatB in anti-TatB-treated thylakoids.
Anti-TatB-treated thylakoids were supplemented with two concentrations of TatB (*0.5μM* and *2μM*) to set up the baseline of reconstituted transport. Based on these conditions, varying amounts of TatA were added into the assays. The concentrations of TatB and TatA are given above the lanes. Both TatA and TatB were supplemented prior to transport reaction. The upper pane represents an autoradiogram of this experiment. The lower pane is the statistical analysis of TatA effect on TatB-mediated reconstituted Tat transport. For each condition, the "TatA effect rate" was defined as the ratio of the mature protein signal intensity in '*+ protease*' lane in the presence of TatA to that in the absence of TatA *(0μM)*, under the same TatB supplementation condition. Both mean values and standard deviations were calculated from at least three independently repeated experiments. For further experimental details see the legend to Fig.4.2.

4.2.4 The effect of external TatB on TatA-supplemented Tat transport

To further explore the hypothesis that TatA and TatB compete for their binding sites on TatC, which potentially leads to a decrease in Tat transport efficiency when either protein is in excess, we next examined the effect of TatB on TatA-supplemented Tat transport (Fig.4.12). In this experiment, an excessive concentration of TatA (3μM) was added to non-antibody-treated thylakoids to establish a transport condition in this deceasing phase (Fig.4.9). Upon this background, varying concentrations of TatB were supplemented to evaluate their effect on TatA-mediated transport (Fig.4.12, orange bars). For comparison, the same range of TatB concentrations were also tested in non-TatA-supplemented thylakoids (Fig.4.12, blue bars).

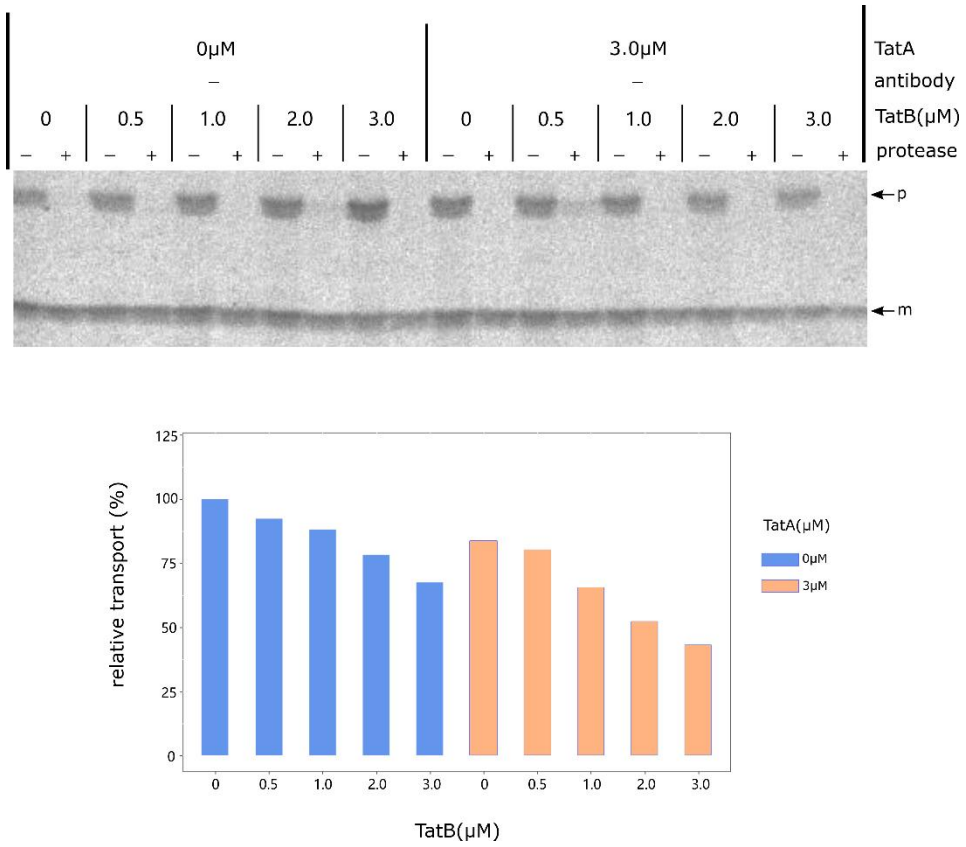

Fig.4.12 The effect of external TatB on high concentration of TatA-supplemented Tat transport.
Thylakoids were incubated with ^{35}S-radiolabeled pOEC16 *(p)*, 3μM TatA and a range of concentrations of TatB for 20min at 25℃ in the light *(orange bars)*. For comparison, same amount of substrate and same range of TatB concentrations were supplemented into non-TatA-added thylakoids *(blue bars)*. The upper pane shows an autoradiogram of this experiment. The lower pane is the quantification of the amount of translocated protein*(m)* from transport reactions which is identical to that shown in upper pane. For each lane, the relative amount of translocated protein *(m)* was calculated in terms of percentage of the control reaction *(0μM TatA, 0μM TatB)* in *+ protease* lanes. For further experimental details see the legend to Fig.4.2.

When TatB was added into non-TatA-supplemented thylakoids, a gradual decrease in Tat transport activity was observed across the range from 0 to 3µM TatB (Fig.4.12, blue bars). In thylakoids supplemented with 3µM TatA but without TatB, Tat transport activity was reduced to approximately 80% of the mock-treated thylakoids (Fig.4.12, orange bar, 0µM), consistent with the previously observed reducing effect of high TatA concentrations. Upon additions of TatB to thylakoids that already containing 3µM TatA, a further decline in transport activity was observed (orange bars). Specifically, transport efficiency decreased by approximately 40% at 3µM TatB (from ~80% to ~40% of the level in mock-treated thylakoids) (orange bars, compare 0µM and 3µM). Similarly, in non-TatA-supplemented thylakoids, Tat transport also decreased by approximately 35% at 3µM TatB (from ~100% to ~65% of the level in mock-treated thylakoids) (blue bars, compare 0µM and 3µM). It seems that TatB has no additional effect on TatA-supplemented Tat transport. Although precise statistical comparison between individual treatments was not possible due to limited replicates, both TatA-supplemented and non-TatA-supplemented conditions exhibited a similar decreasing trend in transport efficiency with increasing TatB concentrations. This indicates that TatB likely has no competition with TatA (See Discussion 5.1.2).

4.3 The effect of external TatB on the stability of TatBC complexes

As shown previously (Fig. 4.5, Fig. 4.6), high concentrations of external TatB led to a progressive decrease in Tat transport activity, rather than reaching a saturation plateau. This unexpected pattern prompted further investigation into the underlying mechanism. Since TatBC complexes serve as the core functional units of Tat translocase, any disruption in their integrity could likely impact Tat transport. Therefore, we next examined the status of TatBC complexes under varying concentrations of TatB supplementation.

Blue Native polyacrylamide gel electrophoresis (BN-PAGE) is a suitable method for analyzing solubilized membrane protein complexes. Upon solubilizing thylakoid membranes with detergents such as digitonin, a predominant TatBC complex of approx. 620kDa (complex#1) could be detected, followed by a smaller complex of approx. 520kDa (complex#2). A third, less abundant complex of approx. 420 kDa (complex#3) was also observed, although its signal intensity was notably weaker than that of the other two complexes (Fig.4.13A). Both complex#1 and complex#2 could be observed by

indirect labeling using radiolabeled TatB or Tat substrates (Fig.4.13B) (Berghöfer and Klösgen 1999). When radiolabeled substrate OEC16 was added to thylakoids, a slightly shift in the migration of both complex#1 and complex#2 was observed, compared to labeling with radioactive TatB alone. The shift may reflect substrate association with the TatBC complexes (Fig.4.13B).

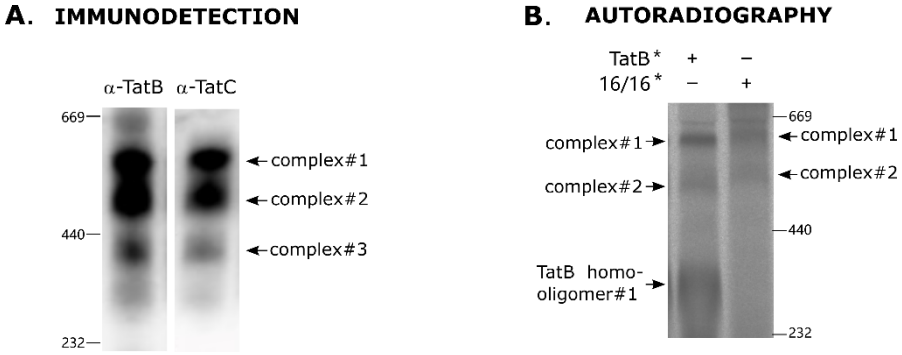

Fig.4.13 Detection of TatBC complexes on thylakoid membranes.
Mock-treated thylakoids (A) or thylakoids supplemented with ^{35}S-radiolabeled substrate or TatB (B) were incubated for 20min at 25℃ in the light, followed by once washing. Then samples were solubilized by BN lysis buffer with 1.67% digitonin (see Method 3.4.6) and subsequently incubated in 4℃ for 1h. The BN-lysis samples corresponding to 30μg of chlorophyll were loaded on a 5%-13.5% gradient blue native polyacrylamide (BN-PA) gel (see Method 3.2.2). (A) BN-PA gels were blotted and developed with specific antibodies against the respective proteins as shown above the lanes. (B) an autoradiograph of the gel with ^{35}S -radiolabeled OEC16 or TatB is shown. *Asterisks* represent ^{35}S-radiolabeled proteins. The *arrows* point to the positions of three Tat complexes of approximately 620 kDa (complex#1), 520kDa (complex#2) and 420kDa (complex#3).

To examine whether TatB supplementation affects the status of TatBC complexes, varying concentrations of TatB were supplemented to thylakoid membranes (Fig.4.14). At higher TatB levels (1μM, 2μM, 3μM), externally supplied TatB predominantly formed homo-oligomers within the membrane, while no defined oligomers were detected at a relatively low concentration of TatB (0.5μM) (right pane). However, the signals of TatBC complexes by anti-TatB immunodetection was difficult to be observed due to strong background signals and the relatively weak signal intensity of TatBC complex bands (right pane). In contrast, anti-TatC immunodetection provided clearer signals of these complexes (left pane). At 0.5μM and 1μM TatB, TatC signals corresponding to complexes#1, #2, and #3 were slightly reduced compared to the mock-treated control. And signal of complexes#4 was disappeared. Notably, complexes#4 observed in mock-treated thylakoids cannot be consistently detected by BN-PAGE across independent experiments, likely due to its low abundance in the membrane. But by comparing the method used in this study with that of Rimers (Fig.S2) (Matthias Reimers Dissertation,

MLU, 2021, Section 4.2), we confirmed that this signal represents complex#4 (TatC monomers), rather than a nonspecific band. Taken together, these results suggest that external TatB may mildly destabilize all four TatBC complexes.

However, this interpretation of destabilizing effect alone cannot fully explain why the disassembly occurred at relatively low TatB concentrations (left pane, 0.5µM and 1µM) while higher concentrations of TatB (2µM and 3µM) did not cause further disruption. From 1µM TatB to 3µM TatB, the signals of complexes#1, #2, and #3 stayed stable (left pane). Moreover, this disassembly effect was unexpected, since TatBC complexes, especially the TatC core structure, are structurally stable in the membrane (Behrendt, et al. 2007). Even when TatB was dissociated from TatBC complexes either by high-temperature treatment or hash detergent extraction, the TatC core structure remained intact in the membrane (Matthias Reimers Dissertation, MLU, 2021).

Thus, we propose an alternative possibility that externally supplied TatB may not disassemble TatBC complexes, but instead bind to them and promote a stepwise transition between complex forms. Specifically, TatB may bind to complex #4 to form complex #3; similarly, complex#3 may transition to complex #2, and complex#2 may change to complex#1; eventually complex#1 progresses to even a bigger complex which cannot be detected by BN-PAGE. As a consequence, complex#4 would be the first to disappear, as observed at 0.5µM TatB supplementation (Figure 4.13, left pane, 0.5µM lane). Due to the low abundance of complex#4, its conversion into complex#3 was unable to compensate for the simultaneous consumption of complex#3 to form complex#2, resulting in a decline in complex#3 signal (0-3µM lanes). A similar trend for complex#1 and complex#2 during the early stage, where their formation rate could not compensate for their consumption in forming higher-order complexes, leading to a reduction in their signals (0-1µM lanes). When the rates of formation and consumption reached equilibrium, the signal intensities of the complexes would remain stable, as seen for complex#1 and complex#2 in the later stage (1-3µM lanes). However, this interpretation still cannot fully explain why the signal of complex#3 showed only minimal changes between 1-3µM TatB supplementation and why the highest-order TatBC complex formed by complex#1 is undetectable by BN-PAGE.

Alternatively, at high concentrations (1-3µM), supplemented TatB may tend to form homo-oligomers within the membrane rather than integrating into TatBC complexes. Thus, excessive TatB would not

have further effect neither on complex disruption or complex transition, resulting in stable signal intensities of TatBC complexes (left pane) along with increased signal intensities of TatB homo-oligomers (right pane). However, questions mentioned above for both two models – disruption model and transition model – are still not fully resolved.

Overall, TatB did not show significant effect on the stability of TatBC complexes. As a result, we initially lacked a clear hypothesis to explain why excessive TatB negatively influences Tat transport. However, when examining the effect of TatA on the stability of TatBC complexes, we observed some intriguing results that may provide new insights into the roles of both TatA and TatB in modulating Tat translocation (see Section 4.4 and Discussion 5.1.3 and 5.1.4).

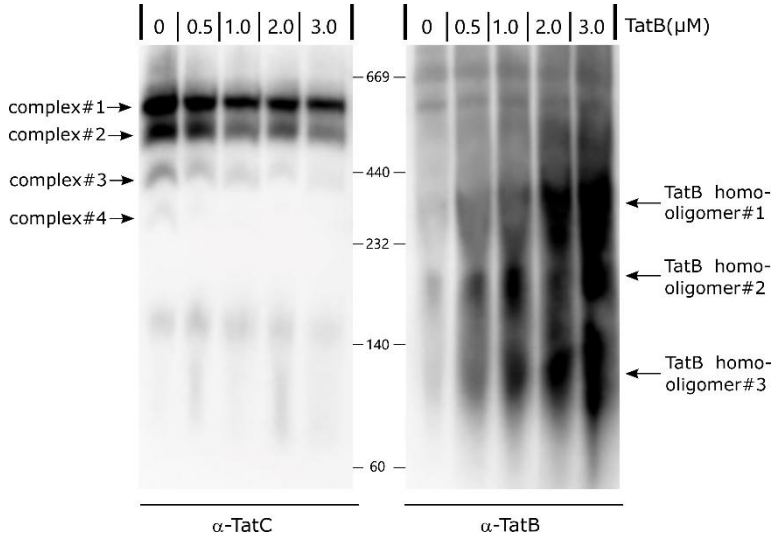

Fig.4.14 Externally supplemented TatB majorly forms oligomers on thylakoid membranes.
Thylakoids corresponding to 30μg chlorophyll were incubated with purified TatB proteins at 25℃ for 20min in light. TatB was obtained from heterologous overexpression. The concentrations of TatB are given above the lanes. Subsequently, thylakoid membranes were washed once and solubilized by BN lysis buffer with 1.67% digitonin (see Method 3.4.6) followed by incubated in 4℃ for 1h for solubilization. The BN-lysis samples corresponding to 30μg of chlorophyll were loaded on a 5%-13.5% gradient BN-PA gel to separate protein complexes (see Method 3.2.2). BN-PA gels were then blotted and developed with specific antibodies against the respective proteins as shown blow the lanes.

4.4 The effect of external TatA on the stability of TatBC complexes

4.4.1 External TatA destabilizes TatBC complexes

As shown previously (Section 4.2.2, Fig.4.9), supplementation of 0.5μM to 2.5μM of TatA into non-antibody-treated thylakoids resulted in a progressive decline in Tat transport activity, rather than reaching a saturation plateau. This unexpected trend prompted further investigation into the underlying mechanism. Given the high similarity in structure and transmembrane helix (TMH) sequence between TatA and TatB (Fig.4.15A), it is plausible that TatA may displace or compete with TatB from its binding site on TatC. Since TatB and TatC form receptor complexes that are essential for substrate recognition and initiation of Tat transport, such competition could disrupt the integrity of TatBC complexes and impair transport efficiency. To test this hypothesis, we analyzed the status of TatBC complexes in non-antibody treated thylakoids supplemented with increasing concentrations of TatA (Fig.4.15).

Surprisingly, TatA affected TatBC complexes even in the absence of substrate (Fig.4.15B). Since the recruitment of TatA into TatBC complexes is based on substrate presence (Mori and Cline 2002), this result was initially unexpected. Along with the increasing concentrations of TatA, a clear and progressive decline in the signals of both TatBC complex#1 and complex#2 was observed (Fig.4.15B). At 1μM TatA, the signal intensities of both two complexes were already significantly reduced compared to non-TatA-supplemented thylakoids; and at 4μM TatA, the signals of them were almost vanished. These observations suggest that the stability of TatBC complex#1 and complex#2 is highly sensitive to external TatA concentration. On the other hand, the signal intensity of complex#3 was already relatively weak under control conditions (0μM TatA), likely reflecting its low abundance in thylakoid membranes. While with 4μM TatA supplementation, the signal intensity of complex#3 remained similar to that of complex#1 and complex#2 (Fig.4.15B). The overall decline in complex#3 signals from 0μM to 4μM TatA was less pronounced than that observed for complex#1 and complex#2, suggesting that complex#3 may be less sensitive to external TatA supplementation.

In addition, since substrate binding may stabilize TatBC complexes by engaging them in their receptor function, we tested whether the presence of Tat substrates affected their stability (Fig.4.15C).

Intriguingly, in the presence of substrates, TatA supplementation led to a similar decline in the signal intensities of TatBC complexes (Fig.4.15C), compared to it observed in the absence of substrates (Fig.4.15B). These results indicate that substrate binding does not protect TatBC complexes from TatA-induced destabilization. Therefore, to avoid potential effects by substrate binding or components from *in vitro* translation system, we decided to exclude substrate supplementation from subsequent experiments.

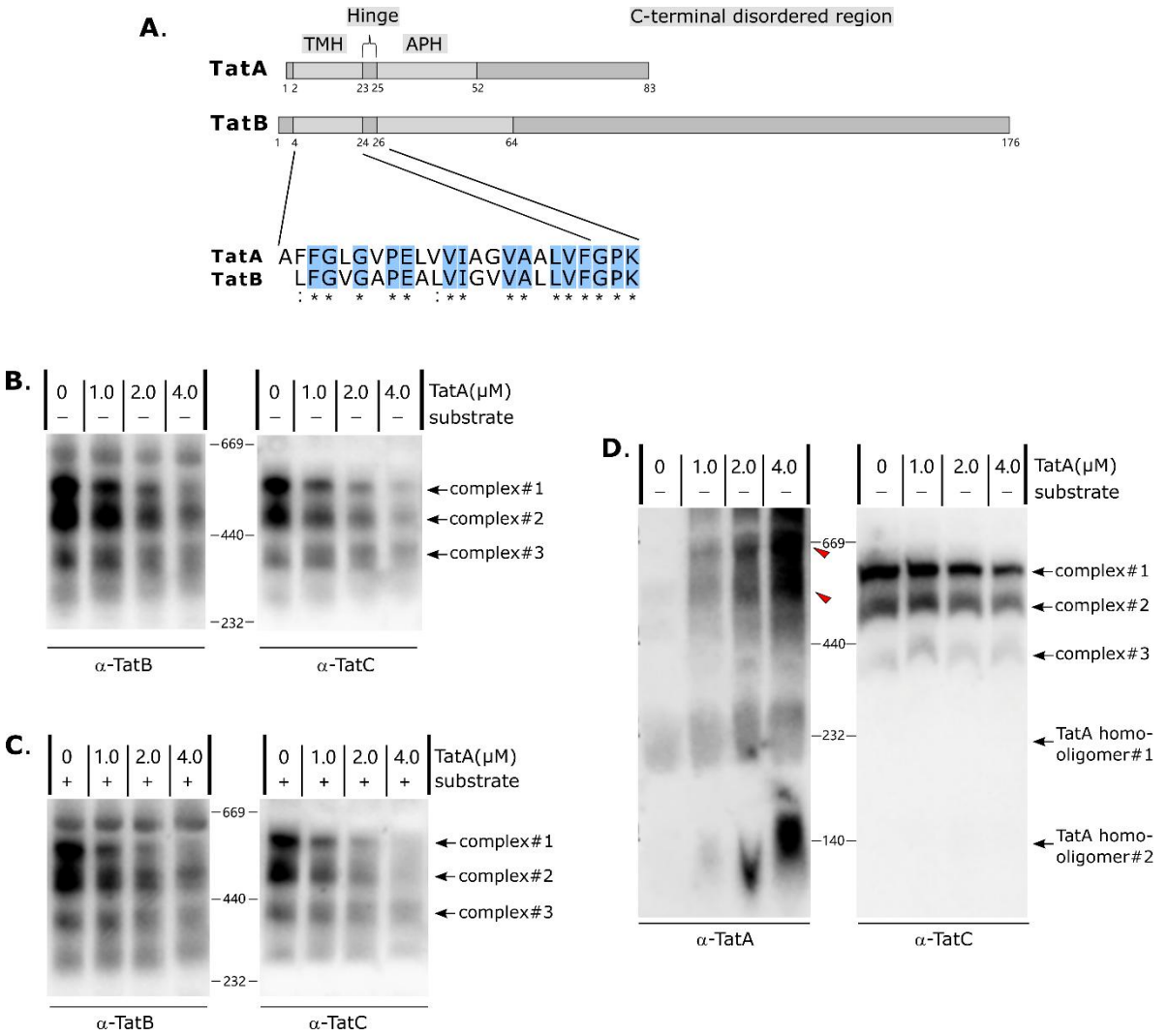

Fig.4.15 The effect of external TatA on TatBC complexes analyzed by BN-PAGE and Western blotting.
(A) Scheme of comparison between the TMH and overall structure of TatA and TatB proteins from pea. (B)(C) Thylakoids were incubated with radiolabeled substrate OEC16 and purified TatA proteins obtained by heterologous overexpression (C) or without substrate (B). OEC16 was synthesized by *Rabbit reticulocyte Lysate System* in the presence of ^{35}S-methionine. Samples were loaded on a BN-PA gel for protein complexes separation. the concentrations of TatA are given above the lanes and the specific antibodies for immunodetection are given below the lanes. For further details see the legend to Fig.4.14. (D) same treatments as (B), but with different antibodies immunodetection as shown below the lanes.

Based on the hypothesis that TatA may displace or compete with TatB for its binding sites on TatC, we next examined TatA-containing complexes by BN-PAGE and Western blot analysis using TatA-antibodies for immunodetection. As a control, TatC was probed in parallel to assess the status of TatBC complexes under the same conditions (Fig.4.15D). Theoretically, TatABC complexes are expected to migrate around ~ 620kDa similar as TatBC complex#1. Upon detection with TatA antibodies, two bands were observed that migrated slightly above the positions of TatBC complex#1 and complex#2 (Fig.4.15D, red triangles). However, these signals were not consistently detected across independent experiments, raising doubts that whether they represent genuine TatA-containing complexes, or they are nonspecific signals. To clarify this, we employed two additional methods for further analysis (Section 4.4.2). On the other hand, TatA oligomers were consistently detected, indicating that the majority of supplemented TatA assembled into oligomers in thylakoid membranes (Fig.4.15D). At 4µM TatA, TatA appeared to form a bigger TatA oligomer#2 than 2µM TatA (Fig.4.15D). However, this shift in migration was not consistently observed and was also seen at other TatA concentrations (Fig.4.15D and Fig.S6A, left pane). Additionally, when radiolabeled TatA was used, only two oligomeric forms of TatA were detected - oligomer#1 around ~250kDa and oligomer#2 around ~120kDa (Fig.S4). Therefore, the migration shift of the ~120kDa complex in Fig.4.15D likely reflects anomalous behavior of this complex during electrophoresis, instead of representing two different TatA complexes.

As shown by Western blot analysis (Fig.4.15B, 4.15C), TatA supplementation led to a decline in the signal intensities of TatBC complexes detected by both TatB and TatC antibodies, whereas no alternative TatB- or TatC-containing complexes appeared or accumulated in parallel. This raises the question of whether the observed signal reduction is due to a genuine structure change in TatBC complexes, or it is simply a result of membrane disruption caused by excessive TatA inserted into thylakoid membranes.

The integrity of thylakoid membranes upon TatA supplementation

Next, we examined whether high concentrations of TatA affect the overall integrity of thylakoid membranes. For this, various concentrations of TatA were supplemented into thylakoids and then the stability of other major thylakoid protein complexes was analyzed (Fig.4.16).

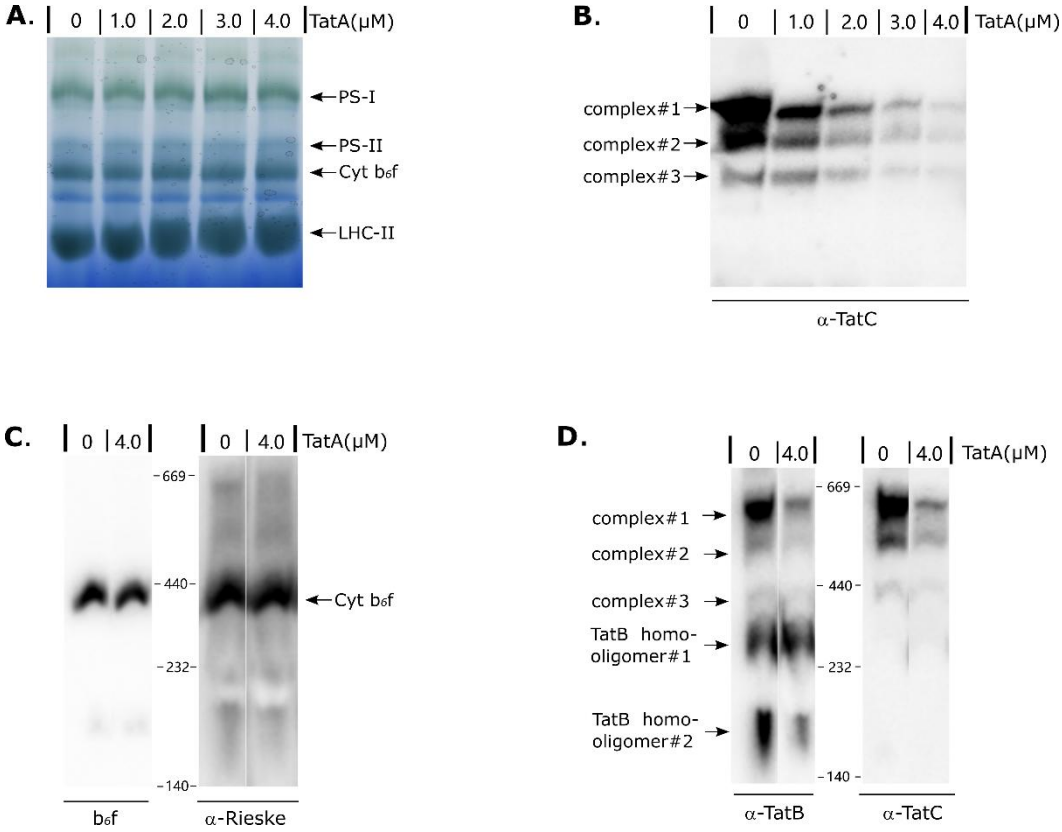

Fig.4.16 The effect of external TatA on other thylakoidal membrane-bound complexes.
Thylakoids were incubated with purified soluble TatA proteins without substrate supplementation. Samples were loaded on a BN-PA gel for protein complexes separation. The concentrations of TatA are given above the lanes. (A) Direct visualization of the BN-PA gel. The *black arrows* point to the positions of photosystem I (PS-I, ca.700kDa), photosystem II (PS-II, ca.480kDa), cytochrome b_6f (Cyt b_6f, ca.430kDa) and light harvesting complexes II (LHC-II, ca.280kDad); (B) same BN-PA gel as (A), but gel was subjected to Western analysis using affinity purified antibodies against TatC; (C) Detection of Cyt b_6f via Western analysis. left pane was the visualization of Cyt b_6f via enhanced chemiluminescence (ECL) without specific antibody probing; right pane was the same BN-PA gel as left, but with specific antibodies against chloroplast Rieske protein with H_20_2 pretreatment to block the endogenous ECL signal. (D) same treatment as (C) but with anti-TatB and anti-TatC immunodetection, as a control comparison with (C). For further details see the legend to Fig.4.14.

After BN-PAGE separation, several membrane-bound complexes could be directly observed on the BN-PA gel (Fig.4.16A). Four major complexes - photosystem I (PS-I), photosystem II (PS-II), cytochrome b_6f complex (Cyt b_6f) and light harvesting complexes II (LHC-II) - remained stable regardless of TatA supplementation (Fig.4.16A). These results indicates that the overall membrane architecture was intact under these conditions. In contrast, TatBC complexes were disassembled by TatA supplementation (Fig.4.16B). To further verify membrane integrity, the stability of Cyt b_6f complex was analyzed by using both intrinsic and antibody-based detection (Fig.4.16C). The Cyt b_6f complex was first visualized directly via enhanced chemiluminescence (ECL) (Fig.4.16C, left pane). This method takes the advantage of the intrinsic peroxidase activity of its heme groups, eliminating the need for specific antibody probing (Li,

et al. 2023; Vargas, et al. 1993). For more specific detection, the same PDVF membrane was probed with antibodies against the chloroplast Rieske protein, a subunit of Cyt b_6f complex. To do this, a pretreatment with H_20_2 is required to block the endogenous ECL signal (Fig.4.16C, right pane). Both detection methods confirmed that Cyt b_6f complex remained unaffected at a high TatA concentration (4μM), as evidenced by no significant differences in signal intensity between TatA-treated and untreated thylakoids (Fig.4.16C). In contrast, TatB and TatC signals from complex#1 and complex#2 were clearly reduced with 4μM TatA supplementation (Fig.4.16D). Taken together, these results indicate that the observed loss of TatBC complex signals is not due to general membrane disruption but it represents a specific effect of TatA on Tat translocase.

The association of TatB and TatC in thylakoid membranes upon TatA supplementation

The next question was whether TatB and TatC remained associated within thylakoid membranes upon TatA supplementation. This concern arose because the signals of TatBC complexes disappeared, and no new TatB- or TatC-containing complexes were observed (Fig. 4.15). At first glance, it seemed that TatB and TatC were somehow excluded from thylakoid membranes. However, this contradicts previous findings showing that both TatB and TatC are integral membrane proteins which are resistant to buffer washing or NaBr extraction (Frielingsdorf, et al. 2008) (see Sarah Zinecker Dissertation, MLU, 2020, Section 3.4.1). To clarify this, we examined the total membrane-associated levels of TatB and TatC by SDS-PAGE and Western blot analysis (Fig.4.17).

Clearly, the overall signals of TatB and TatC proteins were not affected by TatA supplementation (Fig.4.17A right pane, 4.17B). This indicates that TatB and TatC were not excluded from thylakoid membranes. In the anti-TatC detection, the signal in the mock-treated sample appeared slightly weaker than in the other treatments, while the other four treatments showed consistently stronger and comparable signals (Fig.4.17B). Therefore, the weaker signal in mock treatment is likely due to inefficient protein transfer at the edge of the PDVF membrane during semi-dry blotting. It is unlikely to represent a biological difference in TatC abundance. For anti-TatB detection, the Western blot analysis clearly showed that TatA supplementation had no effect on the membrane-associated TatB levels (Fig.4.17A, right pane). Notably, an additional signal above ~30kDa was consistently observed in the

anti-TatB detection across independent experiments. Unfortunately, the identity and exact meaning of this band remain unclear.

On the other hand, as expected, supplemented TatA was integrated into thylakoid membranes, evidenced by membrane-associated TatA levels increasing with the amount of TatA added (Fig.17A, left pane). Notably, no TatA signal was detected in the control sample, despite the known presence of endogenous TatA in thylakoid membranes. This absence is likely due to the small molecular size of TatA (~9kDa), which makes it possibly be lost during blotting and subsequent washing steps. Additionally, partial loss of intrinsic TatA also occurs during thylakoid isolation and sample preparation (see Sarah Zinecker Dissertation, MLU, 2020, Section 3.4.1), further reducing detection sensitivity of TatA. Taken together, these results indicate that neither TatB nor TatC is removed from the membrane upon excessive TatA supplementation. Instead, it appears that TatBC complexes become undetectable by BN-PAGE under these conditions (see Discussion 5.2.2).

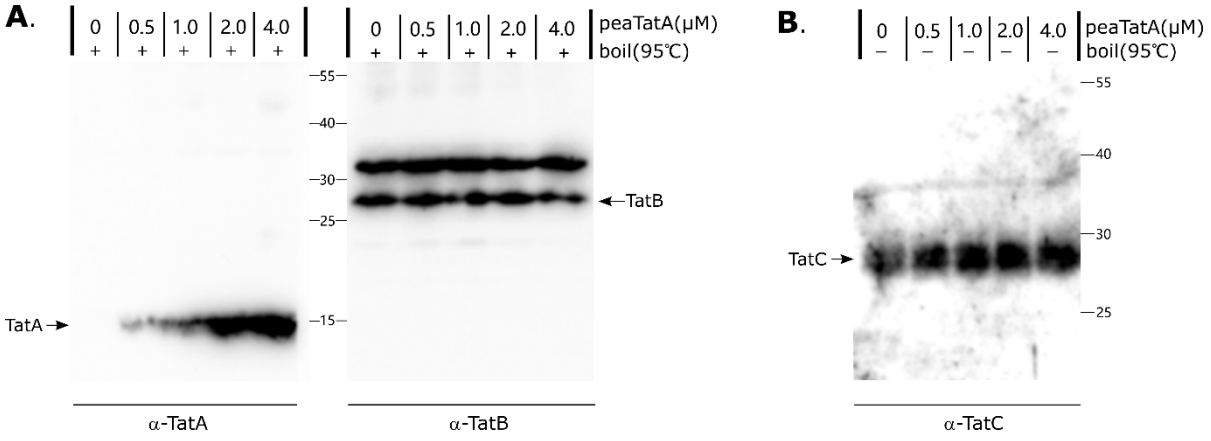

Fig.4.17 Detection of membrane-associated TatA, TatB and TatC levels by SDS-PAGE and Western blotting.
Thylakoids were incubated with purified TatA proteins but without substrate supplementation at 25℃ for 20min in light. The concentrations of TatA are given above the lanes. Subsequently, thylakoid membranes were washed twice and dissolved in Laemmli sample buffer (see Method 3.2.1). For each lane, samples corresponding to 15μg of chlorophyll were loaded on an SDS-PA gel. The SDS-PA gel was subjected to Western analysis with specific antibody immunodetection against the respective proteins as shown blow the lanes. (A) samples was boiled at 95℃ for a better protein degradation and loaded on a 10 – 17.5% SDS-PA gradient gel to separate smaller proteins such as TatA and TatB. (B) For TatC detection, samples were not boiled at 95℃ to prevent aggregation. To get a better separation of TatB and TatC, samples were loaded on a 15% SDS-PA gel and then let the electrophoresis run until the first marker (10kDa) out of the gel.

4.4.2 Can TatABC complexes in thylakoid membranes be detected?

To investigate whether TatABC complexes could be formed upon excessive TatA supplementation, we firstly added ^{35}S-methioine-radiolabeled TatA into non-antibody-treated thylakoids. Membrane-associated complexes were separated by BN-PAGE, and radiolabeled TatA-containing complexes were visualized by autoradiography (Fig.4.18A). The majority of radiolabeled TatA was present as oligomers migrating at approximately 250kDa and 120kDa. Additionally, a faint band was observed around 520kDa (Fig.4.18A, red triangle; Fig.S4, red triangles), which migrated slightly below the position of TatBC complex#2 (Fig.S4). Based on the smaller molecular mass of TatA compared to TatB (8.9kDa and 18.9kDa, respectively), this ~520kDa band may represent a complex formed by TatA replacing TatB. However, this band cannot be considered as convinced evidence of a TatABC complex due to its fairly low signal intensity. Interestingly, when the same amount of ^{35}S-radiolabeled TatA (5µl) was added, a co-supplementation of 2µM unlabeled TatA led to an overall decrease in autoradiograph signal intensity (Fig.4.18A).

Additionally, the membrane complexes from BN-PA gel strips were further separated in the second dimension by SDS-PAGE (Fig.4.18B). In the absence of external TatA supplementation, intrinsic TatA was detected as two dot-like signals around ~120 kDa (upper pane, red asterisks), suggesting that TatA may form two types of oligomers with similar molecular sizes in thylakoid membranes. Two additional signals at ~20kDa and ~35kDa were non-specific cross-reaction by TatA antibodies (upper pane). Upon supplementation with 2µM TatA, TatA formed a broader range of oligomers ranging from approximately 80kDa to 120kDa. The four dot-like signals within this range (lower pane, red asterisks) suggests that excessive TatA formed multiple oligomers of similar but non-identical sizes. In addition, a signal appeared around 232kDa (lower pane) likely corresponds to TatA homo-oligomer#1. However, even with 2µM TatA supplementation, no TatA-containing complexes of higher molecular weight were detected by second dimension separation, suggesting that TatA may not integrate into larger assemblies such as TatABC complexes.

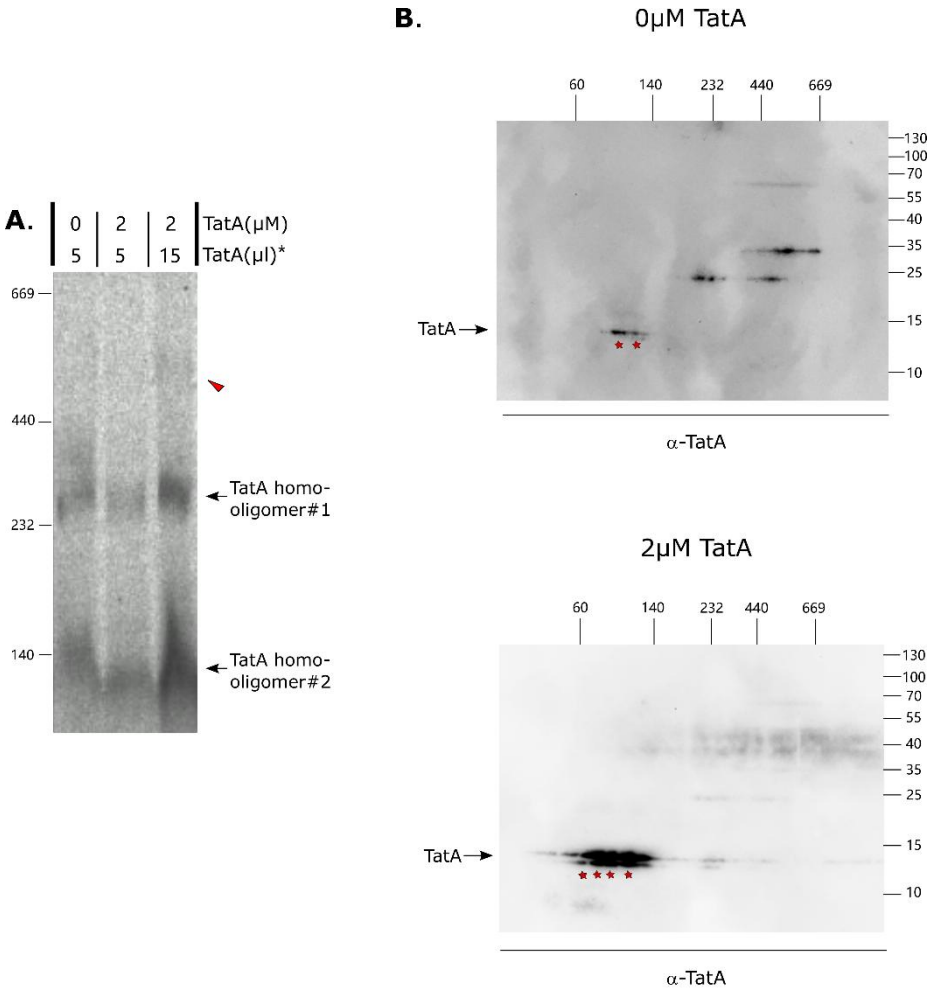

Fig.4.18 Identification of TatA-containing complexes in thylakoid membranes.
(A) Thylakoids membranes corresponding to 30µg chlorophyll were incubated with purified TatA proteins and ^{35}S-radiolabeled TatA obtained from *Rabbit reticulocyte Lysate System*. the concentrations or volumes of TatA are given above the lanes. After solubilization by BN-lysis buffer and 1.67% digitonin (see Method 3.4.6), the samples were loaded on a 5%-13.5% gradient BN-PA gel to separate protein complexes (see Method 3.2.2). Then radioactive signals were detected by phosphorimaging. Here shows the autoradiograph. (B) 2D-analysis of thylakoidal membrane complexes combines BN-PAGE and SDS-PAGE. Thylakoids membranes were incubated with or without 2µM purified TatA. No radiolabeled TatA was supplemented. Further process is same with (A). After BN-PAGE, the strip from BN-PA gel was further analyzed by SDS-PAGE and Western detection using specific TatA antibodies. The *asterisk* indicates multiple TatA oligomers.

4.4.3 Relation between TatA functionality and TatBC complex stability

While the preceding analysis has so far focused exclusively on TatA from pea, which has been shown to functionally reconstitute Tat transport in anti-TatA-treated thylakoids (Hauer, et al. 2017), it was of particular interest to investigate whether other TatA proteins affect the stability of TatBC complexes in thylakoids. For a better comparison, TatA proteins were chosen based on their capability of reaching

successful Tat transport reconstitution in anti-TatA-treated thylakoids. Previous studies demonstrated that wild-type *Arabidopsis* TatA (*atTatA-WT*) was capable of restoring Tat transport activity in anti-TatA-treated thylakoids (Hauer, et al. 2013). In contrast, the *Arabidopsis* E10C-TatA mutant (*atTatA-E10C*) and *E.coli* TatA homolog (*E.coli TatA*) failed to restore the protein transport under same conditions (Hauer, et al. 2017; Hauer, et al. 2013). Therefore, *atTatA-WT* and *pea TatA* are referred as 'functional TatA', while *atTatA-E10C* and *E.coli TatA* are referred as 'unfunctional TatA' in this context. Thus, we examined the impact of all three TatA proteins—*atTatA-WT*, *atTatA-E10C*, and *E. coli TatA*—on the stability of TatBC complexes in pea thylakoids (Fig.4.19).

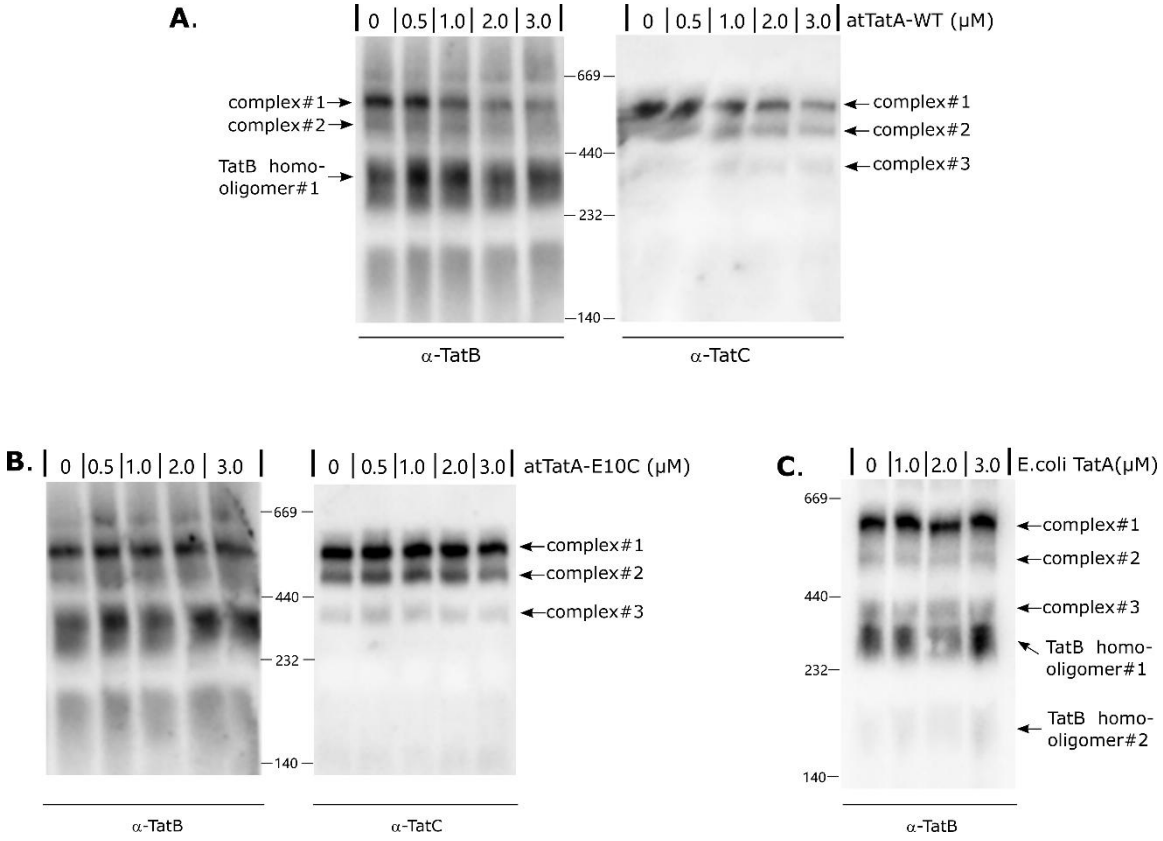

Fig.4.19 The effect of different TatA proteins on the stability of TatBC complexes.
Thylakoids were incubated with three different purified TatA proteins: (A) wild-type *Arabidopsis* TatA (*atTatA-WT*), (B) *Arabidopsis* E10C-TatA mutant (*atTatA-E10C*) and (C) *E. coli* TatA homolog (*E. coli TatA*). The experiment conditions are same with Fig.4.15B the one without substrate supplementation. The concentrations of TatA are given above the lanes and the specific antibodies for immunodetection are given below the lanes. For further details see the legend to Fig.4.14.

As expected, the functional TatA, *atTatA-WT*, influenced TatBC complexes (Fig.4.19A) in a manner similar to pea TatA (Fig.4.15). A concentration-dependent decline in the signal intensities of complex#1

and complex#2 was observed with increasing concentrations of *atTatA-WT*, as detected by both anti-TatB and anti-TatC immunoblotting (Fig.4.19A). In the case of complex#1, even at 1µM *atTatA-WT*, a clear reduction in the signal intensity was observed from both anti-TatB and anti-TatC detection compared to untreated sample; while at 3µM *atTatA-WT*, the complex#1 signal was nearly vanished (Fig.4.19A). Those results suggest that the stability of complex#1 is sensitive to external *atTatA-WT* supplementation.

For complex#2, anti-TatB-detected signals were generally weaker than those of complex#1 (Fig.4.19A, left pane). A faint band was observed in control sample, whereas it almost disappeared with 3µM *atTatA-WT* supplementation (Fig.4.19A, left pane), indicating that TatB in complex#2 was affected by TatA supplementation. On the other hand, TatC signals from complex#2 were more distinct (Fig.4.19A, right pane). The signals at 0µM and 0.5µM TatA were difficult to be distinguished, due to poor blotting efficiency. But a decrease in TatC signal intensity of complex#2 was observed at 3µM TatA compared to 1µM TatA (Fig.4.19A, right pane), suggesting that TatC in complex#2 was affected by TatA supplementation as well. Taken together, *atTatA-WT* also destabilizes complex#2 in a TatA concentration-dependent manner.

Complex#3, however, was more difficult to analyze. In the anti-TatB detection, signals corresponding to complex#3 were hard to distinguish from that of TatB homo-oligomer#1, due to their similar electrophoretic mobility and the strong background associated with TatB antibody probing (Fig.4.19A, left pane). On the other hand, the signals of complex#3 by TatC antibody probing were clear, but the intensities were relatively weak (Fig.4.19A, right pane). When focusing on TatC signals corresponding to complex#3 at 1µM, 2µM and 3µM *atTatA-WT* supplementation, no obvious differences in signal intensities were observed (Fig.4.19A, right pane). This indicates that complex#3 might not be affected, or less affected by high levels of TatA. Altogether, these results indicate that wild-type *Arabidopsis* TatA exerts a similar destabilizing effect on TatBC complexes as pea TatA.

In contrast to *atTatA-WT*, the other two unfunctional TatA proteins, *atTatA-E10C* (Fig.4.19B) and *E.coli TatA* (Fig.4.19C), showed no detectable effect on the stability of TatBC complexes in thylakoids. First, complex#1 remained unaffected by either *atTatA-E10C* (Fig.4.19B) or *E. coli TatA* supplementation (Fig.4.19C). Second, both TatA proteins also had no effect on complex#2. In *atTatA-E10C*-supplemented

assays, complex#2 was difficult to assess by TatB antibody probing, due to weak and ambiguous signals (Fig.4.19B left pane). But by TatC antibody probing, clear signals were observed, which show no significant change in complex#2 (Fig.4.19B, right pane). In the case of *E. coli TatA*-supplemented assays, complex#2 signals detected by anti-TatB were weak but discernible from background, again suggesting no effect on complex#2. Third, complex#3 remained stable across all tested TatA concentrations. Although signals of complex#3 by anti-TatB detection were difficult to be separated with signals of TatB homo-oligomer#1 (Fig.4.19B, 4.19C), TatC antibody probing shows clear complex#3 signals (Fig.4.19B, right pane). These signals showed no significant differences across TatA concentrations. A slightly stronger signal at 0.5µM TatA was observed, but the overall intensity remained stable even at 3µM, indicating that complex#3 was not affected by *atTatA-E10C* supplementation. In short, only those TatA proteins that can functionally reconstitute Tat transport in anti-TatA–treated thylakoids affect the stability of TatBC complexes, whereas non-functional TatA proteins lack this capability.

4.4.4 Does the stability of TatBC complexes correlate to Tat transport efficiency?

In earlier experiments, TatA and substrate OEC16 were supplemented simultaneously prior to light incubation (Section 4.2.2, Fig.4.9), where we observed a TatA concentration-dependent decrease in transport efficiency. This led to the hypothesis that excessive TatA may affect the stability of TatBC complexes, thereby impairing Tat transport. And indeed, we observed destabilization of TatBC complexes by external TatA (Section 4.4.1). However, in the earlier setup, the potential disassembly of TatBC complexes may happened before, coincided with, or after substrate translocation, making it difficult to determine the correlation between the disassembly of TatBC complexes and Tat transport efficiency. To address this, we modified the assay by pre-incubating thylakoids with TatA alone under light for 20 minutes, allowing the disassembly of TatBC complexes. Subsequently, radiolabeled substrates were directly added to the samples and a further 5min incubation under the same light conditions were preformed to enable Tat-dependent protein transport (Fig.4.20).

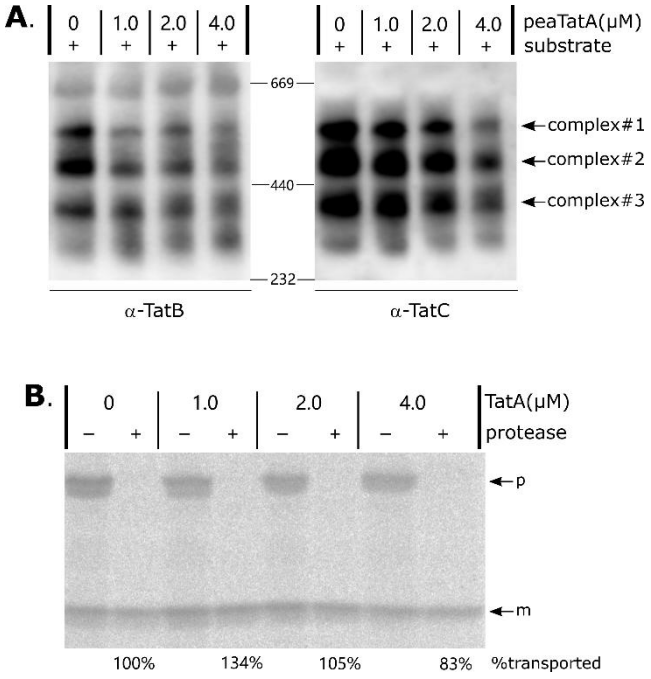

Fig.4.20 Tat transport efficiency was not linear correlated to the stability of TatBC complexes analyzed by BN-PAGE.
Thylakoids were pre-incubated with purified peaTatA at 25°C for 20min in light. The concentrations of TatA are given above the lanes. Following this pre-incubation, 5µl of radiolabeled substrate OEC16 was added into thylakoids followed by another 5min incubation under same conditions. OEC16 was obtained from *Rabbit reticulocyte Lysate System* in the presence of ^{35}S-methionine. As the transport competence of isolated thylakoids tends to decline over time, a short 5-minute incubation was selected which is efficient for OEC16 transport. After transport reaction, samples were wash once and equally divided into two fractions: (A) one fraction was centrifuged down to get the pellet. The pellet was solubilized by BN-lysis buffer and 1.67% digitonin in 4°C for 1h. Then samples were equally divided into two and loaded on a BN-PA gel for anti-TatB and anti-TatC immunodetection respectively. (B) another fraction was also centrifuged down to get the pellet. Then the pellet was dissolved in 200µl HM buffer and subsequently separated into two Epi-tubes, for each containing 100µl sample. One tube was treated with thermolysin and another was treated with HM buffer. For further experimental details, see Fig.4.1. Samples were loaded on an SDS-PA gel for further analysis. Here is the autoradiogram of the gel and radioactive signals were detected by phosphorimaging. Quantification of the amount of translocated protein *(m)* from transport reactions was shown below the lanes. For each TatA concentration, the relative amount of translocated protein*(m)* was calculated in terms of percentage of the corresponding control reaction *(0µM)* in *+ protease* lines.

As expected, preincubation with TatA followed by subsequent supplementation of Tat substrate resulted in a progressive disassembly of the three TatBC complexes, as detected by both anti-TatB and anti-TatC immunoblotting (Fig.4.20A). Interestingly, despite the clear decline in both TatB and TatC signal intensities at 1µM TatA (Fig.4.20A), the same concentration of TatA led to a higher transport efficiency compared to the control (Fig.4.20B). But as the TatA concentration increased from 1µM to 4µM, a corresponding decline in transport efficiency was observed (Fig.4.14B). These results suggest a potential, but not linear, correlation between the stability of TatBC complexes and transport efficiency. Notably, the enhanced transport observed at low concentrations of external TatA is possibly due to

compensation for the loss of intrinsic TatA during thylakoid preparation. Therefore, the interpretation between TatA levels, the stability of TatBC complexes, and transport activity may involve a balance between facilitative and disruptive effects of TatA, rather than a direct linear relationship (see Discussion 5.1.4).

4.4.5 Reassembly by TatB of TatA-induced destabilized TatBC complexes

As demonstrated previously (Section 4.4.1), external TatA destabilized TatBC complexes. This observation suggests that TatA may displace or compete with TatB for its binding sites on TatC, thereby leading to the complex disassembly. If this hypothesis holds true, then supplementation with external TatB should counteract the disruptive effect of excessive TatA by competing for its binding sites and promote the reassembly of TatBC complexes. Particularly, the interaction between TatB and TatC is stronger than that between TatA and TatC. To test this, various concentrations of TatB were supplemented in the presence of 3µM TatA, and the status of TatBC complexes was analyzed by BN-PAGE and Western blotting (Fig.4.21). As control, neither TatA nor TatB was added to assess the intrinsic status of TatBC complexes (lane ①).

Consistent with prior results, 3µM TatA supplementation alone led to the disassembly of TatBC complex#1 and complex#2, while complex#3 could not be reliably distinguished from background signals (Fig.4.21, lane ②). When TatB was added to thylakoids already containing 3µM TatA, a partial reappearance of complex#1 and complex#2 was observed, as evidenced by increasingly discernible bands at 2µM and 3µM TatB (lanes ⑤ and ⑥). However, due to increased background signals, particularly at higher TatB concentrations, it remains inconclusive whether complex#1 and complex#2 were truly reassembled by the added TatB. Interestingly, the signal of complex#3 became slightly distinguishable at 0.5µM and 1µM TatB (red triangles), whereas it was undetectable in both non-TatB added thylakoids (lanes ① and ②). This suggests that complex#3 may have been reassembled. However, at 2µM and 3µM TatB supplementation (lanes ⑤ and ⑥), the signal of complex#3 could not be separated from the signal of TatB oligomer#1, making it difficult to determine whether reassembly had occurred or not. Notably, at high concentrations (2µM and 3µM), the majority of

externally supplemented TatB formed homo-oligomers (lanes ⑤ and ⑥).

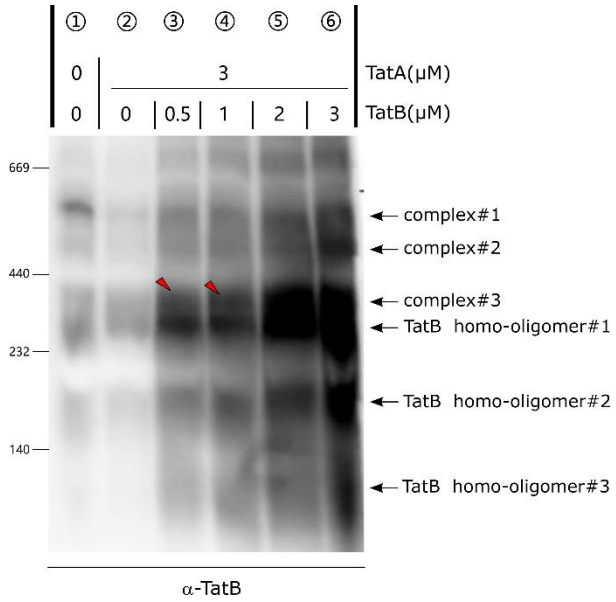

Fig.4.21 The effect of TatB supplementation on disassembled TatBC complexes by external TatA.
Thylakoids were incubated with 3μM purified TatA proteins and a range of concentrations of TatB proteins. As a positive control, thylakoid membranes were not supplemented with neither TatA or TatB proteins *(lane①)*. As a negative control, thylakoid membranes were only supplemented with 3μM TatA *(lane②)*. Lane ③-⑥ were to examine whether supplemented TatB was able to rescue the disassembly of TatBC complexes. The composition of TatA and TatB were shown above the lanes. Samples were solubilization by BN-lysis buffer and 1.67% digitonin, followed by Western analysis and specific TatB antibodies immunodetection. For further experimental details see the legend to Fig.4.14

4.5 The effect of PMF on the stability of TatBC complexes

It is well-established that the recruitment of TatA is dependent on the proton motive force (PMF) across the thylakoid membrane (Aldridge, et al. 2014). Our results showed that TatA affected the stability of TatBC complexes (Chapter 4.4). This raises the question of whether PMF also plays a role in modulating TatBC complexes stability. Before directly assessing TatBC complexes, we first performed a time-course analysis of Tat transport efficiency, using two compounds, ADP and $NADP^+$ (Fig.4.22). They were chosen because both of them are involved in energy-related reactions that influence PMF across the thylakoid membrane.

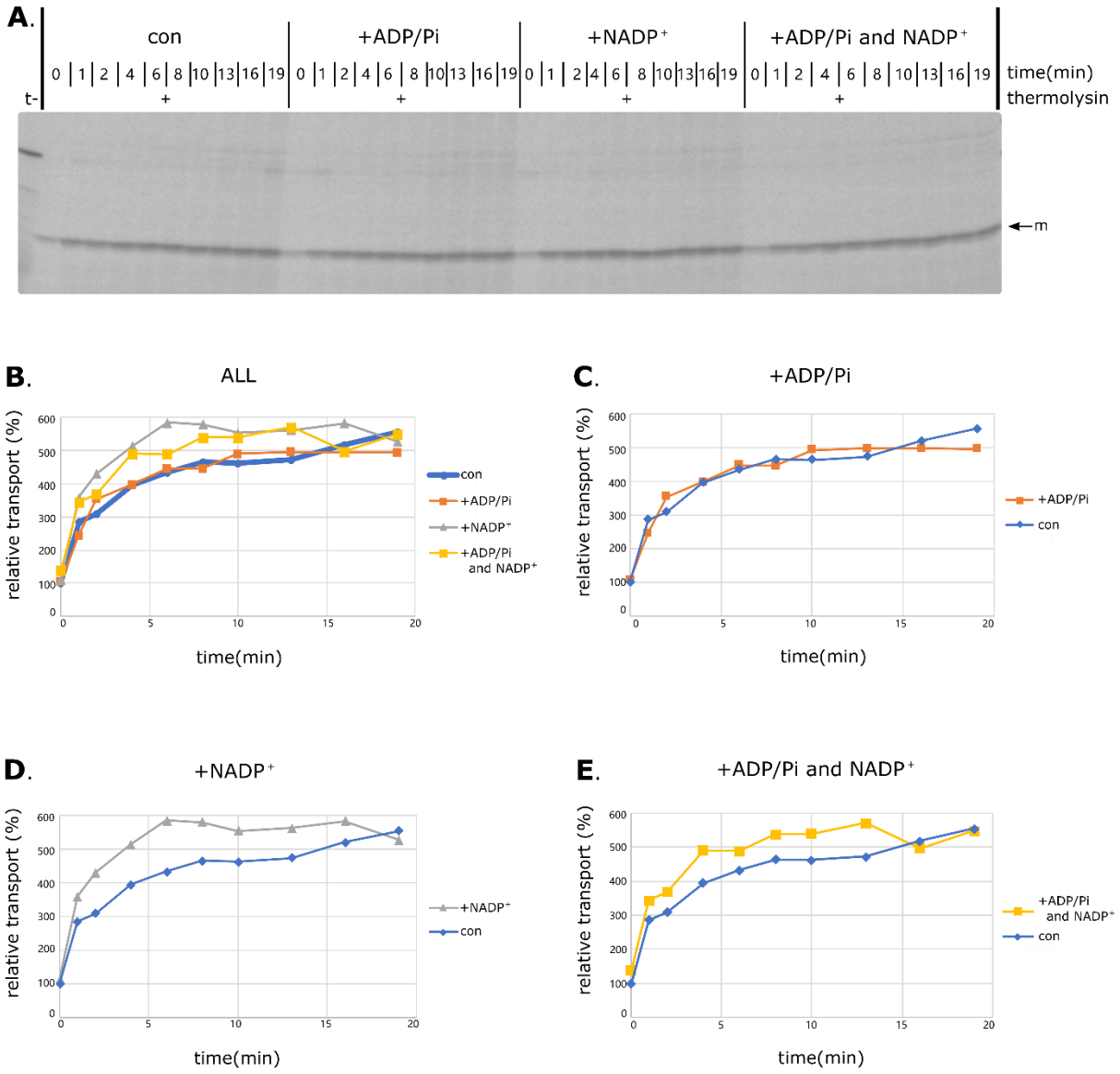

Fig.4.22 The effect of NADP+ and ADP/Pi on Tat transport efficiency in thylakoid membranes.
Time-course of OEC16 transport was analyzed with supplementation of ADP/Pi and NADP+, separately and combined. Substrate OEC16 was synthesized by *Rabbit reticulocyte Lysate System* in the presence of ^{35}S-methionine. 2.5ul of substrate was added into the thylakoids corresponding to 15μg of chlorophyll. ADP, Pi (KH_2PO_4), NADP+ was dissolved in water as a stock with the concentration of 100mM for all. The final concentrations of ADP, Pi (KH_2PO_4), NADP+ in the assays were 0.5mM, 1mM, 0.5mM respectively. Thylakoids were supplied with the substrate and corresponding components and then were incubated at 25℃ in the light for the time periods indicated on top of the lanes. After the indicated incubation time, the transport reaction was stopped by adding 40μl ice-cold HM buffer and immediately transferred to centrifugation at 4000rpm for 4min. Subsequently, the pellet was dissolved in Laemmli buffer and load on an SDS-PA gel. (A) The autoradiogram of this experiment. (B)-(E) quantification analysis of the amount of translocated protein *(m)* from transport reactions which is identical to that shown in (A). For each lane, the relative amount of translocated protein *(m)* was calculated in terms of percentage of the control reaction at 0min *(con, lane 0min)*.

Interestingly, under all experimental conditions, even at 0min (i.e., before light incubation), a low level of Tat transport was still detectable (Fig.4.22A). This residual activity may be attributed to a weak

but persistent H^+-gradient that remains across thylakoid membranes in the dark. Upon light stimulation, even a brief one-minute illumination led to a significant increase in protein transport across all conditions, suggesting that a rapid buildup of PMF stimulating Tat transport (Fig.4.22A). In the control assays, Tat transport was largely stimulated by the first one-minute illumination and continued to gradually increase until 19min (Fig.4.22B). Compared to the control, supplementation with ADP/Pi showed no clear stimulatory or inhibitory effect on Tat transport (Fig.4.22C). Tat transport with ADP/Pi supplementation appeared to reach a saturation plateau after 10min, whereas the intrinsic Tat transport (i.e., control treatment) continued to show slowly increased import until 19min (Fig.4.22C). In contrast, $NADP^+$, a compound directly involved in photosynthetic electron flow that generates the H^+-gradient across thylakoid membranes, enhanced Tat transport throughout the 19-minute time course (Fig.4.22D). However, due to the rapid saturation point (6min) observed in $NADP^+$-supplemented assays, it seemed that $NADP^+$ primarily boosted the initial rate of transport but without providing additional benefit at later time points. When ADP/Pi and $NADP^+$ were combined, Tat transport was still enhanced (Fig.4.22E), but the combined effect did not exceed the benefit observed with $NADP^+$ alone (Fig.4.22B, compare yellow line and gray line).

Assessment of TatBC complexes

Following the analysis of Tat transport efficiency in the presence of ADP and $NADP^+$, we next investigated whether these compounds also affect the stability of TatBC complexes. In addition, we introduced an ionophore, gramicidin, into the assays to disrupt the H^+-gradient across the thylakoid membrane. Moreover, given that the H^+-gradient is primarily generated by photosynthetic electron transport, two additional conditions were established as reference: one with light control to regulate the photosynthetic activity, and the other with temperature control to regulate overall enzymatic activities on thylakoid membranes (Fig.4.23A).

Under fully activated conditions (25℃, light; Fig.4.23A, lane ①), all three TatBC complexes were detected, although the signal of complex#3 was much weaker than it of complex#1 and complex#2. However, when photosynthesis was selectively inhibited - by maintaining the temperature at 25℃ while omitting light (lane ②) - the predominant TatBC complex#1 disappeared, and more complex#3

arose. This indicates that the H^+-gradient generated by photosynthesis is important for maintaining complex#1 under fully activated conditions and that its absence leads to a redistribution of bigger complexes into smaller complexes. Moreover, the overall signal intensities of TatBC complexes under 25 ℃ and dark conditions was lower than that under fully activated conditions (compare lanes ① and ②), suggesting that some TatBC complexes may disassemble into smaller complexes or monomers undetectable by immunodetection. On the other hand, under restricted conditions (4℃, dark; lane③) where the overall enzymatic activities were restricted by low temperature and dark environment, the status of TatBC complexes remained similar to that observed under fully activated conditions. This suggests that TatBC complexes stay stable in inactive membranes. In short, under fully active conditions, photosynthetically generated H^+-gradient is required to maintain predominant complex#1 (compare lanes ① and ②); while under restricted conditions, the stability of TatBC complexes appear to be unaffected despite the lack of H^+-gradient (compare lanes ①②③).

Unexpectedly, under conditions where photosynthesis was eliminated but other enzymatic activities was stay active (25℃, dark), supplementation with ADP/Pi appeared to stabilize complex#1 and complex#2 (Fig.4.23A, compare lane ② and ADP/Pi assays). Specifically, 9mM ADP/Pi seemed to promote the reassembly of complex#3 into complex#1 and complex#2, while 16mM ADP/Pi may reassemble those undetectable smaller complexes or monomers into complex#2 and complex#3 (Fig.4.23A, ADP/Pi assays). These observations were surprising, as external ADP/Pi is expected to help dissipating the H^+-gradient by facilitating ATP synthase activity, promoting proton pumped from lumen to stroma. Based on this, an enhanced disassembly of complex#1 would be expected, rather than stabilization or reassembly. Possible explanations are discussed in Discussion 5.2.1.

Given the central role of $NADP^+$ in photosynthesis and its contribution to creating the H^+-gradient across thylakoid membranes, we supposed that $NADP^+$ supplementation might help stabilize TatBC complexes. However, no clear differences were observed between $NADP^+$-supplemented samples and the control (Fig.4.23A, compare lane① and $NADP^+$ assays). Taken together that TatBC complexes stayed stable under restricted conditions, these results suggest that a small level of H^+-gradient may be sufficient for keeping TatBC complexes stable. At 9mM $NADP^+$, it appeared to be a mild increase in the signal intensity of complex#2, while the signal of complex#1 remained unchanged (compare lane ① and lane-$NADP^+$ 9mM). Increasing the $NADP^+$ concentration to 16 mM did not further enhance the

complex#2 signal (compare $NADP^+$ 9mM and 16mM lanes). However, since $NADP^+$ supplementation seemed to have no significant impact on TatBC complexes, this experiment was only conducted once. Hence, we cannot draw definitive conclusion regarding the effect of $NADP^+$ on the stability of complex#2.

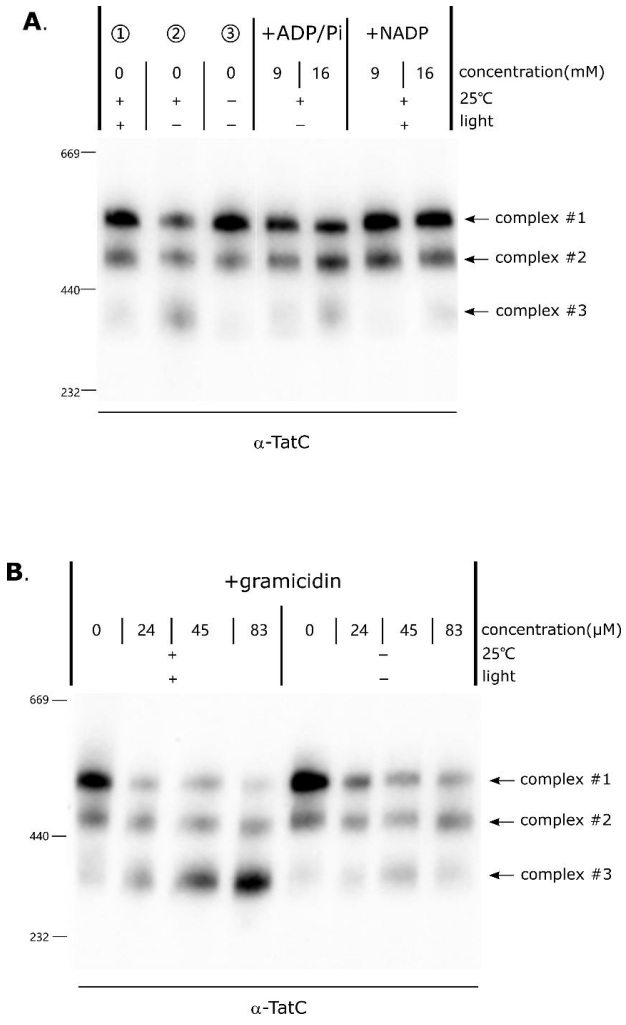

Fig.4.23 PMF across thylakoid membrane influence the state of TatBC complexes.
(A) the status of TatBC complexes under conditions of different proton gradients across the thylakoid membrane was analyzed. As a positive control, *lane*① is the standard conditions *(+ 25℃, + light)* used for our import assays, referring as 'fully activated conditions' in the context. As a negative control, *lane*② incubated samples under same conditions as *lane*① but prevented light stimulation by wrapping samples with aluminum foil *(- light)*, to eliminate the proton gradients generated by photosynthesis, referring as 'photosynthesis was selectively inhibited' in the context. *Lane*③ is to estimate the status of TatBC complexes in relatively inactive thylakoid membranes under the conditions of 4℃ on ice *(- 25℃)*, with aluminum foil *(- light)*, referring as 'restricted conditions' in the context. *Lanes ADP⁺/P*i were to examine whether the activity of ATPase showed an impact on TatBC complexes. *Lanes NADP⁺* were to examine whether the activity of photosynthesis showed an impact on TatBC complexes. The incubation time was 20min with the indicated conditions as shown above the lanes. All the thylakoid samples were solubilization by BN-lysis buffer and 1.67% digitonin, followed by Western analysis and specific TatC antibodies immunodetection. (B) Thylakoid membranes were treated with a range of concentrations of gramicidin under two different conditions: standard import condition *(+ 25℃ , + light)* and restricted condition *(- 25℃, - light)*. The concentrations of gramicidin are given above the lanes. The incubation time was 20min. Thylakoid samples were solubilization by BN-lysis buffer and 1.67% digitonin, followed by Western analysis and specific TatC antibodies immunodetection.

Moreover, to investigate the status of TatBC complexes in the complete absence of proton gradients, we introduced an ionophore, gramicidin, into the assays to dissipate the H^+-gradient across thylakoid membranes (Fig.4.23B). Regardless of whether enzymatic activities were fully activated (25℃, light) or restricted (4℃, dark), gramicidin treatment led to a clear reduction in the signal of TatBC complex#1, indicating that the integrity of this complex depends on the presence of proton gradients. In contrast, the signal of complex#2 was unaffected by gramicidin. The behavior of complex #3, on the other hand, appeared to be dependent on additional light-dependent processes. Under fully activated conditions, increasing concentrations of gramicidin led to an accumulation of complex#3, concurrent with the reduction of complex#1 (Fig.4.23B, left part). However, under restricted conditions, complex#3 did not accumulate despite the disappearance of comple#1 (Fig.4.23B, right part). Those results suggests that when proton gradients were dissipated, some additional light-dependent processes under fully activated conditions facilitated the formation of complex#3. Intriguingly, under restricted conditions (4℃, dark), addition of 24mM gramicidin significantly induced the disassembly of complex#1, whereas increasing concentrations of gramicidin did not further enhance this effect. This suggests the possible involvement of so-called localized protons that are not equilibrated with the aqueous phase proton (see Discussion 5.2.1). Taken together, the formation of TatBC complex#1 depends on the presence of H^+-gradient across thylakoid membranes; when H^+-gradient is dissipated, complex#3 is formed but depends on additional light-dependent processes (see Discussion 5.2.1).

5 Discussion

5.1 The role of TatA and TatB in thylakoidal Tat-dependent protein transport

5.1.1 Functional substitution of TatA by TatB in Tat translocase

TatA and TatB are two essential subunits in Tat translocase, which belong to same protein family but fulfill distinct functions (Hauer, et al. 2013; Lee, et al. 2002; Zinecker, et al. 2020). Given their high similarity in both overall structure and transmembrane helix (TMH) sequences (Fig.1.2, Fig.4.15A), a potential functional-redundancy between TatA and TatB has been considered, raising the possibility that they may substitute for each other within Tat translocase. In pea thylakoids, our results partially support this hypothesis by showing that TatB is able to achieve functional substitution of TatA within Tat translocase. However, on the other way around, TatA is unable to functionally substitute TatB (see Section 4.2, Fig.4.7 and Fig.4.10). Apparently, TatB possesses some unique functional regions that cannot be compensated for by TatA, while the functional regions of TatA can be compensated for by TatB.

The N-terminal region including TMH have been implicated in the functional importance of TatA. cross-linking studies have shown that some residues within the N-terminus of TatA are important for the interaction with other TatA molecules, TatB, TatC and Tat substrates (Aldridge, et al. 2014; Blummel, et al. 2015; Taubert, et al. 2015). In addition, mutagenesis studies also show the functional importance of TatA N-terminal residues (Alcock, et al. 2016; Barrett and Robinson 2005; Hao, et al. 2023). Even minor alterations in the TMH of TatA, such as single or double amino acids substitutions, could completely diminish the function of TatA protein (Dabney-Smith, et al. 2003; Hauer, et al. 2017; Hauer, et al. 2013). Unlike the TMH of TatA harbors functional importance, the C-terminal region of TatA appears dispensable for its function. For instance, a truncated TatA, which lacks nearly half of the amino acids from C-terminus, still retains a full activity (Lee, et al. 2002). Therefore, although TatB diverges significantly from TatA in its C-terminal region, its high sequence similarity to TatA in the N-terminal TMH (Fig.S3 A,B) has led to the hypothesis that TatB may be capable of functionally substituting for

TatA. Indeed, our results demonstrate that TatB is able to substitute for TatA in thylakoidal Tat translocase (Fig.4.7). Hence, our observations reinforce the conclusion that the N-terminal regions of TatA are essential for its function, whereas the C-terminal region is not.

On the other hand, the functional uniqueness of TatB has been indicated to lie in its amphipathic helix (APH) and C-terminal region. First, exogenous TatB protein is well-established to restore Tat-dependent transport lacking intrinsic TatB activity. Either TatB expressed from a plasmid in a TatB-absence background in *E. coli* (Lee, et al. 2002) or supplemented externally into a TatB-blocked thylakoid system (Zinecker, et al. 2020), is able to fully restore Tat transport. However, a chimeric TatBA protein, composed of the N-terminus, TMH and the hinge region of TatB fused to the APH and C-terminal region of TatA, fails to complement the absence of intrinsic TatB in Tat transport (Lee, et al. 2002)(see Sarah Zinecker Dissertation, MLU, 2020, Section 3.6.3). Those results indicate that the APH and C-terminal region of TatA cannot functionally substitute for the corresponding regions of TatB. Second, a truncated TatB with the length comparable to the TatBA chimeric protein still retains a diminishing but distinct level of Tat-dependent transport activity (Lee, et al. 2002). This result further suggests that the failed substitution by TatBA for TatB is not a matter of protein length but is due to the loss of functional specificity of TatB in the APH and the adjacent C-terminal region. Third, a chimeric TatAB protein, which comprises the N-terminus, TMH and the hinge region of TatA fused to the APH and C-terminal region of TatB, can successfully complement the loss of intrinsic TatB in Tat transport in thylakoid membranes (see Sarah Zinecker Dissertation, MLU, 2020, Section 3.6.3), indicating that the TMH of TatA and TatB are replaceable. Also, TatB can functionally substitute for TatA (Fig.4.7) reinforce this indication (see Discussion above). Taken together, our finding that TatA is not able to functionally substitute for TatB in Tat translocase confirms that the residues of TatB in its APH and C-terminal region, rather than in its TMH region, are functionally indispensable and cannot be replaced by the corresponding residues in TatA (comparison between TatA, TatB and chimeric proteins, see Fig.5.1).

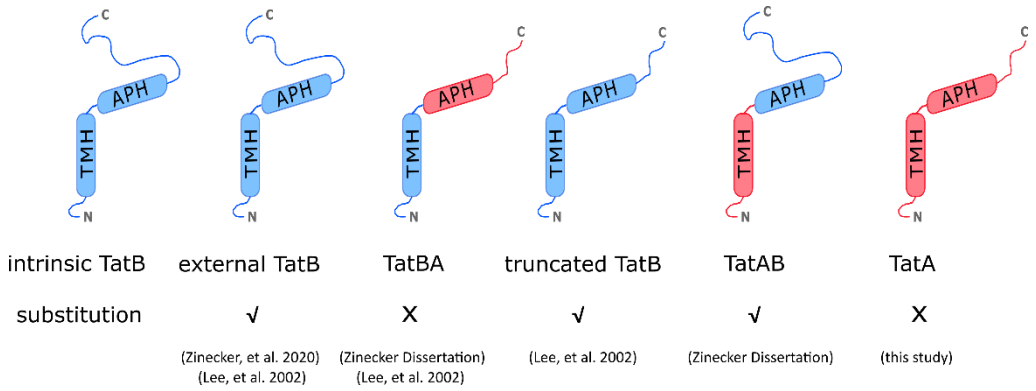

Fig.5.1 Comparison between chimeric proteins, TatA, and TatB in the substitution of intrinsic TatB function.
Schematic representation of TatB, TatA and chimeric proteins. To create chimeric constructs, the N-terminus, TMH, and the hinge region (as a line between TMH and APH) were exchanged between TatA and TatB. This region is referred to as the 'TMH region'. Therefore, TatBA is TatB-TMH region fused with APH and C-terminal region of TatA. TatAB is the reverse chimera. *Blue* represents the part from TatB and *red* represents the part from TatA. Here we did not distinguish TatA or TatB from *E. coil* or pea, since they show similar structure. Notably, in the study of Lee, et al. (2002), they tested TatA, TatB and chimeric proteins from *E. coil*, while in the study of Zinecker, et al. (2020), Zinecker dissertation and of the thesis, we tested proteins from pea.

Intriguingly, our study shows that both TatB and TatBA chimeric protein are capable of functionally substituting for intrinsic TatA in Tat translocase in the pea thylakoid (Fig.4.7) (see Sarah Zinecker Dissertation, MLU, 2020, Section 3.6.3). This contrasts with previous reports showing that neither of these proteins could complement TatA deficiency in *E. coli* (Lee, et al. 2002) and that even in pea thylakoids TatB failed to functionally replace TatA (Dabney-Smith, et al. 2003). Notably, the latter study also used pea thylakoids, but TatB was synthesized by *in vitro* translation, a method that generally yields relatively low protein concentrations. Given that a relatively high TatB concentrations are required for the substitution of TatA in our assays (Fig.4.7), it is possible that TatB produced in their study did not reach the effective concentration threshold that is necessary for functional replacement. Moreover, we observed that TatB proteins which were expressed from the same cDNA source exhibited different activities depending on *in vitro* translation systems used for protein synthesis (see Section 4.1.1.1, Fig.4.1). This suggests that certain systems may exhibit post-translational modifications, or contain interfering proteins that affect TatB activity. In contrast, the present study (Fig.4.7) used purified TatB protein produced by heterologous overexpression, which minimizes potential contamination and produces protein in high purity. Therefore, differences in protein production methods may account for the apparent discrepancies in TatB functionality across studies.

When aligning the TMH sequences of TatA and TatB from *Pea Sativum* and *E. coli*, respectively

(Fig.S3 C), we observed a notable difference in sequence conservation. In *Pea Sativum*, TatA and TatB share 60.87% identity within the TMH region, whereas in *E. coli*, TatA and TatB show only 35% identity, with 40% gap. Notably, the TatBA chimeric protein can substitute for intrinsic TatA in pea thylakoids (see Sarah Zinecker Dissertation, MLU, 2020, Section 3.6.3) but fails to do so in *E. coli* (Lee, et al. 2002). this contrast implies that TMH domain of *E. coli* TatB may lack some critical residues which are required for TatA function.

The observation that TatB can substitute for TatA in pea thylakoid membranes but not in *E. coli* cytoplasmic membranes may reflect the evolutionary divergence within the TatA protein family. In *Campylobacter jejuni*, a single TatA protein is sufficient to mediate Tat-dependent protein transport (Liu, et al. 2014). While *Bacillus subtilis* has three TatA proteins (TatAc, TatAd, TatAy), where TatAy exhibits similar function as *E. coli* TatB and TatAc functions analogously to *E. coli* TatA, suggesting *B. subtilis* represents an intermediate stage in the evolution of TatA-TatB specialization (Goosens, et al. 2015). Furthermore, TatAd from *B. subtilis* is able to functionally substitute for both TatA and TatB in *E. coli* (Barnett, et al. 2011), indicating that *B. subtilis* TatA proteins evolved prior to the full functional differentiation of TatA and TatB. Here, our results demonstrate that pea TatB can functionally replace TatA in pea thylakoids. This functional substitution may reflect an early evolutionary stage of TatA-TatB specialization, where TatA and TatB still retain overlapping functional features. In contrast, in later evolutionary stages, TatA and TatB have evolved distinct, more specific functions, where they are no longer interchangeable, such as *E. coli* TatA and TatB.

5.1.2 Do TatA and TatB share the same binding sites?

Some studies have proposed that TatA and TatB share the same binding sites on TatC (Blummel, et al. 2015; Habersetzer, et al. 2017). At first glance, our results appear to support this idea. First, we observed that excessive TatA/TatB result in a decrease in Tat transport efficiency, which likely due to the competition between TatA and TatB (see Section 4.2.1, Fig.4.6; Section 4.2.2, Fig.4.9). Second, TatA could affect the stability of TatBC complexes possibly by replace TatB on the complexes (see Section 4.4.1, Fig.4.15). However, a more detailed analysis of our data reveals that this interpretation is insufficient and may not adequately explain the observed results in our assays.

First, if the decrease by excessive TatA in Tat transport is the result of TatA competing with intrinsic TatB for binding sites on TatC, leading to fewer functional TatBC complexes. In that case, increasing TatB concentrations should outcompete TatA. As a result, transport efficiency would be expected to recover. However, when TatB was supplemented into 3µM-TatA-containing thylakoids, no convinced evidence showed the reassembly of TatBC complexes (Fig.4.21). Moreover, when various concentrations of TatB were added to both 3µM-TatA-supplemented and non-TatA control assays, transport efficiency remained even lower in the presence of 3µM TatA at equivalent TatB concentrations (see Section 4.2.4, Fig.4.12). Additionally, the trend of transport efficiency from 0 to 3µM TatB was similar in both conditions regardless of TatA supplementation (Fig.4.12). Those results suggest that TatB may not compete with TatA in our *in vitro* transport assays.

Similar transport experiments were conducted in order to examine whether TatA could compete with TatB or not. In those experiments, varying amounts of TatA were supplemented into anti-TatB-treated thylakoids with two defined concentrations of TatB for transport reconstitution (see Section 4.2.3, Fig.4.11). At the higher TatB concentration, the reconstituted Tat transport was in the decreasing phase (Fig.4.5). Following the same rationale as described above, if this decrease is the result of TatB competing with intrinsic TatA for binding sites, increasing TatA concentrations should reclaiming these sites from TatB. As a result, transport efficiency would be expected to recover. At the first glance, it appeared that the same amounts of TatA led to a better Tat transport in 2µM-TatB assays compared to 0.5µM-TatB assays (Fig.4.11, bottom pane, compare blue line and red line). However, due to large standard errors and only minor differences between the two curves, no clear improvement is proven. Moreover, upon 0.2µM TatA supplementation, a further increase of TatA concentrations consistently reduced Tat transport in both conditions (Fig.4.11). If the decrease is due to the competition between excessive TatA and TatB for same binding sites, then adding 2µM TatB should shift the TatA concentration, at which transport efficiency starts to drop, to a higher level. However, this shift is not observed (Fig.4.11).

An alternative explanation could be that external TatB indeed occupies TatA binding sites whereas TatA is unable to reclaim them due to weaker binding affinity for TatC compared to TatB. In fact, TatA is generally thought to interact loosely with TatC, since only TatBC complexes, but not TatABC complexes, could be reliably observed using current methodologies (Geise, et al. 2019) (Matthias

Reimers Dissertation, MLU, 2021). Furthermore, evidence for TatA-TatC interaction comes primarily from indirect measurements such as mutagenesis, cross-linking or bioinformatical prediction (Alcock, et al. 2016; Blummel, et al. 2015; Geise, et al. 2019; Habersetzer, et al. 2017), supporting the idea that this interaction is relative weak and transient. Thus, it is plausible that the external TatA cannot effectively compete with excess TatB for binding to TatC, due to its lower binding affinity. However, regardless of TatA's binding affinity, TatB would be expected to always reclaim its binding sites from TatA, because of its nature to form complexes with TatC (Behrendt, et al. 2007). This prediction does not align with our observations (Fig.4.12). Hence, taken together, these findings argue against the propose that TatA and TatB share identical binding sites on TatC.

Moreover, if the destabilization effect of TatA on TatBC complexes (see Section 4.4.1) is due to direct competition between TatA and TatB, we would expect to observe stepwise transition from complex#1 to complex#2 and then to complex#3, corresponding to sequential dissociation of TatB from TatC core (Matthias Reimers Dissertation, MLU, 2021). Alternatively, we would expect to detect TatABC complexes of similar sizes to the corresponding TatBC complexes, which reflects the replacement of TatB by TatA in complex formation. However, no stepwise transitions were observed; instead, all three TatBC complexes signals from BN-PAGE progressively diminished in response to TatA supplementation (Fig.4.15 B,C). Also, no convinced TatABC complexes were detected. It seems that two TatABC-like complexes appeared upon TatA addition, which presumably contain more than one TatA molecule associated with the TatC core according to their sizes (Fig.4.15D). However, characterization of these complexes remains inconclusive, as attempts to analyze TatA-containing complexes in the second dimension did not provide definitive results (Fig.4.18B). Besides, faint bands of large TatA-containing complexes were observed by using radiolabeled TatA in BN-PAGE, which may represent a complex formed by TatA replacing TatB according to its size (Section 4.4.2, Fig.4.18A; Fig. S4). But these signals were too weak to be consider as definitive evidence for the existence of stable TatABC complexes. Therefore, TatA appears to affect TatBC complexes through a mechanism that remains to be elucidated, rather than by replacing or dissociating TatB from TatBC complexes.

5.1.3 The role of external TatB in Tat transport in thylakoids

In the analysis of TatB effect on Tat transport in thylakoids, we observed a clear threshold effect at

1μM, above which TatB begins to perturb both intrinsic and reconstituted Tat transport, whereas below which TatB has no negative effect in either case (Fig.4.5 and Fig.4.6). Therefore, in this section, we will discuss the role of external TatB in two parts: first, the role of external TatB at non-inhibitory concentrations (≤1μM), and second, the role of excessive TatB that leads to a decrease in Tat transport (>1μM).

1) <u>The role of TatB at low concentrations (≤1μM)</u>

Within the concentration ranging from 0μM to 1μM, external TatB facilitates Tat reconstitution in anti-TatB-treated thylakoids (Fig.4.5), while it has no noticeable effect on Tat transport in untreated thylakoids (Fig.4.6). Previously, our group proposed two potential mechanisms to explain how external TatB facilitates Tat reconstitution (Zinecker, et al. 2020): (1) TatB may utilize potentially surplus TatC molecules in thylakoid membranes to form new functional complexes; or (2) TatB may occupy free binding sites on partially assembled TatBC complexes. Our current data appears to challenge the first hypothesis. If the free TatC is indeed present in the membrane, externally added TatB should promote new complex formation and enhance transport even in untreated thylakoids. Yet no such increase is observed (Fig.4.6). This suggests that free TatC is either absent or alternatively, not accessible for transport enhancement in untreated thylakoids. In the latter scenario, Tat transport may remain limited by the availability of TatA. In this case, the benefit of additional TatBC complexes would be masked. However, TatA supplementation alone is known to enhance Tat transport (see Section 4.2.2,Fig.4.10)(Frielingsdorf, et al. 2008), making it difficult to distinguish whether the observed improvement in Tat transport efficiency upon TatA addition reflects its intrinsic positive role in Tat transport or the compensation for TatA limitation. Hence, whether free TatC is functionally available for incorporation into new TatBC complexes remains to be demonstrated.

On the other hand, recent findings from our group (Matthias Reimers Dissertation, MLU, 2021) showed that the predominant form of TatBC complexes (complex#1) contained a trimeric TatC core associated with three independently bound TatB molecules, while the less abundant forms (complex#2 and complex#3) contained the same core with fewer TatB subunits. This indicates the presence of free binding sites for TatB in thylakoid membranes. Supporting this, the supplementation of radiolabeled TatB into thylakoid membranes resulted in clear detection of complex#1 and complex#2 (Fig.4.13B),

confirming that external TatB is able to integrate into TatBC complexes. Taken together, these findings allow us to refine the second hypothesis: external TatB facilitates Tat reconstitution by binding to unoccupied sites on partially assembled TatBC complexes, restoring transport in TatB-blocked thylakoids; whereas, in untreated thylakoids with sufficient endogenous TatB, these additional binding appear non-functional. Although it is well-established that multiple TatB molecules are incorporated into each TatBC complex (Blummel, et al. 2015; Maurer, et al. 2010; Tarry, et al. 2009), so far, it remains unknown how many TatB molecules per TatBC complex are functionally required for substrate transport. It is possible only one or two TatB molecules actively participate in protein transport, which could be the reason why the incorporation of external TatB into TatBC complexes fails to enhance transport in untreated thylakoids.

2）<u>The role of TatB at high concentrations (>1μM)</u>

Based on typical saturation behavior, one would expect that the transport curve processes into a plateau when TatB concentrations reach a saturate level. However, our results showed that high concentrations of TatB led to a decrease in Tat transport efficiency rather than a steady phase (Fig.4.5 and Fig.4.6). As discussed previously (Section 5.1.2), it is unlikely that TaA and TatB compete for the same binding sites on TatC. Besides, it is also unlikely that excessive TatB perturb the structure of endogenous TatBC receptors, as TatBC complexes stayed stable across high TatB concentrations (Fig.4.14, left pane, 1μM - 3μM). Notably, our data show that TatB predominantly forms homo-oligomers within thylakoid membranes (Fig.4.14, right pane). One possibility is that these TatB oligomers sequester substrates by binding to them prior to their engagement with TatBC complexes, thereby reducing transport efficiency. This is consistent with previous studies showing that TatB oligomers participate in pre-translocational binding with Tat substrates (Blummel, et al. 2015; Maurer, et al. 2010). Albeit since those studies were conducted in the presence of TatC, whether TatB oligomers alone could bind to substrates remains unclear. Alternatively, it is possible that excessive TatB oligomerize at or near the binding sites of endogenous TatB on TatC. These regions are also suggested to be the binding regions of TatA (Alcock, et al. 2016; Aldridge, et al. 2014) and substrates (Blummel, et al. 2015; Rollauer, et al. 2012; Zoufaly, et al. 2012). Thus, such TatB oligomerization may block TatA

binding or disturb substrate recognition, ultimately impairing the efficiency of Tat-dependent transport.

5.1.4 The role of external TatA in Tat transport in thylakoids

In the analysis of TatA effect on Tat transport in thylakoids, we observed that TatA supplementation facilitated Tat reconstitution in anti-TatA-treated thylakoids to levels even higher than mock-treated thylakoids. Across the tested concentration range, higher TatA concentrations had no obviously different impact on transport efficiency, as all concentrations resulted in similarly levels of transport activity. (see Section 4.2.2, Fig.4.8). On the other hand, in non-antibody-treated thylakoids, external TatA initially enhanced intrinsic Tat transport within a certain concentration range. But this enhancement gradually declined as TatA concentration increased (Fig.4.9), eventually leading to lower transport efficiency compared to control treatment (Fig.S1, 3.6µM). The observation of TatA effect on TatA-blocked Tat reconstitution is in accordance with previous studies (Hauer, et al. 2013), where TatA supplementation up to 3µM restored transport to levels comparable to untreated controls. This raises the question of why TatA behaves differently in anti-TatA-treated versus non-antibody-treated thylakoids. The major difference between these two conditions is the functional status of intrinsic TatA. In anti-TatA assays, the function of intrinsic TatA is completely blocked by TatA antibodies. But in non-antibody assays, intrinsic TatA remains active. Thus, a possible explanation is that when intrinsic TatA is non-functional (anti-TatA-treated thylakoids), external TatA acts independently and exerts only a positive effect on transport. In contrast, when intrinsic TatA is functional (non-antibody assays), external TatA may negatively interact with intrinsic TatA. When external TatA is in a lower range of concentrations ($\leqslant$0.5µM), this negative interaction may be negligible. Instead, external TatA may enhanced Tat transport by compensating for the loss of soluble TatA in stroma during thylakoid isolation (Frielingsdorf, et al. 2008) or for the loss of membrane-associated TatA during washing steps. When this negative effect on intrinsic TatA overpasses the positive effect of external TatA due to high concentrations of external TatA, it leads to a decrease in Tat transport efficiency. Unfortunately, due to current methodological limitations, it is not possible to distinguish intrinsic TatA and external TatA in our *in thylakoido* assays. A potential mechanism for the interplay between intrinsic and external TatA is further discussed in Section 5.2.2.

Unilke external TatB, which did not significantly disrupt the structure of endogenous TatBC

complexes (Fig.4.14, anti-TatB detection), our study further showed that external TatA caused a clear destabilization of these complexes (Fig.4.15). Interestingly, this apparent destabilization does not coincide with an immediate decrease in Tat transport efficiency (Fig.4.20). Specifically, although the signals of TatBC complexes#1, #2, #3 were already substantially weaker at 1μM TatA compared to untreated controls (Fig.4.20A), the corresponding post-destabilized transport efficiency was even higher (Fig.4.20B). This observation suggests that the 'destabilization' of TatBC complexes analyzed by BN-PAGE may not directly reflect intrinsic structural destabilization or functional inactivity of TatBC complexes. Thus, while the effect of TatA on Tat transport activity has already been discussed above, due to this apparent discrepancy, the effect of TatA on the stability of TatBC complexes will be separately discussed in Section 5.2.2.

5.2 The stability of TatBC complexes

5.2.1 PMF across the thylakoid membrane affects the stability of TatBC complexes

1) <u>The presence of photosynthesis affects the stability of TatBC complexes</u>

It is well established that Tat pathway utilizes the proton motive force (PMF) as its energy source. In thylakoid membranes, the proton gradient (∆pH) plays a major role in energizing Tat-dependent protein transport (Braun, et al. 2007; Mould and Robinson 1991; Musser and Theg 2000). Our results further demonstrate that PMF also contributes to the stability of TatBC complexes (see Section 4.5). Intriguingly, TatBC complexes remained similarly stable in thylakoid membranes under both fully activated and restricted conditions (Fig.4.23A). In the fully activated state, ∆pH is elevated due to photosynthesis, while in restricted conditions, ∆pH is diminished because of limited overall enzymatic activities. However, when photosynthetic activity was selectively inhibited, while other enzymatic processes remained active, the predominant TatBC complex#1 disappeared and complex#3 emerged (Fig.4.23A). This suggests that the PMF generated by photosynthesis is essential for maintaining the stability of complex#1 in functionally active thylakoid membranes.

The next question is why TatBC complex#1 remains stable in thylakoid membranes under restricted conditions, whereas it disappears when photosynthesis is selectively inhibited. In both cases, ∆pH across thylakoid membranes is expected to be low or dissipated. This discrepancy may be due to the

utilization of so-called localized protons. Previous studies have demonstrated the presence of localized protons, which are not in equilibrium with the bulk aqueous phases of protons and are released in the dark to maintain the proton pool within thylakoids (Renganathan, et al. 1991; Theg, et al. 1988). Theg's group further proposesd that Tat-dependent transport in thylakoids under dark conditions was energized by these localized protons (Braun and Theg 2008). Our observations may provide additional support for the existence of these localized protons. Under restricted conditions (dark and cold), these protons appear to sustain the stability of complex#1 and to maintain the Tat transport when other enzymatic activities are also restricted. In contrast, in functionally active membranes where only photosynthesis is selectively inhibited, these protons are likely coupled to other processes, such as ATP synthesis, resulting in the destabilization of complex#1. It is important to note that in our experiments, no Tat substrate was supplied, meaning that the Tat translocase remained in an inactive state (Habersetzer, et al. 2017; Werner, et al. 2024). In this state, protons are not required for Tat transport. This may explain why Tat machinery fails to compete with other enzymatic processes for proton utilization when limited protons in the lumen.

Additionally, the presence of localized protons could also explain one unexpected result from our experiments: the stabilizing effect by ADP/Pi on TatBC complexes under dark conditions (Fig.4.23A, compare ADP/Pi assays with lane ②). Initially, we expected that supplying ADP/Pi would lead to destabilization of TatBC complexes by stimulating ATP synthesis to reduce proton levels in the lumen. However, we observed the opposite effect. Addition of ADP/Pi resulted in stronger signals of complexes#1 and complexes#2. A possible explanation is that, in the presence of localized protons, the addition of ADP/Pi initially promotes ATP synthesis and reduces ∆pH; once ∆pH drops below a certain level, ATPase switches from ATP synthesis to ATP hydrolysis, pumping protons back into the lumen. As ∆pH rises again, the excessive externally-supplied ADP/Pi may switch ATPase back to ATP synthesis. As a result, a cycle between ATP synthesis and hydrolysis is established, coupled with proton pumping out of and in the lumen. These cycled protons may be utilized by Tat translocase to stabilize TatBC complexes. Supporting this, previous studies showed that adding ATP in dark-treated thylakoids stimulated Tat transport which was independent of ATP hydrolysis (Braun and Theg 2008). This suggests that ATP could drive ATPase into ATP hydrolysis mode, thereby pumping protons into the lumen and increasing ∆pH, which can be utilized by Tat pathway. However, whether exogenous ADP/Pi combined

with localized protons can sufficiently stimulate ATPase activity to sustain this cycle remains to be further elucidated.

2) <u>proton pumping by photosynthesis potentially affects the stability of TatBC complex#3</u>

Additionally, we also examined the status of TatBC complexes under conditions where the PMF was completely dissipated by gramicidin treatment (Fig.4.23B). Gramicidin is an ionophore that forms ion channels on membranes, permitting the free movement of monovalent cations down to their concentration gradients, including H^+, Na^+ and K^+, leading to a collapse in PMF (Tikhonov, et al. 2008). Our results consistently showed that, under light conditions, gramicidin treatment led to the disappearance of complex#1 and the concurrent appearance of complex#3 (Fig.4.15B; Fig. S5). In contrast, under dark conditions, complex#3 remained less pronounced (Fig.4.15B). It should be noted that only a single experiment was conducted for each of two experiments with different gramicidin concentrations (Fig.4.15B; Fig. S5), while the extent of signal change varied between the two assays. But the overall response patterns of TatBC complexes, the disappearance of complex#1 and the appearance of complex#3, were similar across these assays. Therefore, in the following discussion, we focus on this consistent effect of gramicidin on TatBC complexes.

As expected, dissipating PMF across thylakoid membranes by gramicidin negatively affected the stability of TatBC complex#1 (Fig.4.23B), consistent with the previous observation that complex#1 disappeared when ∆pH is low (Fig.4.23A, compare lane ① and ②). This confirms that the formation of complex#1 requires certain ∆pH across thylakoid membranes. Intriguingly, complex#3 only formed when thylakoid membranes were illuminated but ∆pH was dissipated by gramicidin (Fig.4.23B, left part; Fig. S5). When ∆pH was dissipated by gramicidin but under dark conditions (Fig.4.23B, right part) or by other enzymatic activities (Fig.4.23A, lane ②), no major formation of complex#3 could be observed. This suggests that while ∆pH is crucial for maintaining complex#1, when ∆pH is low or absent, the assembly of complex#3 depends on additional light-dependent processes beyond the proton gradient alone.

To explain this light-specific effect on complex#3 assembly, one possibility is that Tat translocase utilizes energy derived directly from proton pumping by photosynthesis, when the bulk ∆pH across the thylakoid membrane is dissipated. Supporting this idea, Braun and Theg (2008) demonstrated that

proton pumping by the photosynthetic electron transport chain, which initiated before dark incubation, determines Tat transport under dark conditions. Moreover, proton pumping can still occur in thylakoid membranes even when ∆pH is dissipated (Ewy and Dilley 2000; Shikanai and Yamamoto 2017). Therefore, it is plausible that in gramicidin-treated and light-stimulated thylakoids, proton pumping could still happen which provides energy for the assembly of TatBC complex#3 under ∆pH-dissipated conditions.

If localized protons are presented in thylakoid membranes, one may assume that Tat translocase could also utilize these localized protons to facilitate the formation of TatBC complex#3 when ∆pH is dissipated by gramicidin. However, those localized protons are proposed to be utilized when ∆pH is low, without requiring illumination for their release (Braun and Theg 2008; Laszlo, et al. 1984; Theg, et al. 1988). Our results, on the other hand, showed the formation of complex#3 in gramicidin-treated thylakoids occurred only under light conditions (Fig.4.23B). Therefore, it seems that localized protons are not the primary energy source driving complex#3 formation in this specific situation. Then the question is: if localized protons can be utilized by enzymatic activities under dark conditions (Laszlo, et al. 1984; Renganathan, et al. 1991), including Tat transport (Braun and Theg 2008), why they cannot be utilized under gramicidin treatment?

A possible explanation is that gramicidin treatment negatively influences the release of localized protons. When previous studies demonstrated the existence of localized protons (Braun and Theg 2008; Laszlo, et al. 1984; Renganathan, et al. 1991; Theg, et al. 1988), they dissipated ∆pH via dark treatment or ionophores such as nigericin and valinomycin, which primarily influence H^+ flux across the membrane. In contrast, gramicidin allows the passive diffusion of monovalent cations, including H^+, Na^+, K^+ (Petersen and Beitz 2020; Schönknecht, et al. 1992). The resulting disruption of ionic balance may consequently affect the activity of membrane proteins. Several studies have proposed that some of thylakoidal membrane proteins are involved in releasing localized protons through buried regions (Ewy and Dilley 2000; Vershubskii, et al. 2017). Therefore, it is plausible that gramicidin, by altering ion fluxes and consequently affecting activities of membrane proteins, may lead to unavailability of localized protons for processes such as TatBC complex#3 assembly when ∆pH is dissipated.

5.2.2 The relevance between TatA and the stability of TatBC complexes

Our results showed that external TatA led to a decrease in TatBC signals observed by BN-PAGE, while the signal decrease did not immediately lead to a decrease in transport efficiency (Figure 4.20). Therefore, by integrating data from both transport assays (Section 4.2.2 and Section 4.4.4) and BN-PAGE analysis (Section 4.4), we propose two hypothetical mechanisms by which TatA may modulate the status and function of TatBC complexes.

1) <u>External TatA disassembles TatBC complexes</u>

A straightforward hypothesis is that excessive external TatA destabilizes TatBC complexes, resulting in the decrease in signal intensities of TatBC complexes in BN-PAGE. Since TatA is suggested to interact with TM5/TM6 of TatC (Alcock, et al. 2016; Zoufaly, et al. 2012), a possible mechanism is that excessive TatA may form enlarged TatA complexes that overstretch the space between TatC protomers (Fig.5.2), potentially destabilizing TatBC complexes. Here we refer to these as 'enlarged TatA complexes' rather than 'enlarged TatA oligomers' because these TatA complexes may consist of multiple copies of TatA oligomer#1 or oligomer#2.

In this scenario, at lower concentrations, the positive effect of TatA on Tat transport (Frielingsdorf, et al. 2008; Hauer, et al. 2013) may initially compensate for the loss of transport efficiency caused by the partial disassembly of TatBC complexes. However, at higher concentrations, this beneficial effect of TatA is outweighed by the reduced availability of functional TatBC complexes, resulting in a decrease in transport activity. Supporting this idea, Barrett and Robinson (2005) proposed that excessive TatA could disrupt TatBC structure, based on their observation that a TatA mutant led to reduced levels of TatB and TatC along with increased levels of TatA in *E.coli* cytoplasmic membranes. Yet, this explanation does not fully account for the observation that, even when TatBC signals are nearly undetectable at 2μM TatA, the transport efficiency remains comparable to that of mock-treated thylakoids (Fig.4.20).

An alternative, but not mutually exclusive, possibility is that only a small fraction of TatBC complexes is actively engaged in Tat transport under physiological conditions. In this scenario, external TatA may initially destabilize non-active TatBC complexes which has minimal effect on the overall transport efficiency. Once TatA levels become sufficiently high to affect the small pool of active complexes, a

decline in transport efficiency would be observed.

However, both scenarios have limitations. For instance, neither of them fully explains why external TatA only exerts a positive effect on transport efficiency in anti-TatA-treated thylakoids, regardless of TatA concentration (Fig.4.8). It is also difficult to reconcile this interpretation with the reported structural stability of the TatC core, which remains unaffected even under harsh detergent extraction conditions (Matthias Reimers Dissertation, MLU, 2021). Structural insights from Alpha Fold prediction (Fig.5.2B and 5.2C) and cross-linking data (Ramasamy, et al. 2013; Zoufaly, et al. 2012) suggest that TatC protomers interact with each other via the loop L1/L2 (corresponding to loop P1/P2 in *E.coli*, see Fig 1.3A) to form the stable TatC core structure. Since the TatA–TatC interaction is thought to occur around TMH5 and TMH6 of TatC, which near the stromal/cytoplasmic face (Fig.1.3), it seems unlikely that changes in this region by enlarged TatA complexes would disrupt the connection between TatC protomers, which are close to lumen/periplasmic face (Fig.1.3B, cyan-shaded 'cap' region; and also see Fig.5.2).

Thus, the observed disappearance of TatBC complex signals in BN-PAGE upon TatA supplementation may not be due solely to physical disassembly. Instead, it may reflect structural rearrangements or transient interactions between TatA and TatBC complexes that affect their migration behavior during BN-PAGE. In the following section, we therefore consider an alternative explanation centered on such TatA–TatBC interactions.

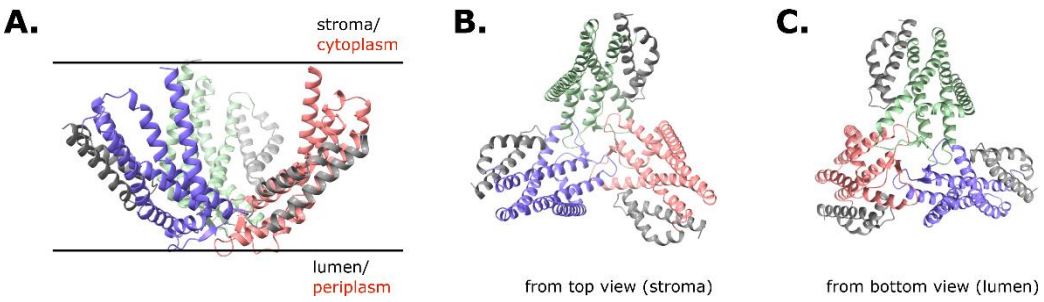

Fig.5.2 Structural model of a trimeric TatC complex, predicted by AlphaFold.
Mature TatC protein sequence from pea was used for Alpha Fold prediction. According to Rimers' results (Matthias Reimers Dissertation, MLU, 2021), we asked for a trimeric TatC core structure. The prediction shows similar structure reported by Ramasamy, et al. (2013)for *Aquifex aeolicus*: TatC protomers are connected by the long loop L1/L2 to form a funnel-like structure; TMH5/TMH6 are away from closed bottom and there is a space between THM5/TMH6 and the nearby TatC protomer. (A) Side view of the TatC trimer from the membrane side, with the stromal/cytoplasmic and lumenal/periplasmic sides indicated. Each TatC monomer is shown in a different color: blue, red, and green. The TMH5 and TMH6 of each monomer are highlighted in grey. (B) Top view from the stromal (cytoplasmic) side, illustrating the spatial arrangement of the TatC subunits. (C) Bottom view from the lumenal (periplasmic) side, showing the connection by L1/L2.

2) External TatA triggers conformational change on TatBC complexes

In Tat research, TatA is thought to associate loosely and dynamically with TatBC complexes, which cause the difficulty in detecting TatABC complexes (Behrendt and Brüser 2014; Bolhuis, et al. 2001). Furthermore, Cléon, et al. (2015) reported that certain mutagenesis on TatC proteins resulted in undetectable TatBC complexes by BN-PAGE, but Tat transport activity remained evident, indicating that BN-PAGE may not capture the intrinsic functional state of them. Additionally, we observed the similar discrepancy that Tat transport remained similar with untreated control when 2uM TatA supplemented, whereas the corresponding signals of TatBC complexes were nearly diminished (Fig.4.20). It is known that BN-PAGE is a powerful method for detecting stable and long-lived protein complexes, whereas it has limitations in capturing dynamic or transiently changed complexes (Jänsch, et al. 1996; Krause 2006; Neff and Dencher 1999). Therefore, this discrepancy between Tat transport efficiency and BN-PAGE-detected TatBC complexes may reflect the highly dynamic nature of Tat translocase. It indicates that the structural status of TatBC complexes analyzed by BN-PAGE may not directly correspond to their functional state *in vivo*.

Moreover, our results suggest that the interaction between TatA and TatBC complexes may affect the detection of TatBC complexes by BN-PAGE. Given that only functionally active TatA affected the signal intensities of TatBC complexes (Fig.4.15 and Fig.4.19), it suggests that the observed reduction in TatBC signals is not simply a consequence of non-specific disruption caused by high levels of external TatA. Instead, it may reflect the interaction between functional TatA and TatBC complexes. In particular, a single amino acid substitution, *Arabidopsis* E10C-TatA mutant, showed completely difference effect on TatBC complexes compared to wild type TatA (Fig.4.19A and 4.19B). These results imply that specific interactions between TatA and TatBC complexes may influence the electrophoretic behavior of TatBC complexes in BN-PAGE.

Next, this interaction may induce a conformational change in TatBC complexes, rendering them less detectable by BN-PAGE. The evidence supporting this hypothesis is the observed discrepancy between the high Tat transport activity and the reduced TatBC signals in BN-PAGE at relatively low concentrations of TatA (Fig.4.20). This suggests that TatBC complexes remain functionally competent but likely undergo structural alterations that render them undetectable by BN-PAGE. Moreover, the conformational change in TatBC complexes may be induced by specific interaction between TatA and

TatC. The hydrophilic residue E10 in pea (Q8 in *E. coli*) has been suggested to play a crucial role in mediating the interaction between TatA and TatC (Alcock, et al. 2016; Rollauer, et al. 2012). In our experiments, *Arabidopsis* wild-type TatA, but not the E10C mutant, led to the loss of TatBC signals, supporting the idea that this specific interaction induces a conformational change that alters the electrophoretic properties of TatBC complexes.

So far, TatA is well established to be functionally essential in Tat transport (Zinecker, et al. 2020). It is believed to integrate into TatBC complexes to form the active Tat translocase (Frain, et al. 2019; Müller and Bernd Klösgen 2005). But the interaction between TatA and TatB/TatC was indirect demonstrated. Previous studies have inferred these interactions through cross linking (Aldridge, et al. 2014; Blummel, et al. 2015; Dabney-Smith and Cline 2009; Geise, et al. 2019), co-immunoprecipitation (Bolhuis, et al. 2001; Mori and Cline 2002), mutagenesis (Barrett, et al. 2007; Barrett and Robinson 2005) and fluorescent tracking (Alcock, et al. 2013; Rose, et al. 2013). While, our results show a direct influence, or interaction, by functionally active TatA on TatBC complexes.

The conformational change on TatBC complexes is triggered by TatA-TatC constitutive interaction

It is widely accepted that substrate-binding triggers the recruitment of TatA to TatBC receptors, either to assemble into an active Tat translocase (Alcock and Berks 2022; Hao, et al. 2023; Mehner-Breitfeld, et al. 2022) or to activate TatBC complexes as a regulatory factor (Hauer, et al. 2013). Less studies are focused on the TatA activity in inactive Tat translocase. Our results show that TaA can interact with TatBC complexes even in the absence of substrate, as evidenced by external TatA affects TatBC complexes without substrate supplementation (Fig.4.15B, Fig.4.19A). This interaction may lead to a conformational change on TatBC, as discussed above. Moreover, this interaction may be mediated by so-called constitutive TatA-TatC interaction, which has been reported to be independent of substrate supplementation (Alcock, et al. 2016; Aldridge, et al. 2014; Habersetzer, et al. 2017; Zoufaly, et al. 2012).

Next, our results do not exclude the substrate-triggered recruitment of TatA to TatBC complexes. It seems that there was no additional recruitment of TatA by substrates supplementation, based on the similar reducing level of TatBC signals in both substrate-supplemented and non-supplemented assays (Fig.4.15B, C). First, it is important to note that BN-PAGE is not a reliable method for drawing any

quantitative conclusions. Second, even if substrates recruit more TatA into TatBC complexes, maybe only a small fraction of recruited TatA could interact with TatC. It is known that TatA tend to form oligomers within membranes (Behrendt, et al. 2007; Dabney-Smith and Cline 2009; Pettersson, et al. 2021). Our results also showed a robust detection of TatA oligomers by BN-PAGE (Fig.4.15D, Fig.4.18, Fig.S4). On the other hand, most evidence indicates the interaction between TatA and TatC primarily involves the TMH of TatA and the TMH5/TMH6 of TatC (Alcock, et al. 2016; Aldridge, et al. 2014; Zoufaly, et al. 2012). Due to the close proximity of TM5 and TM6 (Fig.1.5B), it is deducible that only one or two TatA protomers within an oligomer are positioned to directly interact with TatC, which lead to a conformational change in TatBC complexes. This conformational change results in less sensitivity by BN-PAGE detection. The remaining TatA protomers are unlikely able to interact with TatC. Therefore, even when substrates trigger more external TatA to TatBC complexes, only a limited number of TatA protomers could trigger the conformation change by TatA-TatC interaction. Thus, it is difficult to distinguish the number of recruited TatA between substrate-added and no-substrate-added assays by the signal changes of TatBC complexes.

Additionally, we observed an indication of TatA responding to substrates supplementation in our assays. Compared to no-substrate condition, the overall signals of TatA oligomer#2 appeared weaker upon substrate supplementation, as detected by BN-PAGE and western blotting with anti-TatA detection (Fig.S6). This reduction may reflect substrate-triggered recruitment of TatA, leading to the less formation of oligomer#2 and the formation of Tat(A)BC complexes which are undetectable by BN-PAGE. However, due to limited experimental replication, this observation should be interpreted cautiously and considered only as a preliminary indication inside of final conclusion.

Excessive amounts of TatA block TatB binding on TatBC complexes

One noteworthy observation is that intrinsic Tat transport efficiency shows a biphasic response to TatA concentrations, characterized by an initial increase and a subsequent decrease (Fig.4.9). On possible explanation for the decline of Tat transport is that excessive TatA form enlarged TatA complexes which block the coalescence region located near TMH5 and TMH6, but not destabilize TatBC complexes as hypothesized at beginning of this section. This coalescence region has been suggested to

be the interaction region for TatA, TatB, TatC and substrates (Fig.5.2, space between two TatC protomers) (Alcock, et al. 2016; Habersetzer, et al. 2017; Rollauer, et al. 2012). Thus, when the size of these TatA complexes becomes sufficiently large, they may hinder TatB binding on TatC, interfering with substrate recognition or binding. It is important to note that this hypothesis does not necessarily imply that TatA and TatB share same binding sites. Rather, it suggests that their binding sites may be spatially close - a condition that remains consistent with our earlier discussion (Section 5.1.2).

Last but not least, it seems that the blocking effect observed upon TatA supplementation is mediated by endogenous (intrinsically expressed) TatA, whereas externally added TatA alone does not exhibit this blocking effect. This hypothesis is supported by the observation that external TatA does not impair Tat-dependent protein transport in anti-TatA-treated thylakoids (Fig.4.8), whereas it leads to a decrease in Tat transport when intrinsic TatA remains active (Fig.4.9). One possible scenario is that the intrinsic TatA directs the orientation or organization of TatA complexes assembly within the membrane, leading to the formation of TatA complexes inside the coalescence region. Thus, these TatA assembly may block access to the functional sites of TatB or substrates. In contrast, when only external TatA is present, TatA assembly may orient away from the functional site. In this scenario, TatA complexes may has a linear arrangement (Mehner-Breitfeld, et al. 2022) or a ring-like structure (Pettersson, et al. 2021) that physically blocks the region (Fig.5.3).

Notably, TatA assembly has been suggested to be highly context-dependent, undergoing structural rearrangements depending on the membrane environment (Pettersson, et al. 2021). In addition, TatA has been shown to generate a hydrophobic mismatch with the membrane (Mehner-Breitfeld, et al. 2022), indicating that it can actively interact with the membrane and possibly alter local membrane properties. These characteristics provide a mechanistic basis for the scenario proposed above: the presence of intrinsic TatA may locally influence the membrane environment, thereby promoting the assembly of external TatA within the coalescence region; in contrast, when intrinsic TatA is blocked by antibodies, external TatA may assemble differently, avoiding interference with this region.

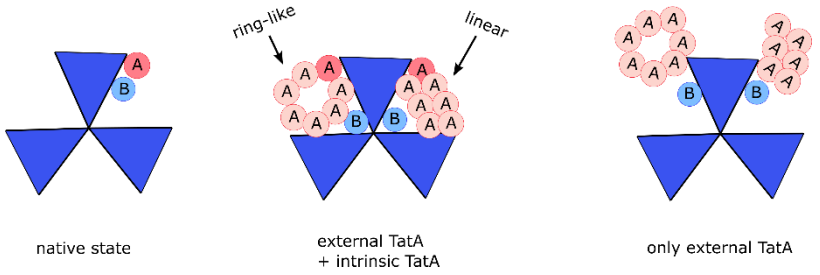

Fig.5.3 Scheme of a possible explanation for the blocking effect of external TatA on Tat-dependent protein transport. Left: In the native state, the translocase is composed of equivalent stoichiometry of TatC (*blue*), intrinsic TatB (*light blue*), and intrinsic TatA (*red*). Middle: Upon addition of external TatA (*light red*), intrinsic TatA potentially leads to the formation of TatA complexes inside the space between two TatC protomers, leading to an imbalance in subunit interactions that may block the TatB interaction with TatC. TatA complexes may has a linear arrangement (Mehner-Breitfeld, et al. 2022) or a ring-like structure (Pettersson, et al. 2021). Right: In the absence of intrinsic TatA, externally supplied TatA *(light red*) forms complexes at outside face of TatC core structure. This location does not have an impact on TatB binding therefore would not negatively influence Tat transport. This model proposes that intrinsic TatA leads the external TatA assembly into the coalescence region, disturbing the binding of TatB.

5.3 Towards the role of TatA in Tat translocase

One of the most surprising findings from our experiments is the apparent 'disappearance' of TatBC complexes even in the resting state (without substrate triggering) (Fig.4.15B). So far, most studies on TatA focus on its role during the substrate-translocation step, where TatA is believed to be recruited by TatBC-substrate complexes. In contrast, the potential role of TatA in the resting state has been largely overlooked. Our findings suggest that TatA can constitutively interact with TatBC complexes even in the absence of substrate, potentially inducing conformational changes that destabilize or remodel these complexes.

First, the effect of TatA on TatBC complexes was observed independently of substrate supplementation (Fig.4.15B and Fig.4.19A) but dependently on TatA functionality (Fig.4.19). Although these experiments were conducted under high TatA concentrations relative to intrinsic TatA level on thylakoid membranes (estimated at 0.17µM according to Hauer, et al. (2013)), only functionally active TatA induced changes in TatBC complexes (Fig.4.19). This specificity implies that the observed effects reflect an interaction between TatA and TatBC, rather than a non-specific or concentration-dependent phenomenon. Second, high concentrations of external TatA led to a significant decrease in Tat transport activity in the presence of intrinsic TatA while external TatA alone does not have such effect (Fig.4.9). If intrinsic TatA is freely diffusing in thylakoid membranes, such high levels of external TatA would be

expected to sequester the small amount of intrinsic TatA, thereby preventing it from exerting any influence on Tat transport. This scenario, however, does not align with our observations (Fig.4.9). Therefore, our data indicates that intrinsic TatA is not freely diffusing in thylakoid membranes but rather constitutively interacts with TatBC complexes. Third, in thylakoid membranes, the ratio of TatA:TatB:TatC has been estimated to be approximately 1:1:1 (Jakob, et al. 2009). Although three working models of TatA are currently discussed (see Introduction 1.3.2), it is generally agreed that substrate binding triggers the recruitment of TatA to TatBC complexes (Alcock and Berks 2022; Hao, et al. 2023; Mehner-Breitfeld, et al. 2022). Thus, if TatA are entirely free and unbound in the membrane, such substrate-driven recruitment would likely be inefficient in the crowded environment of thylakoid membranes. It would be more effective for Tat translocase if TatA constitutively interacts with TatBC complexes, thereby rapidly initiating Tat transport for substrate engagement. This scenario is further supported by the observations that the signal peptide recognition sites (Aldridge, et al. 2014; Fröbel, et al. 2019; Rollauer, et al. 2012) are located near the predicted TatA–TatC interaction region (Alcock, et al. 2016; Aldridge, et al. 2014), which is the region close to the TMH5 and TMH6 of TatC. Taken together, we propose that TatA is constitutively, albeit loosely, interact with TatBC, possibly via its N-terminus (Aldridge, et al. 2014). This interaction may induce conformational changes on TatBC complexes, leading to less sensitivity by BN-PAGE detection. And this interaction itself is likely too weak to allow detergent extraction or Coomassie treatment during BN-PAGE analysis.

Previously, our group proposed that Tat translocase functioned as an allosteric enzyme (Hauer, et al. 2013). This hypothesis is further strengthened by our observation that TatA may trigger the conformation change of TatBC complexes, which is a classic hallmark of allosteric enzyme activity. In contrast, many working models, especially in *E.coli*, propose that TatA predominantly or exclusively forms translocation pores of varying diameters to facilitate membrane transport of Tat substrates of different sizes (Alcock and Berks 2022; Mehner-Breitfeld, et al. 2022). Here, our results suggest that at least in thylakoid membranes, TatA is unlikely to function as forming pores of variable diameters.

First, the relative abundance of TatA is suggested to be low in thylakoid membranes. In *E. coli*, the pore model is supported by the finding that the expression level of TatA is significantly higher than that of TatB and TatC (Jack, et al. 2001). Whereas, in thylakoids, TatA:TatB:TatC ratio is estimated to be approximately 1:1:1 (Jakob, et al. 2009). Our results further suggest that Tat translocase in thylakoids

requires a tightly regulated and relatively low ratio of TatA, by showing that excessive TatA negatively affects Tat transport. Specifically, supplementation with 1μM of external TatA, which is approximately 5-fold higher than intrinsic TatA concentration, already led to a decrease in Tat transport (Fig.4.9). Taken together, these results suggest that it is unlikely for form pores by overproduced TatA in thylakoid membranes.

Second, no TatA oligomers of various sizes are detected in thylakoids in this study. In *E.coli*, TatA forms oligomers with various sizes (Behrendt, et al. 2007), a finding that supports the flexible pore model. In contrast, across a range of TatA concentrations have been tested in this study, we consistently observed only two distinct forms of TatA oligomers regardless of Tat substrate supplementation (Fig.4.15D, Fig.4.18A, Fig.S4 and Fig.S6). Although two-dimensional separation shows that excessive TatA appeared to form multiple oligomers (Fig.4.18B, lower pane), they are in similar sizes around 120kDa rather than showing a broad size distribution. Therefore, our results argue against a variable-diameter TatA pore model in thylakoid membranes.

Third, if TatA forms pores adjacent to TatBC complexes, as proposed by Alcock and Berks (2022), externally supplemented TatA would be expected to assemble into oligomers (or pores) at the periphery of TatBC complexes. In this scenario, excessive TatA should not interfere with the structure of TatBC complexes. However, our data shows that external TatA does affect TatBC complexes, likely by directly interacting with them and inducing conformational change (see Discussion 5.2.2). This observation argues against a model in which TatA forms pores adjacent to TatBC complexes. At the same time, our data seems do not contradict an alternative model that TatA is recruited in between of TatBC protomers and form a pore structure with TatBC protomers, as proposed by Hao, et al. (2023). However, this model also appears unlikely, due to the relatively low abundance of TatA in both pea (Mori, et al. 2001) and *Arabidopsis* (Jakob, et al. 2009). Our results also suggest that thylakoidal Tat translocase requires a tightly regulated stoichiometry of TatA. Thus, it seems improbable that additional intrinsic TatA is available to support such pore formation in thylakoid membranes.

Taken together, our findings strengthen the hypothesis that Tat translocase operates as an allosteric enzyme, and indicate that pore formation by TatA is unlikely at least in thylakoid membranes.

References

Aitken, Alastair, and Michèle P Learmonth

1996 Protein determination by UV absorption. *In* The protein protocols handbook. Pp. 3-6: Springer.

Alami, Meriem, et al.

2003 Differential interactions between a twin-arginine signal peptide and its translocase in Escherichia coli. Molecular cell 12(4):937-946.

Alcock, Felicity, et al.

2013 Live cell imaging shows reversible assembly of the TatA component of the twin-arginine protein transport system. Proceedings of the National Academy of Sciences 110(38):E3650-E3659.

Alcock, Felicity, and Ben C Berks

2022 New insights into the Tat protein transport cycle from characterizing the assembled Tat translocon. Molecular Microbiology 118(6):637-651.

Alcock, Felicity, et al.

2016 Assembling the Tat protein translocase. elife 5:e20718.

Aldridge, Cassie, et al.

2014 Substrate-gated docking of pore subunit Tha4 in the TatC cavity initiates Tat translocase assembly. Journal of Cell Biology 205(1):51-65.

Aldridge, Cassie, et al.

2012 The chloroplast twin arginine transport (Tat) component, Tha4, undergoes conformational changes leading to Tat protein transport. Journal of Biological Chemistry 287(41):34752-34763.

Allen, Stuart CH, et al.

2002 Essential cytoplasmic domains in the Escherichia coli TatC protein. Journal of Biological Chemistry 277(12):10362-10366.

Asher, Anthony H, and Steven M Theg

2021 Electrochromic shift supports the membrane destabilization model of Tat-mediated transport and shows ion leakage during Sec transport. Proceedings of the National Academy of Sciences 118(12):e2018122118.

Bageshwar, Umesh K, et al.

2009 Interconvertibility of lipid-and translocon-bound forms of the bacterial Tat precursor pre-SufI. Molecular Microbiology 74(1):209-226.

Barnett, James P, et al.

2011 Expression of the bifunctional Bacillus subtilis TatAd protein in Escherichia coli reveals distinct TatA/B-family and TatB-specific domains. Archives of microbiology 193(8):583-594.

Barrett, Claire ML, Roland Freudl, and Colin Robinson

2007 Twin arginine translocation (Tat)-dependent export in the apparent absence of TatABC or TatA complexes using modified Escherichia coli TatA subunits that substitute for TatB. Journal of Biological Chemistry 282(50):36206-36213.

Barrett, Claire ML, and Colin Robinson

2005 Evidence for interactions between domains of TatA and TatB from mutagenesis of the TatABC subunits of the twin-arginine translocase. The FEBS journal 272(9):2261-2275.

Behrendt, Jana, and Thomas Brüser

2014 The TatBC complex of the Tat protein translocase in Escherichia coli and its transition to the substrate-bound TatABC complex. Biochemistry 53(14):2344-2354.

Behrendt, Jana, Ute Lindenstrauß, and Thomas Brüser

2007 The TatBC complex formation suppresses a modular TatB-multimerization in Escherichia coli. FEBS letters 581(21):4085-4090.

Berghöfer, Jürgen, and Ralf Bernd Klösgen

1999 Two distinct translocation intermediates can be distinguished during protein transport by the TAT (Δph) pathway across the thylakoid membrane. FEBS letters 460(2):328-332.

Berks, Ben C

1996 A common export pathway for proteins binding complex redox cofactors? Molecular microbiology 22(3):393-404.

Blaudeck, Natascha, et al.

2003 Genetic analysis of pathway specificity during posttranslational protein translocation across the Escherichia coli plasma membrane. Journal of bacteriology 185(9):2811-2819.

Blümmel, Anne-Sophie, et al.

2017 Structural features of the TatC membrane protein that determine docking and insertion of a twin-arginine signal peptide. Journal of Biological Chemistry 292(52):21320-21329.

Blummel, AS, et al.

2015 Initial assembly steps of a translocase for folded proteins. Nat Commun 6: 7234.

Bogsch, Erik, Susanne Brink, and Colin Robinson

1997 Pathway specificity for a ΔpH-dependent precursor thylakoid lumen protein is governed by a'sec-avoidance'motif in the transfer peptide and a'sec-incompatible'mature protein. The EMBO journal.

Bolhuis, Albert, et al.

2001 TatB and TatC form a functional and structural unit of the twin-arginine translocase from Escherichia coli. Journal of Biological Chemistry 276(23):20213-20219.

Borst, P, and LA Grivell

1978 The mitochondrial genome of yeast. Cell 15(3):705-723.

Bradford, Marion M

1976 A rapid and sensitive method for the quantitation of microgram quantities of protein utilizing the principle of protein-dye binding. Analytical biochemistry 72(1-2):248-254.

Braun, Nikolai A, Andrew W Davis, and Steven M Theg

2007 The chloroplast Tat pathway utilizes the transmembrane electric potential as an energy source. Biophysical journal 93(6):1993-1998.

Braun, Nikolai A, and Steven M Theg

2008 The chloroplast Tat pathway transports substrates in the dark. Journal of Biological Chemistry 283(14):8822-8828.

Brink, Susanne, et al.

1998 Targeting of thylakoid proteins by the ΔpH-driven twin-arginine translocation pathway requires a specific signal in the hydrophobic domain in conjunction with the twin-arginine motif. Febs Letters 434(3):425-430.

Brüser, Thomas, and Carsten Sanders

2003 An alternative model of the twin arginine translocation system. Microbiological research 158(1):7-17.

Brüser, Thomas, et al.

2003 Membrane targeting of a folded and cofactor-containing protein. European journal of biochemistry 270(6):1211-1221.

Castellanos-Serra, Lila, et al.

1999 Proteome analysis of polyacrylamide gel-separated proteins visualized by reversible negative staining using imidazole-zinc salts. ELECTROPHORESIS: An International Journal 20(4-5):732-737.

Celedon, Jose M, and Kenneth Cline

2012 Stoichiometry for binding and transport by the twin arginine translocation system. Journal of Cell Biology 197(4):523-534.

Chaddock, Alison M, et al.

1995 A new type of signal peptide: central role of a twin-arginine motif in transfer signals for the

delta pH-dependent thylakoidal protein translocase. The EMBO journal 14(12):2715-2722.

Clark, Sonya A, and SM Theg

1997 A folded protein can be transported across the chloroplast envelope and thylakoid membranes. Molecular biology of the cell 8(5):923-934.

Cléon, François, et al.

2015 The TatC component of the twin-arginine protein translocase functions as an obligate oligomer. Molecular microbiology 98(1):111-129.

Cline, Kenneth, and Hiroki Mori

2001 Thylakoid ΔpH-dependent precursor proteins bind to a cpTatC–Hcf106 complex before Tha4-dependent transport. The Journal of cell biology 154(4):719.

Creighton, Alison M, et al.

1995 A Monomeric, Tightly Folded Stromal Intermediate on the△ pH-dependent Thylakoidal Protein Transport Pathway. Journal of Biological Chemistry 270(4):1663-1669.

Dabney-Smith, Carole, and Kenneth Cline

2009 Clustering of C-terminal stromal domains of Tha4 homo-oligomers during translocation by the Tat protein transport system. Molecular Biology of the Cell 20(7):2060-2069.

Dabney-Smith, Carole, Hiroki Mori, and Kenneth Cline

2003 Requirement of a Tha4-conserved transmembrane glutamate in thylakoid Tat translocase assembly revealed by biochemical complementation. Journal of Biological Chemistry 278(44):43027-43033.

David, Guillaume, et al.

2019 Phosphorylation and alternative translation on wheat germ cell-free protein synthesis of the DHBV large envelope protein. Frontiers in Molecular Biosciences 6:138.

De Keersmaeker, Sophie, et al.

2007 The Tat pathway in Streptomyces lividans: interaction of Tat subunits and their role in translocation. Microbiology 153(4):1087-1094.

De Leeuw, Erik, et al.

2001 Membrane interactions and self-association of the TatA and TatB components of the twin-arginine translocation pathway. FEBS letters 506(2):143-148.

DeLisa, Matthew P, Danielle Tullman, and George Georgiou

2003 Folding quality control in the export of proteins by the bacterial twin-arginine translocation pathway. Proceedings of the National Academy of Sciences 100(10):6115-6120.

Denks, Kärt, et al.

2014 The Sec translocon mediated protein transport in prokaryotes and eukaryotes. Molecular membrane biology 31(2-3):58-84.

Dilks, Kieran, María Inés Giménez, and Mechthild Pohlschröder

2005 Genetic and biochemical analysis of the twin-arginine translocation pathway in halophilic archaea. Journal of bacteriology 187(23):8104-8113.

DiMauro, Salvatore, and Eric A Schon

2003 Mitochondrial respiratory-chain diseases. New England Journal of Medicine 348(26):2656-2668.

Ellis, R John

1981 Chloroplast proteins: synthesis, transport, and assembly. Annual Review of Plant Physiology 32(1):111-137.

Elstner, M, et al.

2009 The mitochondrial proteome database: MitoP2. Methods in enzymology 457:3-20.

Erdmann, Ralf, and Wolfgang Schliebs

2005 Peroxisomal matrix protein import: the transient pore model. Nature Reviews Molecular Cell Biology 6(9):738-742.

Ewy, Robert G, and Richard A Dilley

2000 Distinguishing between luminal and localized proton buffering pools in thylakoid membranes. Plant physiology 122(2):583-596.

Fincher, Vivian, Carole Dabney-Smith, and Kenneth Cline

2003 Functional assembly of thylakoid ΔpH-dependent/Tat protein transport pathway components in vitro. European journal of biochemistry 270(24):4930-4941.

Fincher, Vivian, Michael McCaffery, and Kenneth Cline

1998 Evidence for a loop mechanism of protein transport by the thylakoid Delta pH pathway. FEBS letters 423(1):66-70.

Frain, Kelly M, et al.

2016 Protein translocation and thylakoid biogenesis in cyanobacteria. Biochimica et Biophysica Acta (BBA)-Bioenergetics 1857(3):266-273.

Frain, Kelly M, Colin Robinson, and Jan Maarten van Dijl

2019 Transport of folded proteins by the Tat system. The Protein Journal 38:377-388.

Frielingsdorf, Stefan, Mario Jakob, and Ralf Bernd Klosgen

2008 A stromal pool of TatA promotes Tat-dependent protein transport across the thylakoid membrane. Journal of biological chemistry 283(49):33838-33845.

Frielingsdorf, Stefan, and Ralf Bernd Kloösgen

2007 Prerequisites for terminal processing of thylakoidal Tat substrates. Journal of Biological Chemistry 282(33):24455-24462.

Fröbel, Julia, et al.

2019 Surface-exposed domains of TatB involved in the structural and functional assembly of the Tat translocase in Escherichia coli. Journal of Biological Chemistry 294(38):13902-13914.

Fröbel, Julia, et al.

2012 Transmembrane insertion of twin-arginine signal peptides is driven by TatC and regulated by TatB. Nature communications 3(1):1311.

Fröbel, Julia, Patrick Rose, and Matthias Müller

2011 Early contacts between substrate proteins and TatA translocase component in twin-arginine translocation. Journal of Biological Chemistry 286(51):43679-43689.

Gé, Fabien, and Kenneth Cline

2007 The thylakoid proton gradient promotes an advanced stage of signal peptide binding deep within the Tat pathway receptor complex. Journal of Biological Chemistry 282(8):5263-5272.

Geise, Hendrik, et al.

2019 A potential late stage intermediate of twin-arginine dependent protein translocation in Escherichia coli. Frontiers in Microbiology 10:1482.

Gérard, Fabien, and Kenneth Cline

2006 Efficient twin arginine translocation (Tat) pathway transport of a precursor protein covalently anchored to its initial cpTatC binding site. Journal of Biological Chemistry 281(10):6130-6135.

Gohlke, Ulrich, et al.

2005 The TatA component of the twin-arginine protein transport system forms channel complexes of variable diameter. Proceedings of the National Academy of Sciences 102(30):10482-10486.

Goosens, Vivianne J, et al.

2015 A Tat ménage à trois—the role of Bacillus subtilis TatAc in twin-arginine protein translocation. Biochimica et Biophysica Acta (BBA)-Molecular Cell Research 1853(10):2745-2753.

Goosens, Vivianne J, Carmine G Monteferrante, and Jan Maarten Van Dijl

2014 The Tat system of Gram-positive bacteria. Biochimica et Biophysica Acta (BBA)-Molecular Cell Research 1843(8):1698-1706.

Gouffi, Kamila, et al.

2004 Dual topology of the Escherichia coli TatA protein. Journal of Biological Chemistry

279(12):11608-11615.

Greene, Nicholas P, et al.

2007 Cysteine scanning mutagenesis and disulfide mapping studies of the TatA component of the bacterial twin arginine translocase. Journal of Biological Chemistry 282(33):23937-23945.

Gutensohn, Michael, et al.

2006 Toc, Tic, Tat et al.: structure and function of protein transport machineries in chloroplasts. Journal of plant physiology 163(3):333-347.

Habersetzer, Johann, et al.

2017 Substrate-triggered position switching of TatA and TatB during Tat transport in Escherichia coli. Open biology 7(8):170091.

Halbig, Dirk, et al.

1999 The efficient export of NADP-containing glucose-fructose oxidoreductase to the periplasm of Zymomonas mobilis depends both on an intact twin-arginine motif in the signal peptide and on the generation of a structural export signal induced by cofactor binding. European journal of biochemistry 263(2):543-551.

Hamsanathan, Shruthi, et al.

2017 A hinged signal peptide hairpin enables Tat-dependent protein translocation. Biophysical Journal 113(12):2650-2668.

Hao, Binhan, Wenjie Zhou, and Steven M Theg

2023 The polar amino acid in the TatA transmembrane helix is not strictly necessary for protein function. Journal of Biological Chemistry 299(4).

Hauer, René Steffen, et al.

2017 How to achieve Tat transport with alien TatA. Scientific reports 7(1):8808.

Hauer, René Steffen, et al.

2013 Enough is enough: TatA demand during Tat-dependent protein transport. Biochimica et Biophysica Acta (BBA)-Molecular Cell Research 1833(5):957-965.

Hicks, Matthew G, et al.

2003 The Escherichia coli twin-arginine translocase: conserved residues of TatA and TatB family components involved in protein transport. FEBS letters 539(1-3):61-67.

Hinnah, Silke C, et al.

2002 The chloroplast protein import channel Toc75: pore properties and interaction with transit peptides. Biophysical journal 83(2):899-911.

Hou, Bo, et al.

2018 The TatA component of the twin-arginine translocation system locally weakens the cytoplasmic membrane of Escherichia coli upon protein substrate binding. Journal of Biological Chemistry 293(20):7592-7605.

Huang, Qi, and Tracy Palmer

2017 Signal peptide hydrophobicity modulates interaction with the twin-arginine translocase. MBio 8(4):10.1128/mbio. 00909-17.

Hynds, Peter J, David Robinson, and Colin Robinson

1998 The sec-independent twin-arginine translocation system can transport both tightly folded and malfolded proteins across the thylakoid membrane. Journal of Biological Chemistry 273(52):34868-34874.

Ize, Bérengère, et al.

2004 Novel phenotypes of Escherichia coli tat mutants revealed by global gene expression and phenotypic analysis. Journal of Biological Chemistry 279(46):47543-47554.

Jack, Rachael L, et al.

2001 Constitutive expression of Escherichia coli tat genes indicates an important role for the twin-arginine translocase during aerobic and anaerobic growth. Journal of bacteriology 183(5):1801-1804.

Jakob, Mario, et al.

2009 Tat subunit stoichiometry in Arabidopsis thaliana challenges the proposed function of TatA as the translocation pore. Biochimica et Biophysica Acta (BBA)-Molecular Cell Research 1793(2):388-394.

Jänsch, Lothar, et al.

1996 New insights into the composition, molecular mass and stoichiometry of the protein complexes of plant mitochondria. The Plant Journal 9(3):357-368.

Jongbloed, Jan DH, et al.

2004 Two minimal Tat translocases in Bacillus. Molecular microbiology 54(5):1319-1325.

Karnauchov, Ivan, et al.

1994 The thylakoid translocation of subunit 3 of photosystem I, the psaF gene product, depends on a bipartite transit peptide and proceeds along an azide-sensitive pathway. Journal of Biological Chemistry 269(52):32871-32878.

Kim, Soo Jung, Colin Robinson, and Alexandra Mant

1998 Sec/SRP-independent insertion of two thylakoid membrane proteins bearing cleavable signal peptides. FEBS letters 424(1-2):105-108.

Klösgen, Ralf B, et al.

1992 Proton gradient-driven import of the 16 kDa oxygen-evolving complex protein as the full precursor protein by isolated thylakoids. Plant molecular biology 18:1031-1034.

Klösgen, RB, et al.

2004 Protein transport across the thylakoid membrane. Endocytobiosis and Cell Research 15:518-526.

Koch, Sabrina, et al.

2012 Escherichia coli TatA and TatB proteins have N-out, C-in topology in intact cells. Journal of Biological Chemistry 287(18):14420-14431.

Krause, Frank

2006 Detection and analysis of protein–protein interactions in organellar and prokaryotic proteomes by native gel electrophoresis:(membrane) protein complexes and supercomplexes. Electrophoresis 27(13):2759-2781.

Kreutzenbeck, Peter, et al.

2007 Escherichia coli twin arginine (Tat) mutant translocases possessing relaxed signal peptide recognition specificities. Journal of Biological Chemistry 282(11):7903-7911.

Laemmli, Ulrich K

1970 Cleavage of structural proteins during the assembly of the head of bacteriophage T4. nature 227(5259):680-685.

Laszlo, Joseph A, Gary M Baker, and Richard A Dilley

1984 Nonequilibration of membrane-associated protons with the internal aqueous space in dark-maintained chloroplast thylakoids. Journal of Bioenergetics and Biomembranes 16:37-51.

Lausberg, Frank, et al.

2012 Genetic evidence for a tight cooperation of TatB and TatC during productive recognition of twin-arginine (Tat) signal peptides in Escherichia coli. PloS one 7(6):e39867.

Lee, Philip A, et al.

2002 Truncation analysis of TatA and TatB defines the minimal functional units required for protein translocation. Journal of bacteriology 184(21):5871-5879.

Lee, Philip A, et al.

2006a Cysteine-scanning mutagenesis and disulfide mapping studies of the conserved domain of the twin-arginine translocase TatB component. Journal of Biological Chemistry 281(45):34072-34085.

Lee, Philip A, Danielle Tullman-Ercek, and George Georgiou

2006b The bacterial twin-arginine translocation pathway. Annu. Rev. Microbiol. 60(1):373-395.

Leister, Dario

2003 Chloroplast research in the genomic age. TRENDS in Genetics 19(1):47-56.

Li, Na, et al.

2023 The thylakoid membrane protein NTA1 is an assembly factor of the cytochrome b6f complex essential for chloroplast development in Arabidopsis. Plant Communications 4(1).

Liu, Yang-Wei, et al.

2014 It takes two to tango: two TatA paralogues and two redox enzyme-specific chaperones are involved in the localization of twin-arginine translocase substrates in Campylobacter jejuni. Microbiology 160(9):2053-2066.

Lüke, Iris, et al.

2009 Proteolytic processing of Escherichia coli twin-arginine signal peptides by LepB. Archives of microbiology 191:919-925.

Ma, Qianqian, et al.

2018 Thylakoid-integrated recombinant Hcf106 participates in the chloroplast twin arginine transport system. Plant Direct 2(10):e00090.

Ma, Xianyue, and Kenneth Cline

2010 Multiple precursor proteins bind individual Tat receptor complexes and are collectively transported. The EMBO journal 29(9):1477-1488.

Maldonado, Barbara, et al.

2011 Characterisation of the membrane-extrinsic domain of the TatB component of the twin arginine protein translocase. FEBS letters 585(3):478-484.

Maurer, Carlo, et al.

2010 TatB functions as an oligomeric binding site for folded Tat precursor proteins. Molecular biology of the cell 21(23):4151-4161.

McDevitt, Christopher A, et al.

2006 Subunit composition and in vivo substrate-binding characteristics of Escherichia coli Tat protein complexes expressed at native levels. The FEBS journal 273(24):5656-5668.

Mehner-Breitfeld, Denise, et al.

2022 TatA and TatB generate a hydrophobic mismatch important for the function and assembly of the Tat translocon in Escherichia coli. Journal of Biological Chemistry 298(9).

Michl, Doris, et al.

1994 Targeting of proteins to the thylakoids by bipartite presequences: CFoII is imported by a novel, third pathway. The EMBO journal 13(6):1310-1317.

Molik, Sabine, et al.

2001 The Rieske Fe/S Protein of the Cytochromeb 6/f Complex in Chloroplasts: MISSING LINK IN THE EVOLUTION OF PROTEIN TRANSPORT PATHWAYS IN CHLOROPLASTS? Journal of Biological Chemistry 276(46):42761-42766.

Mori, Hiroki, and Kenneth Cline

1998 A signal peptide that directs non-Sec transport in bacteria also directs efficient and exclusive transport on the thylakoid delta pH pathway. Journal of Biological Chemistry 273(19):11405-11408.

—

2002 A twin arginine signal peptide and the pH gradient trigger reversible assembly of the thylakoid ΔpH/Tat translocase. The Journal of cell biology 157(2):205-210.

Mori, Hiroki, Elizabeth J Summer, and Kenneth Cline

2001 Chloroplast TatC plays a direct role in thylakoid ΔpH-dependent protein transport. FEBS letters 501(1):65-68.

Mori, Hiroki, et al.

1999 Component specificity for the thylakoidal Sec and Delta pH–dependent protein transport pathways. Journal of Cell Biology 146(1):45-56.

Mould, Ruth M, and Colin Robinson

1991 A proton gradient is required for the transport of two lumenal oxygen-evolving proteins across the thylakoid membrane. Journal of Biological Chemistry 266(19):12189-12193.

Mould, Ruth M, Jamie B Shackleton, and Colin Robinson

1991 Transport of proteins into chloroplasts. Requirements for the efficient import of two lumenal oxygen-evolving complex proteins into isolated thylakoids. Journal of Biological Chemistry 266(26):17286-17289.

Müller, Matthias, and Ralf Bernd Klösgen

2005 The Tat pathway in bacteria and chloroplasts. Molecular membrane biology 22(1-2):113-121.

Musser, Siegfried M, and Steven M Theg

2000 Proton transfer limits protein translocation rate by the thylakoid ΔpH/Tat machinery. Biochemistry 39(28):8228-8233.

Neff, Dirk, and Norbert A Dencher

1999 Purification of multisubunit membrane protein complexes: isolation of chloroplast FoF1-ATP synthase, CFo and CF1 by blue native electrophoresis. Biochemical and biophysical research communications 259(3):569-575.

Neuhoff, Volker, Reinhard Stamm, and Hansjörg Eibl

1985 Clear background and highly sensitive protein staining with Coomassie Blue dyes in polyacrylamide gels: a systematic analysis. Electrophoresis 6(9):427-448.

Oates, Joanne, et al.

2005 The Escherichia coli twin-arginine translocation apparatus incorporates a distinct form of TatABC complex, spectrum of modular TatA complexes and minor TatAB complex. Journal of molecular biology 346(1):295-305.

Ouyang, Min, et al.

2020 Liquid-liquid phase transition drives intra-chloroplast cargo sorting. Cell 180(6):1144-1159. e20.

Peltier, Jean-Benoît, et al.

2002 Central functions of the lumenal and peripheral thylakoid proteome of Arabidopsis determined by experimentation and genome-wide prediction. The Plant Cell 14(1):211-236.

Petersen, Lea Madlen, and Eric Beitz

2020 The ionophores CCCP and gramicidin but not nigericin inhibit Trypanosoma brucei aquaglyceroporins at neutral pH. Cells 9(10):2335.

Petrů, Markéta, et al.

2018 Evolution of mitochondrial TAT translocases illustrates the loss of bacterial protein transport machines in mitochondria. BMC biology 16:1-14.

Pettersson, Pontus, et al.

2021 Soluble TatA forms oligomers that interact with membranes: Structure and insertion studies of a versatile protein transporter. Biochimica et Biophysica Acta (BBA)-Biomembranes 1863(2):183529.

Pettersson, Pontus, et al.

2018 Structure and dynamics of plant TatA in micelles and lipid bilayers studied by solution NMR. The FEBS Journal 285(10):1886-1906.

Pop, Ovidiu I, et al.

2003 Sequence-specific binding of prePhoD to soluble TatAd indicates protein-mediated targeting of the Tat export in Bacillus subtilis. Journal of Biological Chemistry 278(40):38428-38436.

Punginelli, Claire, et al.

2007 Cysteine scanning mutagenesis and topological mapping of the Escherichia coli twin-arginine translocase TatC Component. Journal of bacteriology 189(15):5482-5494.

Ramasamy, Sureshkumar, et al.

2013 The glove-like structure of the conserved membrane protein TatC provides insight into signal sequence recognition in twin-arginine translocation. Structure 21(5):777-788.

Randall, Linda L, and Simon JS Hardy

1995 High selectivity with low specificity: how SecB has solved the paradox of chaperone binding. Trends in biochemical sciences 20(2):65-69.

Renganathan, M, et al.

1991 Evidence that localized energy coupling in thylakoids can continue beyond the energetic threshold onset into steady illumination. Biochimica et Biophysica Acta (BBA)-Bioenergetics 1059(1):16-27.

Richter, Christine V, Thomas Bals, and Danja Schünemann

2010 Component interactions, regulation and mechanisms of chloroplast signal recognition particle-dependent protein transport. European journal of cell biology 89(12):965-973.

Richter, Silke, and Thomas Brüser

2005 Targeting of unfolded PhoA to the TAT translocon of Escherichia coli. Journal of Biological Chemistry 280(52):42723-42730.

Richter, Silke, et al.

2007 Functional Tat transport of unstructured, small, hydrophilic proteins. Journal of Biological Chemistry 282(46):33257-33264.

Richter, Stefan, and Gayle K Lamppa

1998 A chloroplast processing enzyme functions as the general stromal processing peptidase. Proceedings of the National Academy of Sciences 95(13):7463-7468.

Robinson, Andrew, and Brian Austen

1987 The role of topogenic sequences in the movement of proteins through membranes. Biochemical Journal 246(2):249-261.

Robinson, Colin, and R John Ellis

1984 Transport of proteins into chloroplasts: partial purification of a chloroplast protease involved in the processing of imported precursor polypeptides. European Journal of Biochemistry 142(2):337-342.

Rodrigue, Agnes, et al.

1999 Co-translocation of a periplasmic enzyme complex by a hitchhiker mechanism through the bacterial tat pathway. Journal of Biological Chemistry 274(19):13223-13228.

Rodriguez, Fernanda, et al.

2013 Structural model for the protein-translocating element of the twin-arginine transport system. Proceedings of the National Academy of Sciences 110(12):E1092-E1101.

Rollauer, Sarah E, et al.

2012 Structure of the TatC core of the twin-arginine protein transport system. Nature 492(7428):210-214.

Rose, Patrick, et al.

2013 Substrate-dependent assembly of the Tat translocase as observed in live Escherichia coli cells. PloS one 8(8):e69488.

Sambrook, Joseph, Edward F Fritsch, and Tom Maniatis

1989 Molecular cloning: a laboratory manual.

Sargent, Frank, et al.

1998 Overlapping functions of components of a bacterial Sec-independent protein export pathway. The EMBO journal.

Sargent, Frank, et al.

2001 Purified components of the Escherichia coli Tat protein transport system form a double-layered ring structure. European Journal of Biochemistry 268(12):3361-3367.

Schäfer, Kerstin, et al.

2020 The plant mitochondrial TAT pathway is essential for complex III biogenesis. Current Biology 30(5):840-853. e5.

Schagger, Hermann, WA Cramer, and G Vonjagow

1994 Analysis of molecular masses and oligomeric states of protein complexes by blue native electrophoresis and isolation of membrane protein complexes by two-dimensional native electrophoresis. Analytical biochemistry 217(2):220-230.

Schatz, Gottfried, and Bernhard Dobberstein

1996 Common principles of protein translocation across membranes. Science 271(5255):1519-1526.

Schatz, Gottfried, and Thomas L Mason

1974 The biosynthesis of mitochondrial proteins. Annual review of biochemistry 43(1):51-87.

Schönknecht, Gerald, Gerd Althoff, and Wolfgang Junge

1992 Dimerization constant and single-channel conductance of gramicidin in thylakoid membranes. The Journal of membrane biology 126:265-275.

Shanmugham, Anitha, et al.

2006 Membrane binding of twin arginine preproteins as an early step in translocation. Biochemistry 45(7):2243-2249.

Shikanai, Toshiharu, and Hiroshi Yamamoto

2017 Contribution of cyclic and pseudo-cyclic electron transport to the formation of proton

motive force in chloroplasts. Molecular plant 10(1):20-29.

Simone, Domenico, et al.

2013 Diversity and evolution of bacterial twin arginine translocase protein, TatC, reveals a protein secretion system that is evolving to fit its environmental niche. PLoS One 8(11):e78742.

Singer, S Jonathan, and Garth L Nicolson

1972 The Fluid Mosaic Model of the Structure of Cell Membranes: Cell membranes are viewed as two-dimensional solutions of oriented globular proteins and lipids. Science 175(4023):720-731.

Smith, Matthew D, et al.

2004 atToc159 is a selective transit peptide receptor for the import of nucleus-encoded chloroplast proteins. Journal of Cell Biology 165(3):323-334.

Stanley, Nicola R, Tracy Palmer, and Ben C Berks

2000 The twin arginine consensus motif of Tat signal peptides is involved in Sec-independent protein targeting in Escherichia coli. Journal of Biological Chemistry 275(16):11591-11596.

Stockwald, Eva R, et al.

2023 Length matters: functional flip of the short TatA transmembrane helix. Biophysical Journal 122(11):2125-2146.

Stolle, Patrick, Bo Hou, and Thomas Brüser

2016 The Tat substrate CueO is transported in an incomplete folding state. Journal of Biological Chemistry 291(26):13520-13528.

Strauch, Eva-Maria, and George Georgiou

2007 Escherichia coli tatC mutations that suppress defective twin-arginine transporter signal peptides. Journal of molecular biology 374(2):283-291.

Tarry, Michael J, et al.

2009 Structural analysis of substrate binding by the TatBC component of the twin-arginine protein transport system. Proceedings of the National Academy of Sciences 106(32):13284-13289.

Taubert, Johannes, et al.

2015 TatBC-independent TatA/Tat substrate interactions contribute to transport efficiency. PloS one 10(3):e0119761.

Teixeira, Pedro Filipe, and Elzbieta Glaser

2013 Processing peptidases in mitochondria and chloroplasts. Biochimica et Biophysica Acta (BBA)-Molecular Cell Research 1833(2):360-370.

Theg, SM, G Chiang, and RA Dilley

1988 Protons in the thylakoid membrane-sequestered domains can directly pass through the

coupling factor during ATP synthesis in flashing light. Journal of Biological Chemistry 263(2):673-681.

Thompson, Simon J, Colin Robinson, and Alexandra Mant

1999 Dual signal peptides mediate the signal recognition particle/Sec-independent insertion of a thylakoid membrane polyprotein, PsbY. Journal of Biological Chemistry 274(7):4059-4066.

Tikhonov, Alexander N, et al.

2008 Spin-probes designed for measuring the intrathylakoid pH in chloroplasts. Biochimica et Biophysica Acta (BBA)-Bioenergetics 1777(3):285-294.

Tymms, Martin J

1998 In Vitro Translation. Molecular Biomethods Handbook:335-346.

Ulfig, Agnes, and Roland Freudl

2018 The early mature part of bacterial twin-arginine translocation (Tat) precursor proteins contributes to TatBC receptor binding. Journal of Biological Chemistry 293(19):7281-7299.

Ulfig, Agnes, et al.

2017 The h-region of twin-arginine signal peptides supports productive binding of bacterial Tat precursor proteins to the TatBC receptor complex. Journal of Biological Chemistry 292(26):10865-10882.

van Dijl, Jan Maarten, et al.

2002 Functional genomic analysis of the Bacillus subtilis Tat pathway for protein secretion. Journal of biotechnology 98(2-3):243-254.

Van Herwynen, John F, and Gregory S Beckler

1995 Translation using a wheat-germ extract. In Vitro Transcription and Translation Protocols:245-251.

Vargas, C, AG McEwan, and JA Downie

1993 Detection of c-type cytochromes using enhanced chemiluminescence. Analytical biochemistry 209(2):323-326.

Verner, Keith, and Gottfried Schatz

1988 Protein translocation across membranes. Science 241(4871):1307-1313.

Vershubskii, Alexey V, et al.

2017 Lateral heterogeneity of the proton potential along the thylakoid membranes of chloroplasts. Biochimica et Biophysica Acta (BBA)-Biomembranes 1859(3):388-401.

Voelker, Rodger, and Alice Barkan

1995 Two nuclear mutations disrupt distinct pathways for targeting proteins to the chloroplast

thylakoid. The EMBO journal 14(16):3905-3914.

von HEIJNE, Gunnar, Johannes Steppuhn, and Reinhold G Herrmann

1989 Domain structure of mitochondrial and chloroplast targeting peptides. European Journal of Biochemistry 180(3):535-545.

Wagener, Nikola, et al.

2011 A pathway of protein translocation in mitochondria mediated by the AAA-ATPase Bcs1. Molecular cell 44(2):191-202.

Walker, Macie B, et al.

1999 The maize tha4 gene functions in sec-independent protein transport in chloroplasts and is related to hcf106, tatA, and tatB. The Journal of cell biology 147(2):267-276.

Weiner, Joel H, et al.

1998 A novel and ubiquitous system for membrane targeting and secretion of cofactor-containing proteins. Cell 93(1):93-101.

Werner, Max-Hinrich, Denise Mehner-Breitfeld, and Thomas Brüser

2024 A larger TatBC complex associates with TatA clusters for transport of folded proteins across the bacterial cytoplasmic membrane. Scientific Reports 14(1):13754.

Wexler, Margaret, et al.

1998 Targeting signals for a bacterial Sec-independent export system direct plant thylakoid import by the ΔpH pathway. FEBS letters 431(3):339-342.

Whitaker, Neal, Umesh K Bageshwar, and Siegfried M Musser

2012 Kinetics of precursor interactions with the bacterial Tat translocase detected by real-time FRET. Journal of Biological Chemistry 287(14):11252-11260.

Wojnowska, Marta, et al.

2018 Precursor–Receptor Interactions in the Twin Arginine Protein Transport Pathway Probed with a New Receptor Complex Preparation. Biochemistry 57(10):1663-1671.

Yen, Ming-Ren, et al.

2002 Sequence and phylogenetic analyses of the twin-arginine targeting (Tat) protein export system. Archives of microbiology 177:441-450.

Yuan, Jianguo, and Kenneth Cline

1994 Plastocyanin and the 33-kDa subunit of the oxygen-evolving complex are transported into thylakoids with similar requirements as predicted from pathway specificity. Journal of Biological Chemistry 269(28):18463-18467.

Zhang, Yi, et al.

2014 Solution structure of the TatB component of the twin-arginine translocation system. Biochimica et Biophysica Acta (BBA)-Biomembranes 1838(7):1881-1888.

Zinecker, Sarah, Mario Jakob, and Ralf Bernd Klösgen

2020 Functional reconstitution of TatB into the thylakoidal Tat translocase. Biochimica et Biophysica Acta (BBA)-Molecular Cell Research 1867(2):118606.

Zoufaly, Stefan, et al.

2012 Mapping precursor-binding site on TatC subunit of twin arginine-specific protein translocase by site-specific photo cross-linking. Journal of Biological Chemistry 287(16):13430-13441.

Appendix

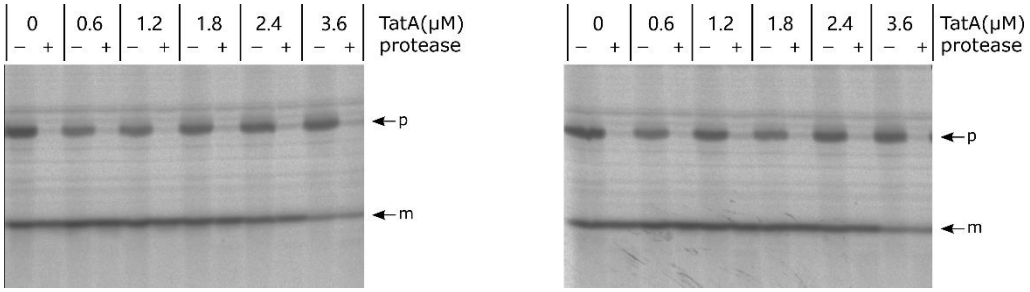

Fig.S1 The effect of external TatA on Tat transport in thylakoids without antibody treatment.
Autoradiograms of two repeated experiments. Mock-treated thylakoids were incubated with 5μl of ^{35}S-radiolabeled pOEC16 *(p)* and heterologously-overexpressed TatA proteins for 20min at 25℃ in the light. Substrate OEC16 was synthesized by *Rabbit reticulocyte Lysate System*. The concentrations of TatA were indicated on top of the lanes. After incubation for 20min in light at 25℃, thylakoids were washed once with HM buffer and subsequently incubated with either thermolysin (182μg/ml, *lanes+*) or HM buffer (*lanes-*) for 30min. For each lane, samples corresponding to 15μg of chlorophyll were loaded on a 10–17.5% SDS-polyacrylamide (SDS-PA) gradient gel. The bands representing the precursor (*p*) and mature proteins (*m*) are indicated by *black arrows*. Radioactive signals are detected by phosphorimaging.

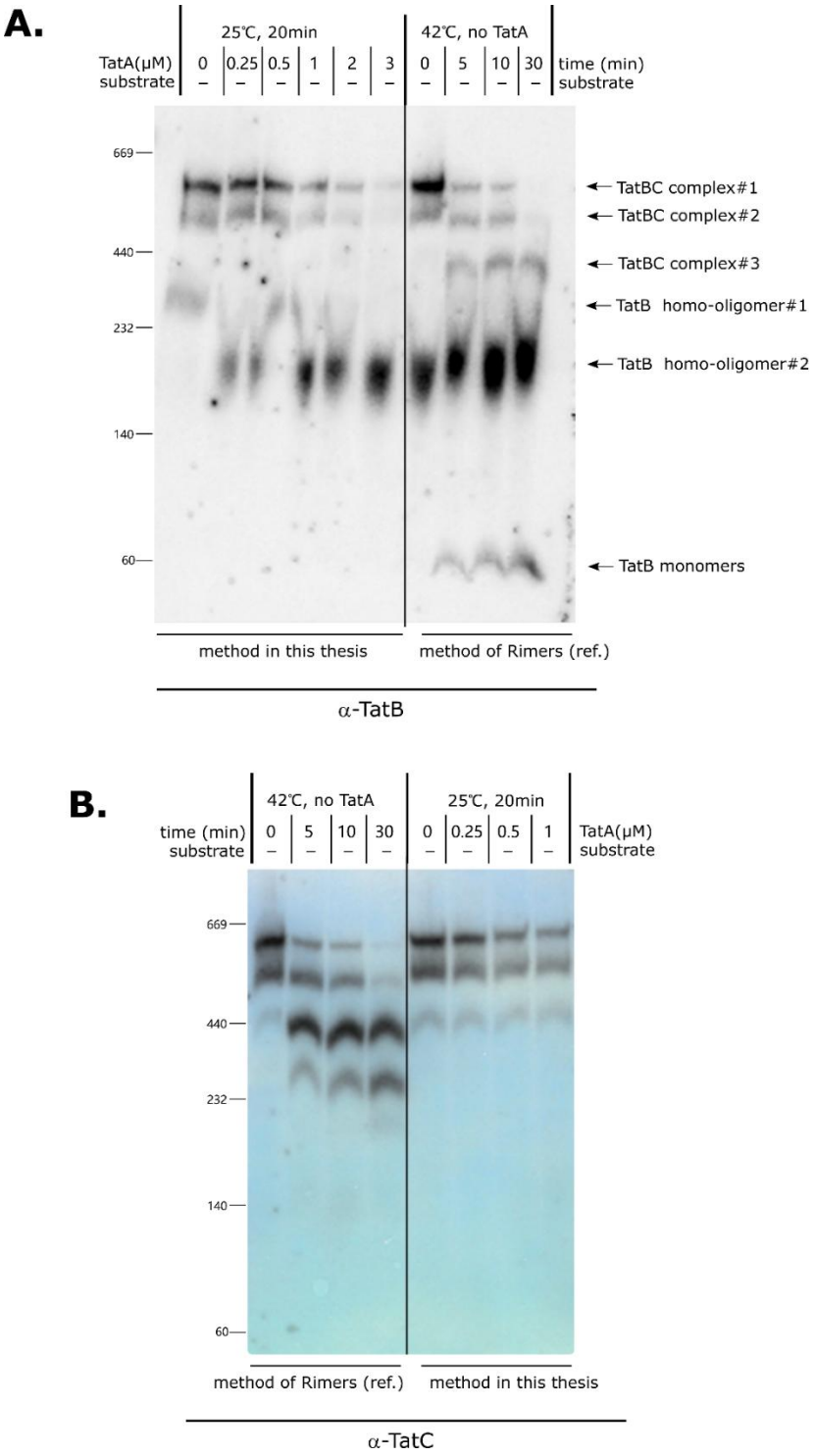

Fig.S2 Comparison between methods used in this thesis and method from Rimers to identify TatBC complexes.
In the method used in this thesis, isolated thylakoids were incubated with purified soluble TatA proteins obtained by heterologous overexpression at 25℃ for 20min in light. The concentrations of TatA are given above the lanes. Subsequently, thylakoids were washed once and solubilized by BN lysis buffer with 1.67% digitonin followed by incubated in 4℃ for 1h. In the method used by Rimers, isolated thylakoids were incubated at 42℃ for a time period as indicated above the lanes. No TatA added. Then, thylakoids were centrifuged down to get the pellet. The pellet was solubilized by BN lysis buffer with 1.67% digitonin followed by incubated in 4℃ for 1h. The BN-lysis samples from both methods corresponding to 30μg of chlorophyll were loaded on a 5%-13.5% gradient blue native polyacrylamide (BN-PA) gel to separate protein complexes. BN-PA gels were then blotted and developed with specific antibodies against the respective proteins as shown blow the lanes.

A. alignment: pea mTatA (full)- pea mTatB (full)

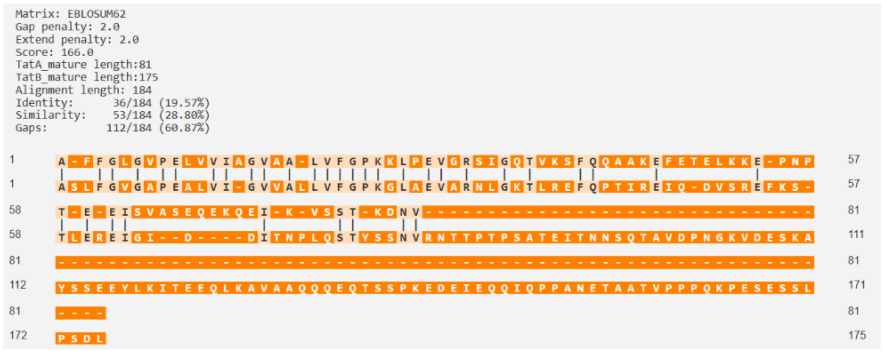

B. alignment: pea mTatA (full)- pea mTatB (1-80)

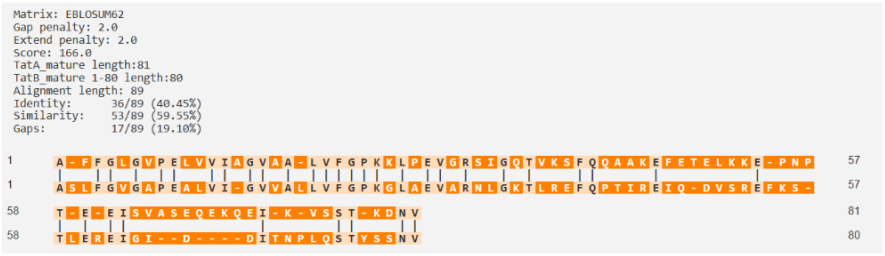

C. alignment: pea mTatA (N+TMH)- pea mTatB (N+TMH)

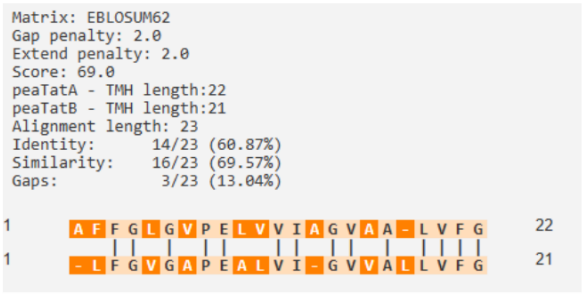

alignment: E.coli TatA (N+TMH)- E.coli TatB (N+TMH)

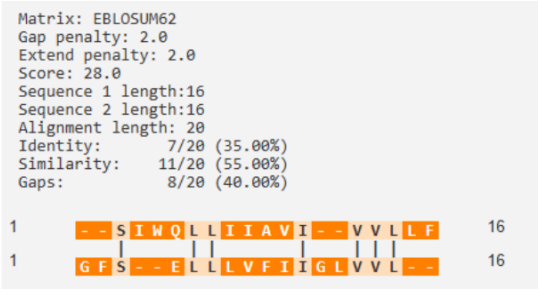

Fig.S3 Comparison between TatA and TatB sequences from *E. coli* and pea.
The details of aligned sequences are given above the pictures. All alignments use EBLOSUM62 matrix with gap penalty and extend penalty in 2.0. Light orange highlights identical amino acids between the two sequences, and the dark orange represents difference. A, comparing full length of TatA and TatB sequences from pea. TatA showed high similarity with TatB at the N-terminus but low similarity at the C-termius. B, comparing full length of TatA and the truncated TatB that has same length as TatA. C, comparing the N-terminus and TMH sequence of TatA and TatB from pea (upper) and from E. coli (bottom).

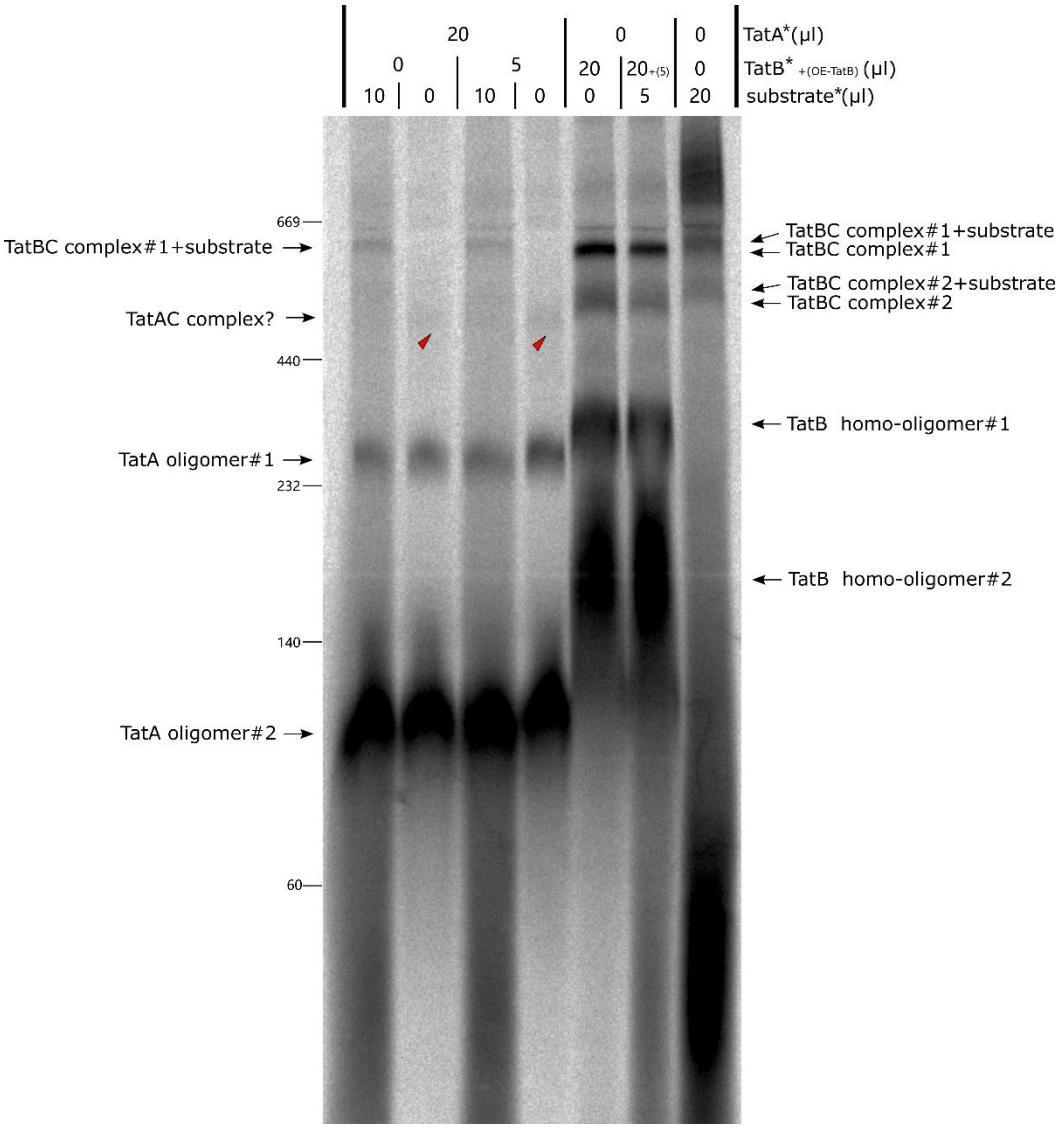

Fig.S4 TatA and TatB complexes by radioactive-labeled TatA, TatB and substrate.
Isolated thylakoids were incubated with radioactive-labeled TatA, TatB and substrate as given above the lanes at 25℃ for 20min in light. *Asterisks* means proteins are synthesized by R*abbit reticulocyte Lysate System* in the presence of ^{35}S-methionine. Purified soluble TatB proteins obtained by heterologous overexpression was also introduced into one of the assays, indicated by smaller letters with brackets above the lanes. After incubation, thylakoids were washed twice and solubilized by BN lysis buffer with 1.67% digitonin followed by incubation in 4℃ for 1h. The BN-lysis samples from both methods corresponding to 30µg of chlorophyll were loaded on a 5%-13.5% gradient blue native polyacrylamide (BN-PA) gel to separate protein complexes. Radioactive signals were detected by phosphorimaging.

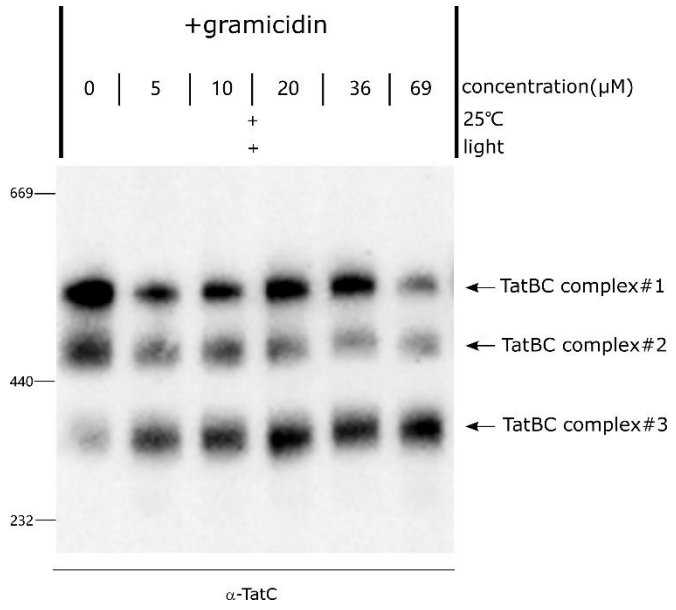

Fig.S5 The detection of TatBC complexes under gramicidin treatment.
Thylakoid membranes were treated with a range of concentrations of gramicidin under standard import condition (+ 25℃ , + light, 20min). The concentrations of gramicidin are given above the lanes. Thylakoid samples were solubilization by BN-lysis buffer and 1.67% digitonin, followed by Western analysis and specific TatC antibodies immunodetection.

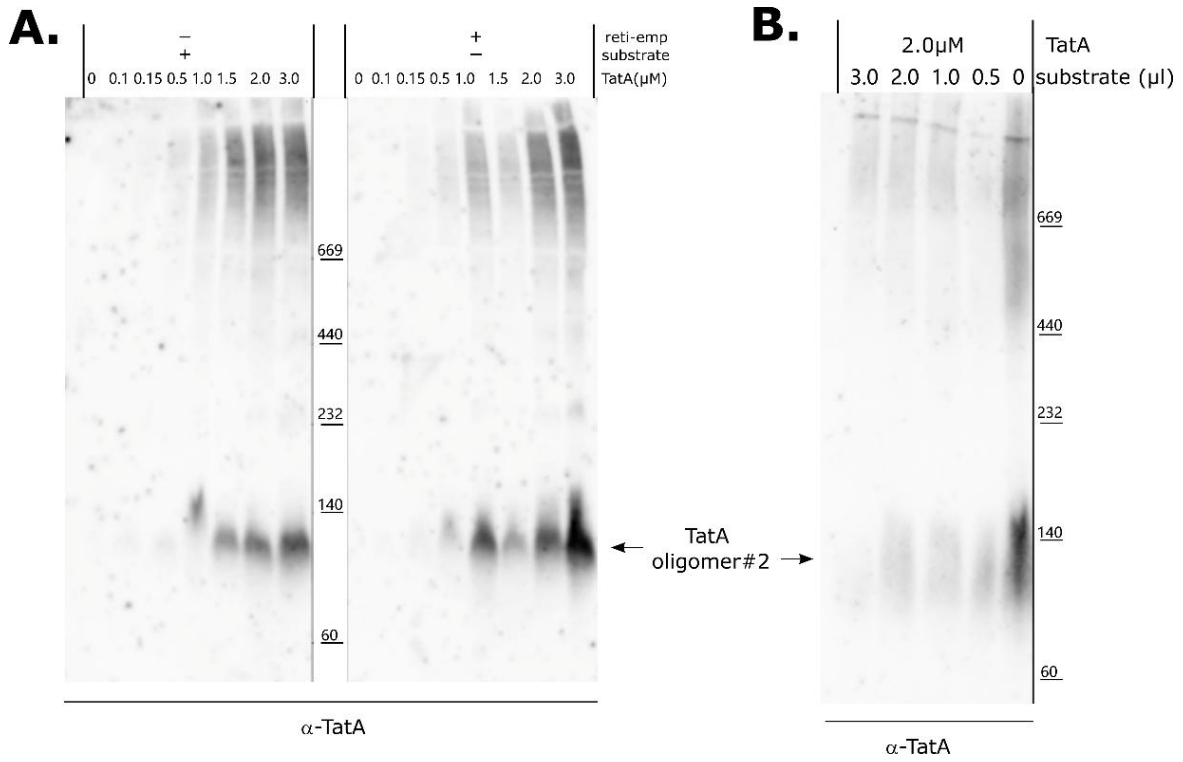

Fig.S6 The influence on TatA oligomers by substrate supplementation.

(A) Isolated thylakoids were incubated with purified TatA proteins and with/without radiolabeled substrate OEC16. TatA proteins were obtained by heterologous overexpression. OEC16 was obtained by *Rabbit reticulocyte Lysate System* in the presence of ^{35}S-methionine. When no substrate was added into assays, same volume of empty translation product (*reti-emp*) was added. The empty product was produced by same procedure as OEC16 synthesis, but did not contain *in vitro* transcription of the respective OEC16. The concentrations of TatA are given above the lanes. (B) thylakoids were incubated with 2μM purified soluble TatA proteins and different volumes of substrate as shown above the lanes. For both cases, after incubation, thylakoids were washed once and solubilized by BN lysis buffer with 1.67% digitonin followed by incubation in 4℃ for 1h. The BN-lysis samples from both methods corresponding to 30μg of chlorophyll were loaded on a 5%-13.5% gradient BN-PA gel to separate protein complexes. BN-PA gels were then blotted and developed with specific TatA antibodies for immunodetection.

List of Figures

Acknowledgement

It has been five years since I come to Halle and start my PhD study. It is a long way, and not easy. But it teaches me a lot and guides me to find my real interest – doing research work. Along my way, from bachelor to PhD, I was exploring, exploring myself and exploring my future. At beginning of my PhD, I didn't know where I would go afterwards. I thought maybe I would turn to industry after I finished my PhD. But during the time, I noticed that I like research work. I like the feeling to explore unknown things and demonstrate it by my hand. So now, I can confidently to say I want to continue on researching. And I think it should attribute to our warming research group.

First, I would like to give my huge appreciation to my supervisor, **Prof. Dr. Ralf Bernd ("Rabe") Klösgen**. I learn a lot from you: how to do research work, how to think scientifically, and how to be a good person. I appreciate every discussion we had for my project, and enjoy every group events after work. Maybe words cannot fully describe my feeling, but I feel really lucky and grateful to be a member in our group, and be your student, for my PhD time. Thank you!

Then, I want to give a warm hug to Dr. Bationa Benewitz. **Bationa**, you are like an elder sister for me. I feel heart-warming to work with you. I remember when we attended the EMBO meeting 2024, you were always with me in the poster session, and taught me how to dance the whole night at the last day^^ I know you didn't want me to feel alone. You give me lots of support both in my PhD project and my everyday life!

I also want to extend my thanks to our group members. **Mario**, you are always kind and patient when I need help. You are a good teacher whenever I asked you about protein purification or biochemical stuff, explaining things really well. **Birgit**, I know I trouble you a lot. Whenever something happened in the lab, I always come to you. But you are nice to me every time. **Nico**, even though you are not so often in the office, the time we spend together like canoeing, mitteldeutsche meeting and etc. that are really fun. You also help me a lot with German language. I'm glad to work with you.

Leander, even though you already finished your work here and continue to the next page, I still feel you are one of the members in our group. You are the one who let me know how fun board game is. And you are the one who always in the lab and willing to help whenever I have some questions about

experiments, about lab stuff. I miss the time when you were still in the lab. But of course, now, I wish you all the best for your next chapter!

Ditya, my dear friend. We always support each other when we have problems, especially in the writing time. We started at almost same time, so we kind of in same stage and understand each other. I'm glad to have a friend and colleague like you that we feel free to share our feelings about everything. I hope you can finish your thesis soon, getting though the hardest time. Then we can go out together, enjoying a relaxing time!

My bachelor supervisor, **Prof. Dr. Yan He**, thank you for giving me support when I apply for master and PhD programs. And when I hesitated in whether should I go further to do a postdoc or not, you wipe out my hesitation and let me know if I want to do it, I should do it. No one knows what will happen in the future, so try my best to get what I want.

My dear **Weizhao** (伟钊), thank you for supporting me all the way. From master to PhD, you always go faster than me and lead me on the way. Even at this moment, when you are going though the most difficult time in your life, you still help me with my thesis and support me. Life is going on, I hope we can support each other on this long, difficult but also beautiful way. 生命它苦涩如歌，亦璀璨如歌，且行且珍惜。

At end, I want to say "thank you" to my parents, **Chenggang Zhou** (周成刚) and **Weiying Wang** (汪伟英). You fully support me and respect my decision. When I said I wanted to go to Beijing for bachelor, you let me go even though at that time I had better choices in universities but in other cities. When I said I wanted to go outside to see the world, you agreed and shouldered the high tuition fees for my master. When I decided to find a PhD still in a foreign country, although you really want me back to China and live close to you, you still respected my decision and let me do it. I'm so lucky and grateful to be your child. 谢谢爸爸和妈妈!

Curriculum vitae

PERSONAL INFORMATION

Name: Ming Zhou

Nationality: Chinese

EDUCATION AND RESEARCH BACKGROUND

10/2020 – present	**PhD student** AG Klösgen, Plant Physiology Department, Martin-Luther University of Halle-Wittenberg (Germany) Thesis title: "Towards the role of TatA and TatB on the activity and stability of Tat translocase" Supervisor: Prof. Dr. Ralf Bernd Klösgen
09/2017 – 06/2019	**Master student** **MSc**, Plant Biotechnology, Wageningen University & Research (the Netherlands) Thesis title: "The role of K^+ transporters in Salinity Stress in *Arabidopsis thaliana*" Supervisor: Prof. Dr. Christa Testerink
09/2013 – 07/2017	**Bachelor student** **BSc**, Agriculture Science, China Agricultural University (China) Thesis title: "QTL mapping to identify polygenes controlling the pollen number of maize" Supervisor: Prof. Dr. Yan He

CONFERENCE ATTENDANCES

24. – 25.09.2021	presentation	Mitteldeutsche Pflanzenphysiologietagung, Wittenberg (Germany)
24. – 25.06.2022	attend	Mitteldeutsche Pflanzenphysiologietagung, Dresden (Germany)
14. – 16.09.2022	poster	GBM Fall Conference 2022, Düsseldorf (Germany)
23. – 24.09.2023	presentation	Mitteldeutsche Pflanzenphysiologietagung, Jena (Germany)
17. – 20.06.2024	poster	Plant Science Student Conference 2024, Halle (Germany)
15. – 19.09.2024	poster	Botanik Tagung - International Conference of the German Society for Plant Sciences, Halle (Germany)
21. – 25.09.2024	poster	EMBO conference – "Advances and challenges in protein translocation across membranes", Sant Feliu de Guixols (Spain)

EIDESSTATTLICHE ERKLÄRUNG (STATUTORY DECLARATION)

Hiermit erkläre ich an Eides statt, dass ich mich mit der vorliegenden wissenschaftlichen Arbeit erstmals um die Erlangung des Doktorgrades bewerbe, die Arbeit selbstständig und ohne fremde Hilfe verfasst, nur die angegebenen Quellen und Hilfsmittel genutzt und die den benutzten Werken wörtlich oder inhaltlich entnommenen Stellen als solche kenntlich gemacht habe.

Halle (Saale),den _____ _____

ZHOU, Ming